Energy Storage Materials 42 (2021) 723–752

Contents lists available at ScienceDirect

Energy Storage Materials

journal homepage: www.elsevier.com/locate/ensm

Rational design of carbon nanotube architectures for lithium–chalcogen batteries: Advances and perspectives

Lianbo Ma [a,c,d,e,1], Junxiong Wu [b,1,*], Yang Li [c], Yaohui Lv [a], Baohua Li [f,*], Zhong Jin [d,e,*]

[a] Key Laboratory of Green Fabrication and Surface Technology of Advanced Metal Materials, Ministry of Education; School of Materials Science and Engineering, Anhui University of Technology, Maanshan 243002, China
[b] College of Environmental Science and Engineering, Fujian Normal University, Fuzhou, Fujian 350007, China
[c] Department of Mechanical and Aerospace Engineering, The Hong Kong University of Science and Technology, Clear Water Bay, Kowloon, Hong Kong, China
[d] MOE Key Laboratory of Mesoscopic Chemistry, MOE Key Laboratory of High Performance Polymer Materials and Technology, Jiangsu Key Laboratory of Advanced Organic Materials, School of Chemistry and Chemical Engineering, Nanjing University, Nanjing 210023, China
[e] Shenzhen Research Institute of Nanjing University, Shenzhen 518063, China
[f] Shenzhen Key Laboratory on Power Battery Safety and Shenzhen Geim Graphene Center, Tsinghua Shenzhen International Graduate School (SIGS), Shenzhen, China

ARTICLE INFO

Keywords:
Li–chalcogen batteries
Carbon nanotubes
Chalcogen cathodes
Lithium anodes
Interlayers

ABSTRACT

Rechargeable Li–chalcogen (S, Se, and Te) batteries (LCBs) have attracted considerable interest owing to their high theoretical capacities and energy densities. However, LCBs normally suffer from dramatic volume expansion of elemental chalcogen, dissolution and shuttling of intermediates in ether electrolytes, and serious Li dendrite growth. Carbon nanotubes (CNTs) have been employed to resolve these pressing issues, including the construction of cathodes, fabrication of interlayers, modification of separators, and design of Li anodes. In this review, the properties of different chalcogen elements and the electrochemistry of LCBs are first provided. Next, the multiple functions of CNTs are presented to mitigate the notorious issues faced by LCBs. More importantly, recent representative studies on CNT-based architectures for LCBs are presented and analyzed in detail, in terms of design concepts, fabrication methods, electrochemical performance, and underlying mechanisms. Finally, the remaining issues and future challenges in the adoption of CNTs for LCBs are discussed. It is believed that this paper can provide new insights into the further development and commercialization of LCBs.

1. Introduction

The global energy crisis and environmental pollution necessitate high-performance energy storage and conversion devices [1, 2]. Lithium-ion batteries (LIBs) are currently popular for powering portable electronics and electric vehicles [3, 4]. However, their energy densities are limited to 300 Wh kg^{-1}, owing to which they cannot meet the increasing demands of modern high-end electronic markets [5, 6]. Therefore, several types of energy storage devices, including sodium-ion batteries, potassium-ion batteries, and supercapacitors, have recently been explored as promising alternatives to the commonly used LIBs [7-11]. Li–chalcogen batteries (LCBs), which rely on the electrochemical redox reactions of Li with chalcogen (S, Se, and Te) elements, have gained immense attention owing to their high theoretical capacities and energy densities (**Fig. 1**) [12-19]. Of them, Li–S batteries are the most attractive because sulfur can store 1672 mAh g^{-1} when fully reduced to Li_2S, resulting in a high theoretical energy density of approximately 2600 Wh kg^{-1}. In addition, sulfur is much cheaper and more abundant than Se and Te. However, the electrical conductivity of S is much lower than those of Se and Te, thus requiring highly conductive matrices to accelerate the conversion kinetics. In terms of volumetric energy density, LCBs exhibit much higher values than conventional LIBs (1190 Wh L^{-1}). Considering the significant importance of volumetric energy density in practical applications, LCBs deserve more attention.

With progress in research on LCBs, five major challenges have emerged, which need to be resolved to promote their commercialization [20-22]. First, the shuttling of soluble polychalcogenides in ether-based electrolytes results in a continuous loss of active species and significant side reactions at the Li anode, both of which contribute to fast capacity decay. Second, the electrical conductivities of S and the polychalcogenides are still relatively low for enabling fast charge/discharge. Third, the volume expansion of chalcogen elements during repeated Li-ion insertion/extraction triggers a large internal strain, resulting in the structural degradation of cathodes and detachment of active materials from the current collector. Fourth, the uncontrollable Li dendrite growth during the repeated plating/stripping cycles gives rise to serious safety con-

* Corresponding authors.
E-mail addresses: jwuba@connect.ust.hk (J. Wu), libh@mail.sz.tsinghua.edu.cn (B. Li), zhongjin@nju.edu.cn (Z. Jin).
[1] Lianbo Ma and Junxiong Wu contributed equally to this work.

https://doi.org/10.1016/j.ensm.2021.08.023
Received 15 June 2021; Received in revised form 30 July 2021; Accepted 16 August 2021
Available online 18 August 2021

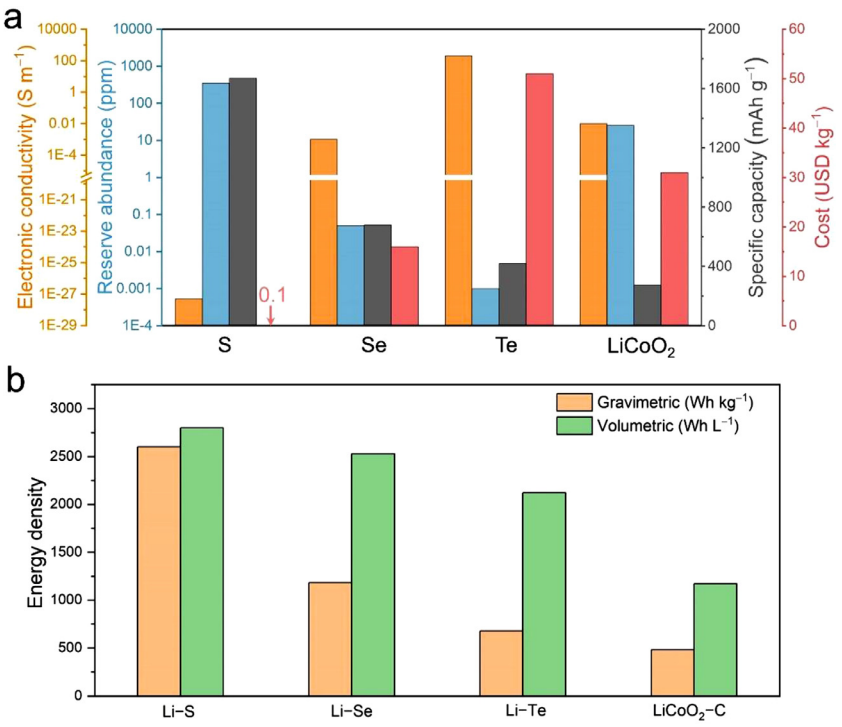

Fig. 1. (a) Comparison of chalcogen elements with the currently used $LiCoO_2$ cathode materials in terms of electronic conductivity, abundance, specific capacity, and cost. (b) Gravimetric and volumetric energy densities of LCBs and the present $LiCoO_2$–C batteries.

cerns [23]. Finally, the slow reaction kinetics at a low electrolyte/sulfur (E/S) ratio compromise the energy density of LCBs. Very recently, Bonnick et al. estimated via modeling that the gravimetric energy density of a Li–S battery with an E/S ratio greater than 3 mL g^{-1} is lower than that of a Li[$Ni_{0.33}Mn_{0.33}Co_{0.33}$]$O_2$||Li cell [24]. All these issues must be addressed to promote the commercialization of LCBs.

Substantial efforts have been made towards resolving these intractable issues faced by LCBs. Ji et al. pioneered the study of using carbon structures to host sulfur species [25]. The ordered carbon matrix, *i.e.*, CMK-3, could conduct electrons to the active sulfur component, thus realizing an efficient conversion between S and Li_2S. Furthermore, they also coated the sulfur/carbon composite with polyethylene glycol to mitigate the dissolution and shuttling of polysulfides because simple physical (spatial) entrapment is not sufficient for long-term cycles. Since then, various carbon matrices, including meso- and microporous carbons, carbon nanotubes (CNTs), carbon fibers, graphene, and mixtures thereof, have emerged as chalcogen and Li hosts, interlayers, and separator modifiers to prolong the lifespan of LCBs [26-29]. These carbon matrices not only offer high-speed electron pathways for active materials but also accommodate the volume changes of chalcogen cathodes and Li anodes, and alleviate the shuttling of soluble intermediates via physical entrapment.

Of diverse carbonaceous materials, CNTs have been extensively studied for use in various batteries owing to their extremely high length-to-width ratio, extraordinary electrical conductivity, remarkable mechanical/chemical/thermal stability, and large specific surface areas [30-33]. CNTs are typically produced by four main methods: arc discharge, laser ablation, gas-phase catalytic growth from carbon monoxide, and chemical vapor deposition (CVD)[34]. Of these methods, the CVD approach offers better potential for producing large quantities of CNTs at a low cost. For this reason, the use of commercial CNTs to construct hierarchical micro-and nanostructures such as CNT spheres, films, and sponges, thus promoting fast ion/electron transport in battery electrodes, is a well-recognized tactic for rechargeable batteries. Moreover, CNTs have also been produced by annealing various precursors comprising Co, Ni, Fe catalysts at high temperatures [35, 36]. In such a way, the CNT frameworks are uniformly distributed on elaborately designed architectures

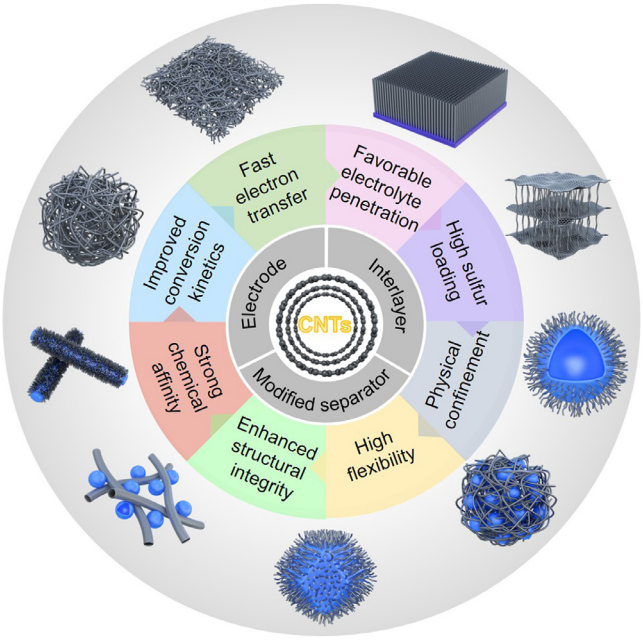

Fig. 2. Schematic of the functions of CNTs in LCBs, and the proposed CNT-based micro-and nanostructures.

without compromising their characteristics, resolving the dispersion issue for making CNT-based electrodes. For example, Co-based metal-organic frameworks (MOFs) can be used to produce CNTs that are grown in situ on MOF-derived frameworks [37-39]. In addition, CNTs can be easily integrated with other carbonaceous materials and assembled into various sophisticated architectures, making them very promising for use in the preparation of flexible electrodes.

CNT-based materials have been used in LCBs to construct hierarchical Li/chalcogen hosts, interlayers and to modify separators to improve their electrochemical performance [40-42], as illustrated in **Fig. 2**. For

Table 1
Summary of the detailed parameters of different chalcogens.

Element	Crystal structure	Mole Mass (g mol^{-1})	Mass Density (g cm^{-3})	Electronic Conductivity (S m^{-1})	Melting point (°C)
S	monoclinic (Ring-like S_8)	32.1	2.07	5×10^{-28}	115
Se	Trigonal(chain-like Se_8), rhombohedral (Se_6), monoclinic (Ring-like Se_8), and amorphous	79.0	4.81	1×10^{-3}	221
Te	Trigonal (Chain-like Te_8)	127.6	6.24	2×10^{2}	450

example, Wei et al. prepared an intriguing structure composed of a graphene/single-walled CNT (SWCNT) hybrid to encapsulate elemental sulfur [43]. The SWCNTs, CVD-grown graphene, as well as the robust connection between SWCNTs and graphene, conducted electrons to the sulfur species, whereas the internal spaces between the two stacked graphene layers and among the SWCNTs offered room for sulfur. However, simple spatial confinement cannot completely block the diffusion and shuttling of polysulfides over long-term cycles. Later, heteroatom doping and polymeric materials were used to modify the CNT networks to enable strong chemical interactions between the intermediates and polar hosts [44, 45]. In addition, metal compounds that demonstrate significant catalytic activities have been hybridized with CNT skeletons to accelerate the conversion of soluble intermediates to solid chalcogens and Li chalcogenides [46, 47]. Apart from the numerous efforts on the development of chalcogen cathodes, modification of separators, construction of interlayers are simple but effective strategies for intercepting the diffusion of intermediates to the anode [48]. Similar to rationally designed hosts, CNT-based materials with high electrical conductivity, large surface areas, and strong interactions with intermediates are desired. In addition, substantial efforts have been directed to constructing CNT assemblies to promote stable and reversible Li plating/stripping by reducing local current density for Li deposition and introducing nucleation sites [49, 50].

The last few years have witnessed tremendous improvements in the fundamental understanding of Li–chalcogen chemistries through a combination of science and engineering approaches, particularly focusing on the chalcogen cathode. CNT-based architectures have been extensively studied for LCBs. However, a systematic yet in-depth overview of this exciting field is still lacking. To facilitate their practical applications, we offer a timely and comprehensive review to present the latest progress in CNT-based materials for LCBs. In this review, we first compare the electrochemical principles of LCBs in different liquid electrolytes and summarize the multiple functions of CNTs in improving chalcogen utilization and mitigating Li dendrite growth. Then, the detailed roles of CNTs in LCBs are discussed from the viewpoint of design concepts, fabrication/synthesis methods, electrochemical performance, and underlying mechanisms. Next, the recent progress of CNT-based hosts for Li-metal batteries is presented. Finally, the persisting issues and future research directions are discussed.

2. Electrochemical principles of LCBs

Prior to discussing the working principles of LCBs, the physicochemical properties of S, Se, and Te are compared to help understand their differences in electrochemistry (**Table 1**)[21]. First, S, Se, and Te possess different crystal structures, which may result in different electrochemical activity and solubility properties of polychalcogenides in the electrolytes, thus significantly affecting their electrochemical performance. For example, Zhou et al. found that amorphous Se underwent multi-step lithiation while trigonal Se delivered single-phase transformation, signifying the impact of Se phase in Li–Se batteries [51]. Second, the electrical conductivity of chalcogen elements varies. S is an insulator, whereas Se and Te are semiconductor and semimetal, respectively. The huge differences in electrical conductivity render S with poor rate capacity and require a significant amount of carbon additives to boost the reaction kinetics. Third, the much higher density (6.24 g cm^{-3}) of Te enables the Li–Te to have a comparable volumetric capacity to that of Li–S and Li–Se batteries, which is of great importance for practical applications requiring limited space. Fourth, the melting point increases with the atomic number of chalcogen (S: 115°C, Se: 220 °C, and Te: 450°C). As a result, using the melting infiltration method to make the carbon/Te composite undergoes inevitable limitations of higher cost, inferior safety, and lower active mass loading. In this section, we will discuss in detail the electrochemical principles of Li–S, Li–Se, and Li–Te batteries.

2.1. Li–S batteries

Li–S batteries normally display a multi-step electrochemical redox reaction characterized by a two-plateau charge/discharge voltage profile in ether-based electrolytes [52]. As shown in **Fig. 3a**, during the discharge process, sulfur molecules (S_8) reacted with Li^+ to form a variety of soluble intermediates, *i.e.*, Li_2S_8, Li_2S_6, Li_2S_4, as reflected by the upper discharge plateau at ~2.3 V. Upon further lithiation, the long-chain polysulfides transformed into short-chain solid-state and insoluble polysulfides (*i.e.*, Li_2S) depositing on the electrode, corresponding to the lower discharge plateau at about 2.1 V. During the charge process, the reversible reactions occur with the conversion of solid-state intermediates to Li_2S_8 or S. Overall, the redox reactions of Li–S batteries undergo a solid to liquid to solid conversions during charge/discharge processes.

For comparison, carbonate electrolytes have been recognized to be incompatible with the cyclo-S_8 cathode because high-order polysulfides will undergo nucleophilic reactions with the carbonate solvent, leading to the failure of the battery after the first discharge [53]. Later on, researchers found that space-confined sulfur molecules $S_{2\text{-}4}$ and covalently bonded organic sulfur show a distinct charge-discharge profile with an inclined plateau in carbonate electrolytes [54, 55]. This phenomenon can be attributed to the absence of soluble polysulfides in the system, indicating a solid–solid conversion mechanism. In addition, the Li–S batteries equipped with a solid electrolyte also display a similar charge/discharge profile, resulting from the absence of polysulfide shuttle [56].

2.2. Li–Se batteries

As a congener of sulfur, Se has a similar lithiation/delithiation mechanism to that of S, and the theoretical volumetric capacity of Li–Se (3253 mAh cm^{-3}) is comparable to that of Li–S (3467 mAh cm^{-3}) although Li–Se has a much lower theoretical gravimetric capacity (675 mAh g^{-1}) than that of Li–S (1675 mAh g^{-1}) [57, 58]. Li–Se batteries also suffer from several pressing issues that prevent their practical application, including the dissolution of intermediate polyselenides and their ensuing shuttle effects in ether-based electrolytes, volume expansion of Se during cycles, and active loss [59, 60]. Li–Se batteries show different charge/discharge behaviors in ether-based and carbonate electrolytes. For Li–Se batteries operating in ether-based electrolytes, their working mechanisms are similar to those of Li–S batteries except for a slightly lower redox potential [61]. Typically, Se is initially reduced to Li_2Se_n ($n \geq 4$), then to Li_2Se_2, and finally to Li_2Se, reflected by the two discharge plateaus at ~2.1 and ~1.9 V, respectively. During charging, only one plateau is observed, which may be attributed to the potential overlapping (**Fig. 3b**) [62]. In this manner, Li–Se batteries share the same challenges as Li–S batteries when an ether-based electrolyte

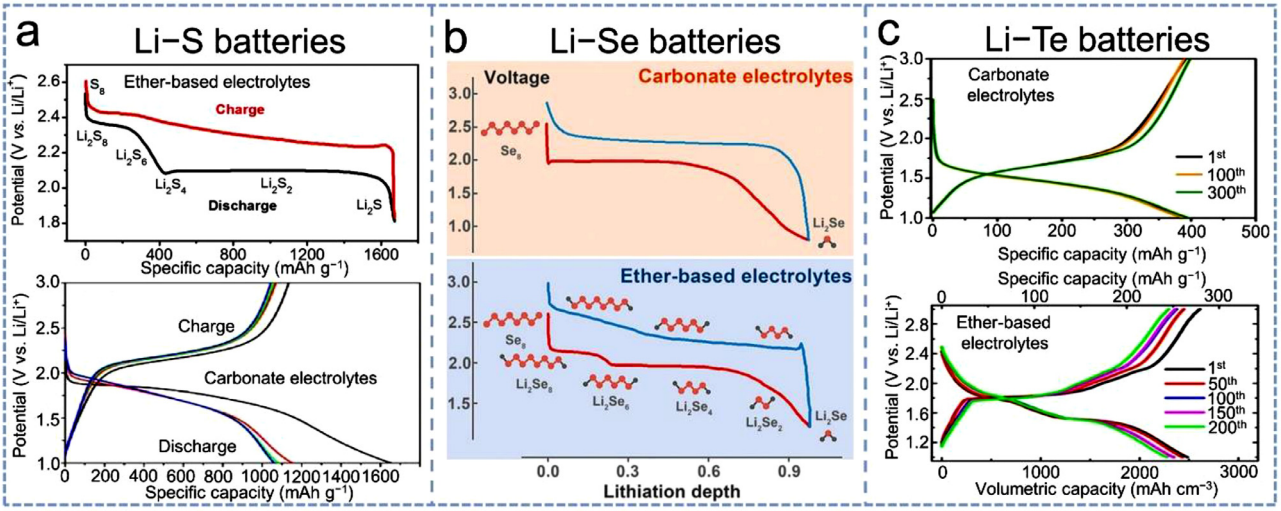

Fig. 3. Charge/discharge profiles of LCBs in carbonate-based and ether-based electrolytes liquid electrolyte. (a) Li–S batteries. Reproduced with permission [52]. Copyright 2016, Royal Society of Chemistry. Reproduced with permission [54]. Copyright 2015, American Chemical Society. (b) Li–Se batteries. Reproduced with permission [62]. Copyright 2021, Wiley-VCH. (c) Li–Te batteries. Reproduced with permission [67]. Copyright 2017, Elsevier. Reproduced with permission [14]. Copyright 2016, American Chemical Society.

is used. Notably, the Se cathodes are compatible with carbonate electrolytes, which is essentially different from cyclo-S_8 [62]. It is revealed that the Li–Se batteries experienced a single-phase transformation between Se and Li_2Se without soluble polyselenides, but unclear multi-step lithiation processes in carbonate electrolytes may exist [51, 63]. In addition, researchers also found the crystal structure of Se significantly affects the lithiation behaviors and electrochemical performance of Li–Se batteries [62]. Overall, the working mechanisms of the Se cathode in carbonate electrolytes remain controversial. Further advanced characterizations are desired to uncover the fundamental mechanisms of the Se cathodes in various electrolyte systems.

2.3. Li–Te batteries

As another chalcogen element, Te locates in the same group as S and Se elements, and Li–Te batteries have recently been studied. Similar to Li–S and Li–Se batteries, Li–Te batteries theoretically exhibit a high volumetric capacity (2558 mAh cm^{-3}) comparable to those of Li–S and Li–Se batteries. In terms of theoretical gravimetric capacity, Li–Te batteries possessed a smaller value (419 mAh g^{-1}) than those of Li–S (1675 mAh g^{-1}) and Li–Se (675 mAh g^{-1}) batteries because of the higher molecular weight of Te [64, 65]. Wang's and Yu's groups pioneered the use of Te cathode for rechargeable Li batteries in 2014 [22, 66]. It has been reported that the Li–Te redox reaction in carbonate electrolytes is a one-step phase transition process associated with the formation of Li_2Te (**Fig. 3c**) [67]. Since Te cathode is more compatible with the conventional carbonate electrolytes compared to the S_8 cathode, carbonate electrolytes have been widely used in Li–Te batteries. For comparison, in ether-based electrolytes, the Te cathode is firstly reduced into chain-like polytellurides and cyclo polytellurides ($Li_2[Te_n]^{2-}$, $2 < n \leq 8$) upon discharge, which are different from those in Li–S and Li–Se batteries (only chain-like polysulfides and polyselenides) [14]. The different structures of polytellurides may be associated with the unique chain-like structure of Te. After that, the polytellurides are reduced into the insoluble Li ditellurides and/or tellurides (Li_2Te_2 or Li_2Te). Upon charge, the insoluble Li ditellurides and/or tellurides are converted into Te. As a consequence, Te electrodes encounter the same shuttling issue as observed in S and Se electrodes in ether electrolytes. Note that the formation of polytellurides is still under debate. In addition, Te cathodes undergo a large volume expansion of approximately 200% during lithiation, thereby resulting in a rapid deterioration in long-term cyclic stability.

3. Multiple functions of CNTs in LCBs

Considering the pressing issues encountered in LCBs, CNTs play an important role in enhancing their electrochemical performance. First, CNTs have excellent electrical conductivity, rendering them an ideal conductive matrix for various chalcogen cathodes and Li anodes accompanied by a small polarization. In addition, the intrinsic large aspect ratio and large surface areas of CNTs would shorten the transport lengths for both electrons and ions and offer large electrode/electrolyte contact areas. Second, the surface chemistry of CNTs can be tailored to graft functional groups or/and support polar components. As such, the soluble intermediates can be anchored within the CNT frameworks, resulting in faster redox kinetics and less intermediate shuttling. In addition, the lithiophilicity of CNTs can be improved to promote uniform Li deposition through surface functionalization. Third, rational construction of micro-and nanostructures based on CNTs, such as CNT spheres, films, and sponges is still an effective approach to restrict the dissolution of intermediates in electrolytes by physical trapping. The pore size, volume, and shape of the CNT-based carbon matrix play significant roles in mitigating the crosstalk of intermediate shuttling. Fourth, the superb mechanical property of CNTs is capable to maintain the structural integrity of chalcogenide cathodes and Li anodes. As a typical example, CNT-based structures such as freestanding films enable the construction of a mechanically robust skeleton with high durability, showing huge potential in making flexible electronics (*e.g.*, implantable devices, touch screens, electronic skins, smart clothes, and stretchable displays). In the following section, we discuss these functions in detail.

(1) **Support of polar nanoparticles**. It is well known that metal compounds (*e.g.*, metal oxides, sulfide, nitrides, and phosphides) possessing high polarities are beneficial for suppressing shuttle effects [68, 69]. In addition, a few metal compounds exhibit significant catalytic activities for polychalcogenides, contributing to faster redox kinetics and less intermediate shuttling. However, the electronic conductivity of these polar materials is unsatisfactory, resulting in poor fast charge/discharge performance. Owing to the extraordinary electronic conductivity of CNTs, they can serve as a support for polar nanomaterials, thereby enabling the best utilization of both components. On one hand, polar particles anchored on CNTs prevent the

agglomeration of CNTs and have a higher utilization efficiency. On the other hand, metal compounds with poor electronic conductivity are integrated with highly conductive CNTs, boosting the electron transfer for redox reactions, especially at high currents.

(2) **Highly conductive pathways**. Chalcogen cathodes should display good electronic conductivity to facilitate fast electron transfer during charge/discharge cycles, which is a prerequisite for achieving good electrochemical performance. However, the electrical conductivity of chalcogen elements, especially sulfur, is not significant. As mentioned previously, CNTs have excellent electrical conductivity, rendering them an ideal conductive matrix for chalcogen cathodes. Initially, sulfur was simply mixed with CNTs to serve as the sulfur cathode. Although this simple treatment can enhance the initial reversible capacity, the improvement is not significant because of the poor ionic transport and large volume variation during electrochemical reactions. Considering the large aspect ratio and high surface area of CNTs, the rational design of three-dimensional (3D) structures would ensure shorter transport lengths for both electrons and ions, larger electrode/electrolyte contact area, and better accommodation of the strains arising from conversion reactions. These characteristics should be optimized to achieve better performance.

(3) **Restriction of intermediate dissolution and shuttling**. The confinement of intermediates through a physical trap is another important function of CNTs in LCBs. Encapsulating elemental chalcogen in the pores and voids of CNTs is an ideal solution to mitigate the notorious shuttle effects of intermediate products, but the strong capillary effect of CNTs limits its realization [70, 71]. Although the interaction between bare CNTs and intermediates is not strong, the design of various micro-and nanostructures based on CNTs, such as CNT spheres, films, and sponges can restrict the dissolution of intermediates. More importantly, heteroatom doping and surface modification of CNTs have been proven to facilitate stronger adsorption of soluble intermediates and stabilize electrochemical reactions, owing to which these methods are gaining significant popularity in the fabrication of chalcogen cathodes.

(4) **Enhancement of cathode structural stability**. As the conversion reactions always induce large volume variations, the structural damage and collapse of chalcogen cathodes inevitably deteriorate the electrochemical performance. The sp^2 carbon–carbon bonding in CNTs results in exceptional mechanical properties. For example, it has been reported that the Youth's modulus and tensile strength of CNTs are 1.2 TPa and 50–200 GPa, respectively [34]. Therefore, the construction of chalcogen cathodes using CNTs can dissipate the internal stress arising from Li-ion insertion/extraction and maintain superior structural integrity. In addition to their attractive physicochemical properties, CNTs with a large length-to-width ratio can form various flexible substrates using diverse methods, including vacuum filtration, layer-by-layer stacking, rolling, and blade casting. After introducing chalcogen-based active materials, the resultant CNT-based cathodes can work well under bending, stretching, and twining. The high flexibility of CNTs enabled the utilization of LCBs in flexible electronics.

(5) **Suppression of the Li dendrite growth**. The high reactivity and large volume change of Li anode have led to severe dendrite growth during repeated plating/stripping cycles, especially under high current densities. Reducing local current density, introducing nucleation sides, and designing a stable solid-electrolyte interface (SEI) are well-accepted methods to alleviate this issue. CNTs, having very high electrical conductivity, large surface area, and tunable surface features, are promising materials for suppressing Li dendrites. In addition, considering the free-standing feature and mechanical properties, it is believed that the CNT-based Li hosts may attract more attention in the field of flexible electronics.

CNTs thus display multiple functions in enhancing the electrochemical performance of LCBs. Owing to the diverse physicochemical properties of elemental chalcogens, the applications of CNTs in LCBs may differ slightly. First, owing to the insulting nature of S, sufficient CNTs are needed to confer S cathodes with satisfying electrical conductivity. In contrast, Se and Te endow much higher electrical conductivities, thus fewer CNTs should be added to ensure a higher capacity. Second, concerning the fabrication of chalcogen electrodes, most S and Se electrodes have been fabricated using a melt infiltration method due to the low melting point of S and Se. For comparison, Te has a much higher melting point of ~450°C, and thereby many Te/CNT electrodes are mainly prepared by ball milling, vacuum infiltration, and sealed tube method. Third, S_8 is inactive in carbonate electrolytes and suffers polysulfide shuttling in ether electrolytes, while Se and Te elements are more compatible with carbonate electrolytes. As a result, CNT frameworks with suitable micropores, functionally polar components, excellent electrical conductivity, and good structural stability should be explored when using carbonate electrolytes. For the Se and Te cathodes operating in carbonate electrolytes, the main roles of CNTs are to accommodate the volume changes of Se and Te cathodes and facilitate electron and ion transportation.

4. CNT-based hosts for chalcogen cathodes

Confining chalcogen elements in various hosts is a simple yet effective strategy to achieve high chalcogen utilization. An ideal host should meet the following requirements: (i) high electrical conductivity to allow the fast speed electron transfer, (ii) stable physical/chemical properties against electrolytes, (iii) high pore volume to realize high chalcogen loading, (iv) special micro-and nanostructures to confine the chalcogen species, thereby avoiding their leakage, and (v) outstanding structural stability to sustain long-term electrochemical tests. In this section, we aim to overview the advanced CNT architectures for different chalcogen hosts and analyze the critical roles of CNTs thereof.

4.1. CNT-based S hosts

The S cathode is an important component of Li–S batteries, which significantly affect the electrochemical performance. Elemental sulfur is an insulator and the generated intermediate polysulfides also possess low electrical conductivity, resulting in sluggish reaction kinetics. As an outstanding conductive agent, the addition of CNTs in sulfur cathodes can effectively enhance the conductivity of the entire sulfur cathode and the utilization ratio of active sulfur species, thereby improving the final electrochemical performance (Table 2). Moreover, owing to the high length-to-width ratio of CNTs, their presence in sulfur cathodes strengthens the structural integrity of the cathodes, enabling better electrochemical performance, especially long-term cyclic stability. However, although many related works on the utilizations of CNTs in Li–S batteries have been reported, these batteries are commonly evaluated with the coin cell form, and few works have been demonstrated in punch cells and/or cable-like format (Table 3).

4.1.1. Pristine CNT architectures

Pure CNTs can be used to construct sulfur composite cathodes for Li–S batteries. However, owing to the high capillary force originating from CNTs, it is extremely difficult to encapsulate elemental sulfur in the internal voids of the CNTs. Depositing elemental sulfur onto the CNT surface is a simple strategy for ameliorating Li–S chemistry [72-79]. As a representative study, Zhang et al. prepared a sulfur cathode composed of multi-walled CNTs (MWCNTs) and sulfur through a typical melt-infiltration strategy, for Li–S batteries [72]. The MWCNTs with high electrical conductivity and good distributions enabled a fast electron transfer and efficient electrical contact, and the as-achieved electrode demonstrated a specific capacity of 740 mAh g^{-1} at 2.0 C and a relatively slow capacity decay for 140 cycles. However, the energy density of the sulfur cathode is low; hence, it cannot meet the requirements for practical applications. One major reason for this is that the sulfur

Table 2
Electrochemical performance comparison of Li–S batteries (coin cell) with CNT-based hosts.

Sulfur cathodes	Morphology	Methods	Areal sulfur loading (mg cm^{-2})/electrode area (cm^2)	Sulfur content (wt.%)	Electrolyte/S ratio(uL/mg)	Rate capability	Cyclic performance	Ref.
CNT/S	Tubular structure	As received	0.32	50	–	1288 mAh g^{-1} at 0.2 C	Capacity fading rate of 0.33% over 100 cycles	[75]
MWCNT/S	Clew-like structure	MOF-derived	0.7-1.7/1.54	70	~7.65	640 mAh g^{-1} at 2.0 C	Capacity fading rate of 0.053% over 1000 cycles	[35]
MWCNT/S	3D framework	Physical mixing	2.0	60	140	~720 mAh g^{-1} at 1.0 C	~580 mAh g^{-1} after 100 cycles at 0.2 C	[109]
CNT/S	3D forest	CVD	2.0	59~63	–	–	812 mAh g^{-1} after 200 cycles at 0.4 A g^{-1}	[126]
CNT@CNT/S	Tube in tube	Template combined with *in situ* growth	2.0	85.2	30	1274 mAh g^{-1} at 2.0 C	954 mAh g^{-1} after 150 cycles at 5.0 C	[132]
CNT microsphere/S	Porous structure	Solution drying	1.0	70	–	~1000 mAh g^{-1} at 2.0 C	901 mAh g^{-1} after 100 cycles at 0.5 C	[113]
Graphene/CNT/S	Hierarchical porous structure	CVD	–	~90	–	~620 mAh g^{-1} at 5.0 C	650 mAh g^{-1} after 100 cycles at 5.0 C	[43]
Graphene/CNT/S	3D aerogel structure	Freeze-drying	2.46	50	16.3	1286 mAh g^{-1} at 0.2 C	Capacity fading rate of 0.06% over 500 cycles at 2.0 C	[143]
Graphene/CNT/porous carbon/S	Hierarchical porous structure	CVD	–	77	–	809 mAh g^{-1} at 10 C	877 mAh g^{-1} after 150 cycles at 1.0 C	[169]
Co-CNT/S	Yolk-shell bamboo-like structure	Spray pyrolysis combined with reduction	1.84/1.54	64	–	752 mAh g^{-1} at 2.0 C	700.2 mAh g^{-1} after 400 cycles at 1.0 C	[192]
TiO_2/CNT/S	Porous hollow structure	Hydrothermal method	3.6-4.0	56	–	888 mAh g^{-1} at 7.0 C	Capacity retention of 90% after 100 cycles at 5.0 C	[205]
1T-ReS_2/CNT/S	Hierarchical porous structure	Self-assembly	4.8	78	4.5	839 mAh g^{-1} at 2.0 C	Capacity retention of 77.1% after 1000 cycles at 1.0 C	[225]
Carbon/CNT/CoP	Porous structure	Solution method combined with thermal annealing	0.7/0.95	70	57.1	527.7 mAh g^{-1} at 3.0 C	Capacity fading rate of 0.076% over 200 cycles at 0.2 C	[36]
CNT/graphene-S-Al_3Ni_2	3D porous structure	Ultrasonication followed by annealing	3.3	65	62.5	812 mAh g^{-1} at 3.0 C	Capacity fading rate of 0.055% over 800 cycles at 1.0 C	[246]
Amine modified CNT/S	Tubular structure	Polymerization	1.2	70	32.8	~310 mAh g^{-1} at 4.0 C	Stable for 100 cycles at 2.0 C	[45]
MOF/CNT/S	Hierarchical porous structure	CVD	3.2-3.5	64	20	840 mAh g^{-1} at 1.0 C	750 mAh g^{-1} after 500 cycles at 1.0 C	[252]

Table 3
Electrochemical performance comparison of Li–S batteries (punch and cable-like cells) with CNT-based materials.

Sulfur cathodes	Morphology	Areal sulfur loading (mg cm^{-2})/electrode area (cm^2)	Sulfur content (wt.%)	Electrolyte/S ratio(uL/mg)	Electrochemical performance	Ref.
CNTs aerogel/S	Porous structure	4.89/4.8	43	7.8	8.8 mAh cm^{-2} after 20 cycles at 0.1 C	[104]
CNT film/S	Porous structure	–/5	60	60	822 mAh g^{-1} after 100 cycles at 0.2 C	[128]
Gra-CNTs/S (cable-like)	Porous structure	2.0/0.071	45	–	volumetric capacity and volumetric energy density of 0.44 × 106 mAh L^{-1} and 917 Wh L^{-1}, respectively	[144]
Co-N-CNTs/carbon fiber paper/S	Hierarchical porous structure	5.0/10	~40	10	4.823 mAh cm^{-2} after 150 cycles at 0.2 C	[196]
VO_x/SWCNTs	Porous hollow structure	1.5/6	67	–	Stable under bending and unbending states for 24 cycles	[200]
MgO/carbon foam/CNTs-S	Porous structure	6.6	78	–	Stable under bending and unbending states	[206]
ReS_2/CNTs/S	Hierarchical porous structure	4.8/38.96	78	4.5	Capacity fade rate of 0.22% per cycle for 131 cycles	[225]

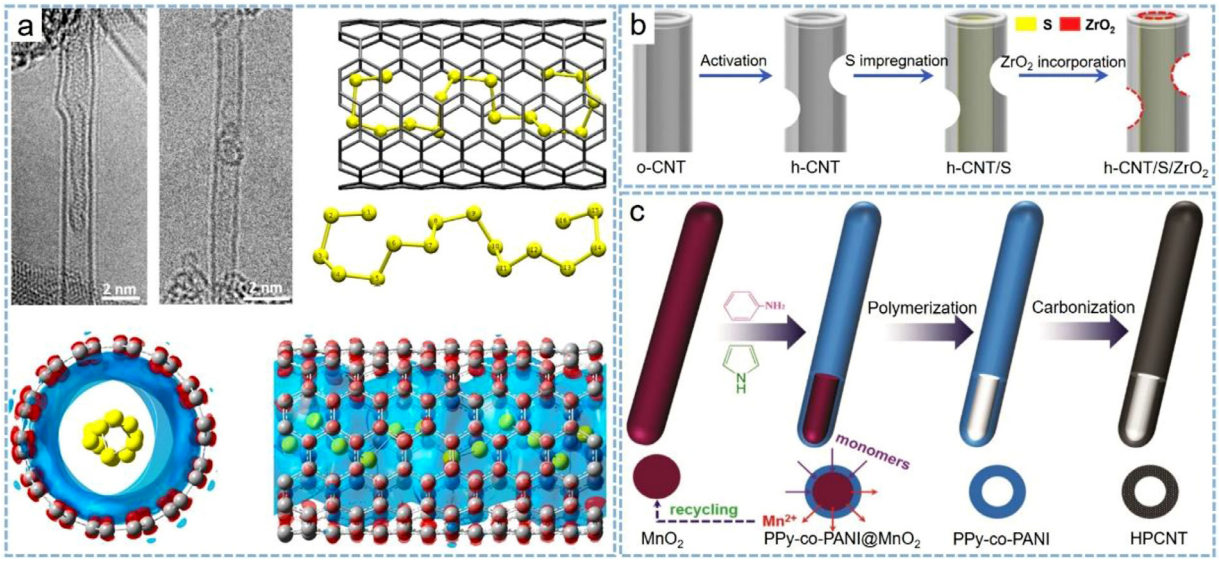

Fig. 4. (a) Narrow-diameter CNTs for use as the sulfur host in Li–S batteries. Reproduced with permission [80]. Copyright 2018, American Chemical Society. (b) Porous holey CNFs as the S host in Li–S batteries. Reproduced with permission [82]. Copyright 2015, Wiley-VCH. (c) Hierarchical porous CNTs as the sulfur host in Li–S batteries. Reproduced with permission [84]. Copyright 2018, Wiley-VCH.

content in the composite cathode is too low. To resolve this issue, Li et al. synthesized sulfurized CNTs with a high sulfur content (68 wt%) by functionalizing CNTs using a solvent exchange method to graft sulfur chains onto the surface of the CNTs [73]. Such a method ensured the thoroughly loading of sulfur chains with stable interactions, and the as-fabricated Li–S batteries demonstrated excellent cyclic stability for 1300 cycles and a high rate capability of up to 2 C, along with Coulombic efficiencies (CEs) above 95.5%. As another example, Hangen et al. grew CNT arrays on a Ni current collector using a CVD approach [74]. Owing to the abundant pores and voids, high length, and high conductivity, the sulfur content was as high as 90 wt%, and the areal sulfur loading was more than three times higher than that in the regular sulfur electrodes prepared by slurry coating. Moreover, Zhu et al. fabricated a CNT/S composite cathode and investigated the impact of areal sulfur loading on the final electrochemical performance [75]. The areal sulfur loading was found to significantly affect the specific capacity and energy density of Li–S batteries. When the sulfur loading is extremely high, the electrochemical performance is restricted by the effective contact between the active sulfur species and the electrolyte.

Encapsulation of elemental sulfur in CNTs is a recognized strategy for improving the electrochemical performance of sulfur cathodes. Guo et al. successfully confined the electrochemical reactions of sulfur in two types of narrow-diameter single-walled CNTs (SWCNTs) with different diameters (1.55 ± 0.1 and 1.0 ± 0.2 nm)[80], as shown in **Fig. 4a**. The sulfur cathode was synthesized by exposing the CNTs to saturated sulfur vapor at 600°C for two days. The sulfur contents in the composites were measured to be approximately 4.57 and 11.33 wt%, respectively. The electrochemical properties could be significantly modulated by varying the diameter of SWCNTs because a suitable diameter of SWCNTs can restrict the dissolution and shuttle of intermediates. Despite the direct encapsulation of elemental sulfur in CNTs, liquid-state long-chain polysulfides can be fully impregnated into CNTs. For instance, Jeong et al. synthesized a flexible sulfur electrode composed of a Li_2S_6 solution-impregnated CNT film with a conductive 3D skeleton structure [81]. Owing to the excellent flexibility and superior electrical conductivity of the CNT film, the constructed Li–S batteries can be applied to flexible electronic devices. A high specific capacity of 975 mAh g^{-1} at 0.5 C and stable cyclic performance for 500 cycles were obtained. More impressively, by using a polysulfide solution as the active sulfur species for making sulfur cathodes, the utilization ratio of sulfur species can be significantly enhanced.

Porous CNTs have been carefully designed and constructed to restrict the dissolution and shuttle effects of polysulfides [82-93]. The pores of CNTs allow the effective contact of active sulfur with electrolytes and enable the fast transport of Li^+, thus improving the electrochemical performance, especially the high-rate capability. This has been verified by

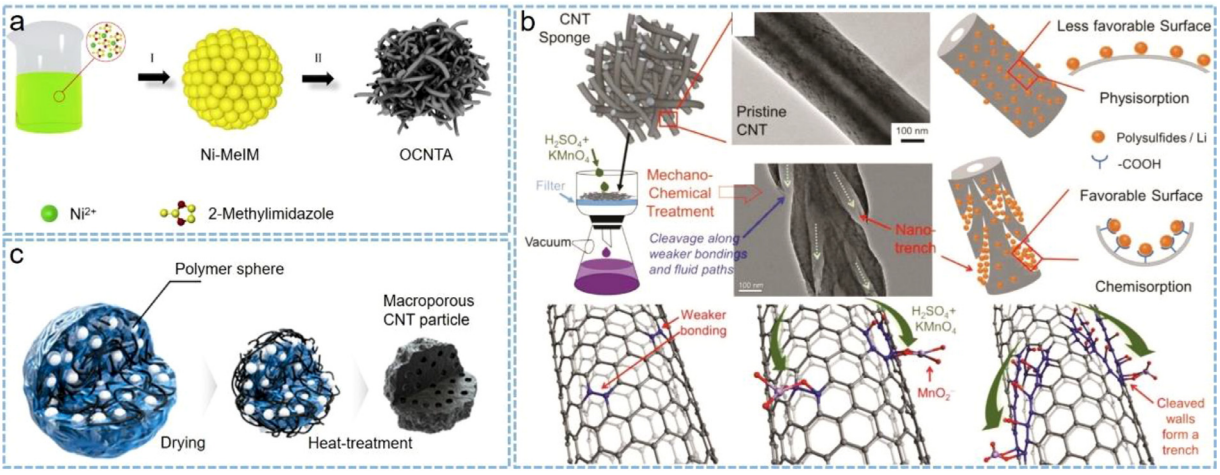

Fig. 5. (a) Schematic of the synthesis of multi-walled CNT aggregates. Reproduced with permission [35]. Copyright 2017, Elsevier. (b) Schematic of the synthesis and utilization of CNTs in Li–S batteries. Reproduced with permission [49]. Copyright 2018, Wiley-VCH. (c) Schematic of the macroporous CNT particle. Reproduced with permission [113]. Copyright 2018, American Chemical Society.

Zhou et al., who fabricated porous, holey CNTs through the chemical activation method as the sulfur host for Li–S batteries (Fig. 4b) [82]. The special structure of CNTs allowed the high sulfur loading in sulfur composite, and thus the as-fabricated CNT/S cathode exhibited a high-rate performance (424 mAh g^{-1} at 6 C). Yang *et al.* prepared a nacre-like CNT sheet with sulfur compactly embedded into the CNT structure via the unidirectional freeze-drying approach [83]. The nacre-like structure enabled the high electrode stability with fast electrolyte penetration, and the Li–S batteries fabricated using this sheet demonstrated a high specific capacity of 1236 mAh g^{-1} at 0.1 C and maintained at 498 mAh g^{-1} at 2 C with an areal sulfur loading of 5.0 mg cm^{-2}. After increasing the sulfur loading to 10 mg cm^{-2}, the areal capacity reached 11.0 mAh cm^{-2}. Kang et al. selected a completely green and straightforward strategy to synthesize hierarchical porous CNTs without the assistance of templates and activation procedures [84]. The as-prepared CNTs (Fig. 4c) possessed a hierarchical micro/meso/macroporous structure with a specific surface area as high as 1419 m^2 g^{-1}. When employed as the sulfur host, an impressive rate performance (391 mAh g^{-1} at 4 C) and stable long-term cyclic stability (947 mAh g^{-1} after 100 cycles at 0.2 C) were attained with the very high sulfur content.

The abovementioned pure CNTs can indeed enhance the electrochemical performance of Li–S batteries; however, the enhancement is not significant. Recently, surface-functionalized CNTs have been adopted as sulfur hosts [35, 44, 94-102]. It is well known that heteroatom doping of carbonaceous materials has two apparent benefits: (i) enhancing the electrical conductivity of the entire sulfur cathode and (ii) strengthening the capability for adsorbing intermediate polysulfides. Both aspects contribute to improving electrochemical performance. For example, Zuo et al. prepared MOF-derived screw-like N-doped MWCNTs as hosts for Li–S batteries [35]. The N-doped MWCNTs possess 3D conductive and interconnected open-ended structures (**Fig. 5a**) and demonstrated an outstanding capability to encapsulate elemental sulfur and immobilize intermediate polysulfides. As a result, the assembled Li–S batteries exhibited an impressive electrochemical performance with ultra-long cyclic stability over 1000 cycles, accompanied by a low capacity decay of 0.053% per cycle. To further enhance the chemical adsorption of intermediate polysulfides by the host, Tao et al. fabricated boron and oxygen co-doped MWCNTs to serve as the sulfur host via chemical doping strategy [44]. Both theoretical and experimental results confirmed that boron and oxygen doping significantly enhanced the adsorption of polysulfides and promoted fast electron transfer, thereby improving the cyclic stability and rate capability.

CNTs can form various micro-and nanostructures, which can maximize the utilization of sulfur in Li–S batteries. 3D CNT architectures are popular as sulfur skeletons for Li–S batteries [49, 103-111], as they provide well-established conductive networks and large voids/spaces for loading sulfur and restricting the dissolution/shuttling of generated polysulfides. Yu et al. fabricated a 3D free-standing porous CNT sponge for Li–S batteries via mechanochemical treatment (Fig. 5b) [49]. Benefiting from the reduced interfacial resistance and charge transfer resistance, the as-fabricated sulfur cathodes exhibited the highest areal capacity ever reported (13.3 mAh cm^{-2}). Moreover, a lightweight, free-standing interconnected 3D CNT foam was prepared via simple one-step spray pyrolysis, as a flexible host for Li–S batteries [103]. The CNT foam ensured high structural integrity and preeminent electron transfer pathways. With a high areal sulfur loading of 7.1 mg cm^{-2}, the sulfur utilization of the total electrode was up to 72%, and the areal capacity was approximately 9 mAh cm^{-2}. The abovementioned electrochemical performance, including the rate capability and cyclic performance, is better than those of most of the reported CNT-based sulfur cathodes. In addition, Wang et al. fabricated a mesoporous CNT aerogel host to obtain high-areal-capacity Li–S batteries via capillary action [104]. The 3D porous structure of the CNT aerogel offers high-speed electron transfer pathways and rapid ion transport channels, whereas the 3D CNT structure itself allows the thorough wetting of the sulfur host with the electrolyte. Consequently, the as-obtained Li–S batteries exhibited an ultrahigh areal capacity of 22.9 mAh cm^{-2} at a high sulfur loading of approximately ~20 mg cm^{-2}. In addition, the 3D CNT aerogel demonstrated potential for application in punch cells.

CNT spheres have been considered as an ideal sulfur host because of the existence of pores, voids, conductive networks, etc. These merits of 3D CNT spheres contributed to the improved electrochemical performance of assembled Li–S batteries [112-117]. For instance, Han et al. proposed a high N-doped CNT microsphere as the sulfur host for Li–S batteries through a simple spray drying and one-step pyrolysis method [112]. The interconnected CNTs with surface modifications offer highly conductive electron/ion channels, block polysulfide shuttling, and ensure fast sulfur infiltration. These synergistic effects contributed to a significantly improved electrochemical performance in terms of high rate capability and stable cyclic performance. Furthermore, porous CNT spheres achieved ultrahigh areal sulfur loading for Li–S batteries (Fig. 5c). As reported by Moon et al., the sulfur content was as high as 70 wt% without the attachment of a sulfur residue, because of the existence of abundant pores and voids [113]. The as-fabricated sulfur

cathode demonstrated a high specific capacity of 1343 mAh g^{-1} at 0.2 C and a high rate capability with a capacity retention of 74% at 2.0 C.

The CNT array is another type of 3D architecture that effectively encapsulates elemental sulfur in Li–S batteries. 3D CNT arrays possess hierarchical and porous structures and enable the prevention of polysulfide dissolution and shuttling in electrolytes [118, 119]. Notably, 3D CNT arrays are commonly synthesized by various template approaches; thus, the porosity and thickness of the shells can be tuned well. As a pioneering study, Wang et al. fabricated 3D CNT arrays using a commercial anodic aluminum oxide (AAO) membrane as a template [118]. Elemental sulfur can be infused into the pores and voids of the 3D CNT arrays via a typical melt-diffusion method. More importantly, the electrolyte can reach the site where liquid elemental sulfur can diffuse, ensuring effective contact between elemental sulfur and the electrolyte. High cyclic stability and CE values were achieved when these arrays were used as sulfur cathodes in Li–S batteries. Wei et al. fabricated similar structures composed of hierarchical tree-like CNT architectures through in situ CVD self-assembly [119]. Catalysts (Fe nanoparticles) were utilized to catalyze the direct growth of SWCNTs and MWCNTs, and these two types of CNTs self-organized into a tree-like architecture because of the decreased interfacial adhesion energy. Such a structure ensured good electron transport networks and stable structural integrity. The Li–S batteries fabricated using it demonstrated an impressive rate performance and long-term cyclic stability (530 mAh g^{-1} after 450 cycles at 1.0 C). Apart from the abovementioned CNT arrays, other types of CNT arrays have demonstrated similar improved electrochemical results [120-125].

Furthermore, other CNT-based architectures, including CNT forest [126], CNT paper/film [127-129], CNT networks [130, 131], and CNTs inside CNTs [132, 133], have been designed and constructed to serve as sulfur hosts for Li–S batteries. As a fundamental study on flexible Li–S batteries, Zhang et al. fabricated a hierarchical free-standing CNT paper electrode with an ultrahigh sulfur loading mass (6.3 mg cm^{-2}) via the bottom-up synthesis strategy [127]. In this study, short MWCNTs were utilized as a short-range electrically conductive skeleton for sulfur accommodation, whereas long CNTs served as a long-range conductive network and interconnected mechanical framework. Consequently, a high areal capacity of 6.2 mAh cm^{-2}, with 60% sulfur utilization and a capacity decay of 0.20% per cycle was successfully achieved. Electrochemical results indicative of practical feasibility were obtained by stacking several layers of sulfur electrode films. Moreover, Wang et al. reported an ingenious CNT-based tube-in-tube architecture, composed of small-sized CNTs inside large CNTs, through the typical self-sacrificing AAO template method [132]. This intriguing structure with a large number of voids and pores efficiently resolves the critical issues including poor electrical conductivity, dissolution/shuttling of polysulfides, and large volume expansion during cycles. With an extremely high sulfur content (85.2 wt%), the sulfur cathode exhibited a high specific capacity of 163 mAh g^{-1} at 0.1 C, and high cyclic stability with a specific capacity of 954 mAh g^{-1} after 150 cycles at 5 C.

4.1.2. CNTs hybridized with carbon matrices

To enhance structural integrity, CNTs need to be hybridized with other carbon matrices, such as graphene, reduced graphene oxide (rGO), carbon nanofibers (CNFs), and porous carbon. Various architectures can be formed by the hybridization of CNTs with other carbon matrices, which can greatly resolve the issues encountered by sulfur cathodes.

Graphene and rGO: Owing to its large specific surface area and good mechanical properties, graphene has been extensively hybridized with CNTs. The interaction between CNTs and graphene offers several structural advantages, including (i) a large specific surface area and high pore volume to encapsulate elemental sulfur; (ii) intact electrical conductive networks for promoting electron transfer; (iii) plenty of pores/voids to accommodate the volume expansion of sulfur during cycles; and (iv) numerous channels generated to allow thorough electrolyte penetration, thereby enabling effective contact between active sulfur species and the electrolyte. The synergistic effects of these merits result in a significant enhancement in electrochemical performance in Li–S batteries. Commercially available graphene sheets can be mixed directly with CNTs, and vacuum filtration is the most widely used approach to fabricate graphene/CNTs [134, 135]. For example, Wu et al. fabricated a lightweight and binder-free sulfur host comprising lignin fibers@CNTs/graphene composite via a vacuum filtrated method [134]. Benefiting from a sandwich-like structure with CNTs stacked between graphene sheets, the as-fabricated sulfur cathode exhibited a high specific capacity of 1632 mAh g^{-1} at 0.1 C and long-term cyclic stability of 987 mAh g^{-1} after 500 cycles at 1.0 C. Furthermore, a remarkable electrochemical performance was obtained using similar CNT/graphene architecture [135].

An in situ growth method can also produce graphene sheets that are then mixed with CNTs. Compared with the physical mixing methods, this approach strengthens the interaction between the CNTs and graphene sheets, thus enhancing the overall structural integrity. With Ni foam serving as the catalyst and glucose and dicyandiamide as the carbon and nitrogen sources, Yu et al. prepared a well-interconnected N-rich CNTs-graphene hybrid with a 3D architecture using a solid-state growth strategy (**Fig. 6a**) [136]. This intriguing framework with CNTs grown on both graphene sides enabled high structural stability, fast electron transfer, and good intermediate restriction during cycles. After the sulfur infiltration process, the sulfur cathode displayed a high reversible capacity of 1314 mAh g^{-1} at 0.1 C and a high capacity retention of 97% after 200 cycles at 2.0 C. Moreover, to improve the structural stability, Wei et al. synthesized an N-doped aligned CNT/graphene sandwich structure via a catalytic growth method [40]. Owing to their high surface area, large pore volume, highly conductive skeletons, abundant interfacial adsorption sites (Fig. 6b), and N-doping feature, the assembled Li–S batteries presented outstanding electrochemical results with a high specific capacity of 1152 mAh g^{-1} at 1.0 C and significant cyclic stability (880 mAh g^{-1} after 880 cycles). The binding of SWCNTs among graphene planes through covalent C–C bonds is expected to produce extraordinary physical properties. Therefore, Wei et al. fabricated an intriguing structure comprising a graphene/SWCNTs hybrid to encapsulate elemental sulfur through a solid-state CVD method [43]. The sulfur cathode delivered an excellent electrochemical performance (a high specific capacity of 928 mAh g^{-1} at 1.0 C and 650 mAh g^{-1} after 100 cycles at 5.0 C with CEs of approximately 92%). Furthermore, other graphene matrices, such as graphene foam [137], graphene networks [138-140], graphene spheres [141], graphene films [142], have been developed for hybridizing with CNTs, and such structures have facilitated improvements in Li–S batteries.

In addition to the direct introduction of graphene sheets into the design and preparation of CNT/graphene composites, rGO has been employed because it possesses numerous oxygen-containing functional groups, which are helpful for the chemical adsorption of intermediate polysulfides and further restrict their shuttle effects. Moreover, structural defects could be generated during the reduction processes, benefiting electrolyte diffusion and penetration as well as lowering the interfacial resistance between the sulfur host and electrolyte. For instance, Wu et al. fabricated a 3D free-standing graphene/CNT aerogel for serving as a 3D sulfur host, *via* a solution-based synthesis method followed by a light heating process [143]. The architecture possessed an interconnected conductive framework, large surface area, and high pore volume (Fig. 6c), which enabled a fast electron transfer and ultrahigh sulfur loading. The free-standing graphene/CNT/S aerogel showed a high specific capacity of 1286 mAh g^{-1} at 0.2 C, and a low capacity decay of 0.06% per cycle over 500 cycles at 2.0 C. Similarly, Kim et al. constructed an ultralight and flexible sulfur host comprising of CNTs intercalated uniformly between the amphiphilic GO sheets through a one-step electrospinning method [144]. Importantly, the oxygen-containing groups on the rGO surface adsorbed the intermediates through chemical interactions, thereby restricting the leakage and shuttle effects of polysulfides. At a moderate sulfur loading mass ranging from 0.028 to 0.13 mg cm^{-2}, the cable-like Li–S batteries exhibited a high capacity of 1255

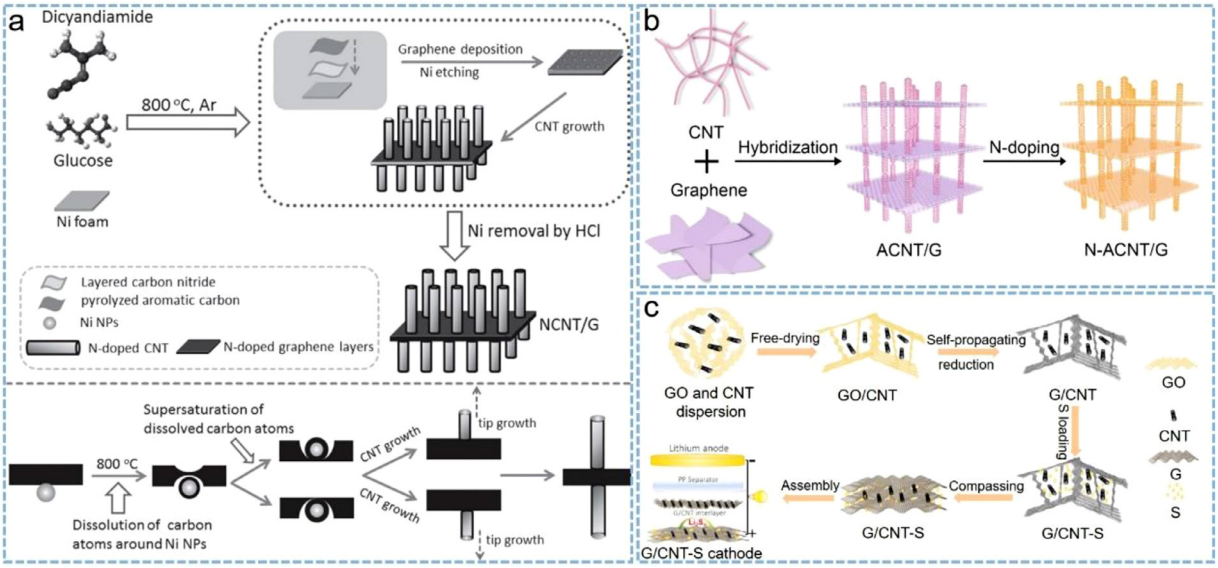

Fig. 6. (a) Schematic of the synthesis of N-CNTs/graphene hybrid. Reproduced with permission [136]. Copyright 2016, Wiley-VCH. (b) Schematic of the N-doped aligned CNTs/graphene. Reproduced with permission [40]. Copyright 2014, Wiley-VCH. (c) Schematic of the synthesis of CNTs/graphene/S composite. Reproduced with permission [143]. Copyright 2019, Elsevier.

mAh g^{-1} at 0.05 C, corresponding to a high areal capacity of 2.49 mAh cm^{-2}. Moreover, the cable-like Li–S batteries demonstrated outstanding flexibility under repeated bending-unbending operations. To improve the utilization efficiency of sulfur species and the ability to withstand volume changes during cycles, solid-state polysulfides, *e.g.*, Li_2S, can be used directly as the active component. Wu et al. fabricated a practical Li_2S cathode consisting of a Li_2S/FWCNTs@rGO nanobundle forest for Li–S batteries through a fast freeze-drying method [145]. In such a structure, FWCNTs serve as axial shafts to direct the structure, Li_2S acts as the internal active material, and rGO sheets supply contact to reduce the resistance of Li_2S toward the electrolyte and adsorb the intermediates. Consequently, the assembled Li–S batteries demonstrated a high discharge capacity of 868 mAh g^{-1} at 0.2 C even after 300 cycles and a high rate capability with a specific capacity of 433 mAh g^{-1} at 10 C. Furthermore, other rGO/CNT-based architectures of various morphologies, including microspheres [146], films [147], aerogels [148, 149], sponges [150], and networks [151-155], have been fabricated for use as sulfur hosts in high-performance Li–S batteries.

CNFs: CNFs with a high aspect ratio, outstanding mechanical properties, high electrical conductivity, and excellent structural integrity, have been considered superior carbon skeletons for energy storage and conversion systems [156, 157]. The combination of CNFs and CNTs can take full advantage of their benefits and overcome the problems of sulfur cathodes for Li–S batteries [158-161]. For example, Gao et al. fabricated a free-standing porous CNF/CNT film where CNTs were decorated on CNF to immobilize sulfur in Li–S batteries via the templated method [158]. As shown in **Fig. 7a**, the interconnected structure facilitates high sulfur loading, good electrolyte diffusion and penetration, strong chemical adsorption of intermediate polysulfides, and reliable accommodation of volume expansion during electrochemical cycles. The stacked S/CNF/CNT cathodes exhibited a high areal capacity of 13.5 mAh cm^{-2}, along with an extremely high sulfur loading of 12 mg cm^{-2}. To further enhance the sulfur content in the sulfur composites, pores and voids were deliberately designed in the CNF/CNT architectures. For instance, Zhou et al. fabricated porous hollow CNT/CNFs (CNTs grown on CNF surfaces) through a CVD method for use as a sulfur host in Li–S batteries [159]. In such a structure, amorphous elemental sulfur was encapsulated in the pores/voids of hollow CNFs enclosed by conductive CNTs, thereby improving the electrical contact with the current collector. The resulting sulfur cathodes with a sulfur content of 55 wt% showed a high reversible capacity of 572 mAh g^{-1} at 5 C and retained approximately 430 mAh g^{-1} after 200 cycles at 5 C.

Porous carbon materials: Porous carbon materials can act alone as sulfur hosts, because of their high specific surface areas, large pore volumes, and good capability to prevent polysulfide dissolution and thereby, shuttle effects [162, 163]. However, porous carbon materials normally exhibit poor electrical conductivity compared to CNTs and graphene, thus affecting the rate performance of Li–S batteries. CNTs hybridized with porous carbon materials can resolve these issues by providing an integrated conductive network for electron transfer and additional physical confinement of polysulfides [164-180]. Wang et al. fabricated a 3D conductive framework of close coverage with seamless junctions of CNTs using N-doped porous carbon through a template method (Fig. 7b) [164]. This architecture inherits and strengthens the advantages of both the high electrical conductivity of CNTs and the strong polysulfide trapping capability of N-doped porous carbon. Consequently, the sulfur cathodes exhibited a high reversible capacity of 1065 mAh g^{-1} at 0.5 C and impressive capacity retention of 817 mAh g^{-1} after 300 cycles. To enhance the restriction of intermediate polysulfide dissolution and shuttle effects, Wang et al. doped heteroatoms (B and O) into a porous carbon matrix (Fig. 7c) that was attached to CNTs via a simple organic condensation reaction [165]. It was demonstrated that the hybrids promoted the chemical adsorption and conversion of intermediate polysulfides through chemical bonding between the heteroatoms and polysulfides. Furthermore, a large specific capacity of 1077 mAh g^{-1} was obtained after 200 cycles at 0.2 C. When the current was increased to 1.0 C, a capacity of 794 mAh g^{-1} was maintained after 500 cycles. Although elemental sulfur is conventionally used as the active component, polysulfides can also be adopted as the active species in Li–S batteries. Zhang et al. synthesized a porous carbon-coated Li_2S-CNT composite for use as a sulfur cathode by heating carbon disulfide and a Li hydride-CNT mixture at a moderate temperature (250°C) [166]. The Li_2S@porous carbon particles were interconnected by a 3D CNT network, and the sulfur cathodes showed a reasonable electrochemical performance (a specific capacity of 573 mAh g^{-1} at 1.0 A g^{-1}).

Other carbon matrices: Other carbon matrices, such as carbon cloth [181], and activated wheat dough [182], have been combined with CNTs to generate elaborate structures. He et al. fabricated a 3D functionalized CNT/graphitic carbon nitride hybrid composite to serve as the sulfur host for Li–S batteries through a self-assembly-assisted method

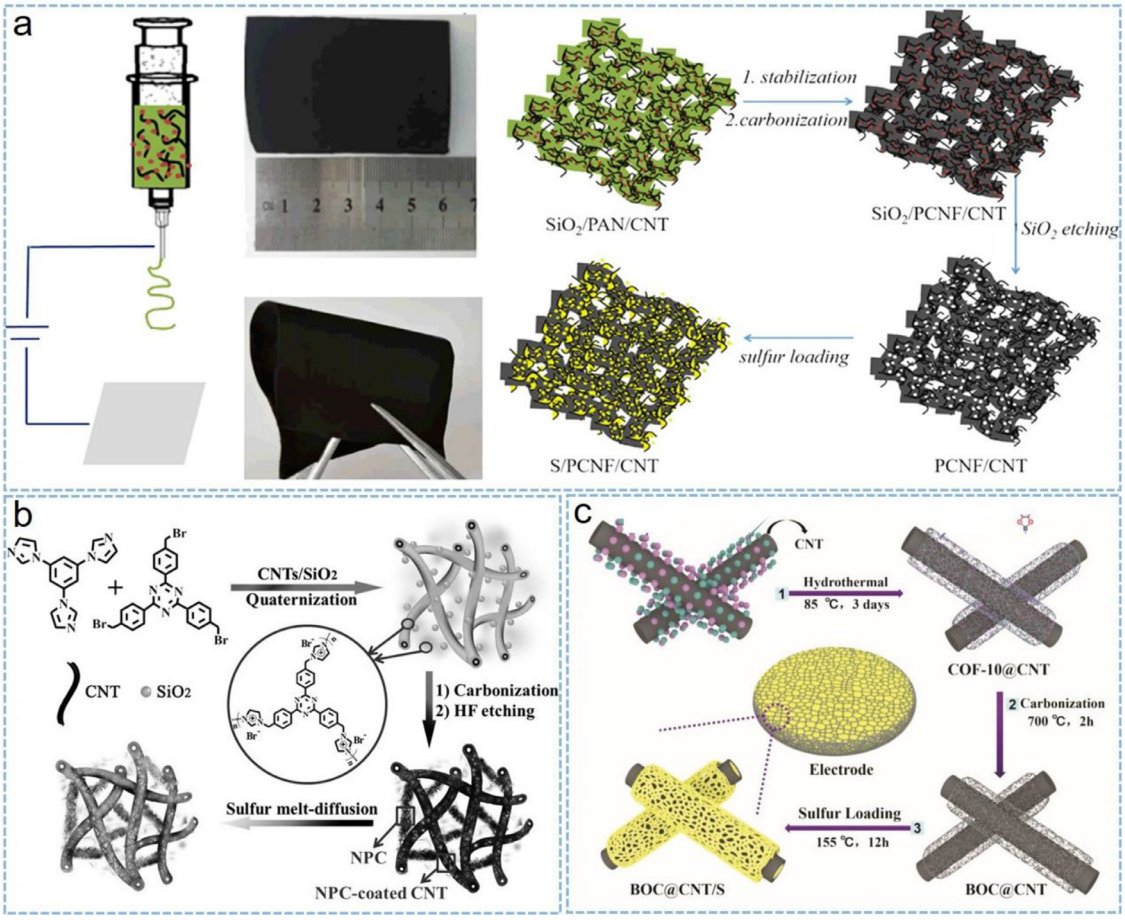

Fig. 7. (a) Schematic of the synthesis of porous CNFs/CNTs. Reproduced with permission [158]. Copyright 2018, American Chemical Society. (b) Schematic of CNTs/N-doped porous carbon hybrid. Reproduced with permission [164]. Copyright 2017, Wiley-VCH. (c) Schematic of the synthesis of B, O co-doped carbon/CNTs/S composite. Reproduced with permission [165]. Copyright 2019, Wiley-VCH.

followed by a calcination process [183]. Such an interconnected framework between CNTs and graphitic carbon nitride directs the electron transfer from CNTs to carbon nitride, thereby enhancing the electrical conductivity of the hybrid composite and providing abundant N-containing functional groups. Owing to this unique design concept, the resultant sulfur cathodes with a high sulfur content (80 wt%) demonstrated a high specific capacity of 1351 mAh g^{-1} at 0.1 C and remarkable cyclic stability of 759 mAh g^{-1} after 200 cycles at 1.0 C, along with a sulfur loading of 5.0 mg cm^{-2}.

4.1.3. CNTs hybridized with polymers

Polymers exhibiting high electrical conductivities and good Li-ion conducting properties have been used with CNTs to produce various composites. For example, Archer et al. fabricated a sulfur host using amine-functionalized CNTs (**Fig. 8a**) [45]. It was found that the amine-functionalized CNTs offer a specific and strong interaction between the sulfur species and amine groups in the interconnected conductive CNT network. Eventually, high specific capacities were obtained at both low and high current rates. Furthermore, other polymers, including polypyrrole [184], polyethylene glycol [185], polyethylenimine [186], and polyphenylene [187], have been utilized to modify CNT/S cathodes, and these sulfur composite cathodes demonstrated considerably improved electrochemical results. Recently, polymeric S/CNTs composites have become popular because the strong chemical bonds between sulfur and the polymers effectively restrict the dissolution and shuttling of intermediate polysulfides, whereas the CNTs ensure efficient electron and ion transfer [188-191]. For instance, an S-rich co-polymer@CNT composite was developed to enable the long-term cycle of Li–S batteries through a template method combined with the CVD process [188]. The S-rich co-polymer can serve as the sulfur cathode, whereas the CNTs acted as the support to adsorb the polysulfides tightly. Benefiting from the compositional and structural characteristics (Fig. 8b), the sulfurized polymer/CNT cathodes exhibited a high reversible capacity of 1300 mAh g^{-1} at 0.1 C, a high rate capability of 700 mAh g^{-1} at 2.0 C, and excellent cyclic performance with a specific capacity of 880 mAh g^{-1} after 100 cycles at 1.0 C. Moreover, a free-standing composite comprising CNTs encapsulated in sulfurized PAN was used as a binder-free sulfur cathode for Li–S batteries via a combined electrospinning and carbonization method [189]. The sulfur bonds well with the PAN skeleton, and the CNT networks strengthen the structural integrity of the sulfur cathode and further ensure their fast electron transfer. When used as the cathode for Li–S batteries, a high specific capacity (1610 mAh g^{-1} at 0.2 C) and remarkable cyclic stability (1106 mAh g^{-1} after 500 cycles at 1.0 C) were achieved.

4.1.4. CNTs hybridized with inorganic compounds

CNTs hybridized with carbonaceous materials can form various impressive architectures, but the prevention of polysulfide dissolution and shuttling in such structures is limited. As discussed in Section 2, polar inorganic compounds are beneficial for suppressing the shuttle effect. The hybridization of CNTs with inorganic materials has demonstrated the following advantages: (i) inorganic materials with highly polar properties enable strong chemical adsorption of polysulfides, thereby limiting their dissolution and further shuttle effects; (ii) CNTs can act as conductive networks to improve the electrical conductivity of the sulfur hosts, by promoting fast electron transfer during cycles; and (iii) CNTs are

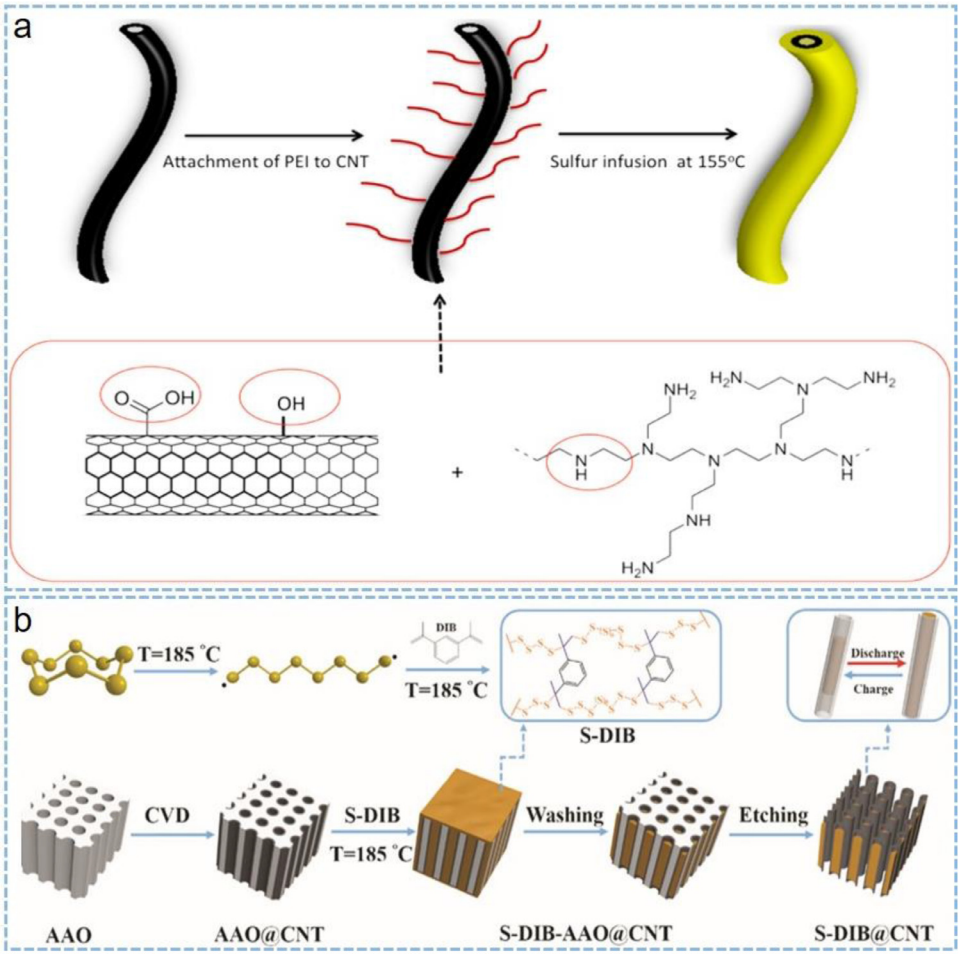

Fig. 8. (a) Schematic of the synthesis of CNTs-PEI/S. Reproduced with permission [45]. Copyright 2016, American Chemical Society. (b) Schematic of the synthesis of sulfurized polymer/CNT composite. Reproduced with permission [188]. Copyright 2017, Wiley-VCH.

able to enhance the structural integrity of sulfur hosts, thereby facilitating long-term cyclic stability tests. Thus far, different inorganic fillers, including metals, metal oxides, metal sulfides, metal phosphides, and MXenes, have been extensively studied.

Metals: Metal nanoparticles have high electrical conductivities and highly polar properties, which can contribute to their strong chemical affinity for polysulfides and promote fast polysulfide conversion kinetics [33, 46, 192-199]. As a typical example, metallic Co can not only catalyze the growth of CNTs but also exhibit strong interactions with polysulfides, making it an attractive material for constructing elaborate architectures in Li–S batteries. For example, a hierarchical yolk-shell microsphere, comprising of Co nanoparticles encapsulated in bamboo-like N-doped CNTs (**Fig. 9a**), was synthesized through a spray pyrolysis method and then used as an efficient S host [192]. This architecture with Co doped yolk-shell microspheres enables high sulfur loading, mitigates polysulfide dissolution, and improves the chemical affinity for intermediate polysulfides. As a result, the Li–S batteries with a high sulfur content (64 wt%) exhibited a specific capacity of 700 mAh g^{-1} after 400 cycles at 1.0 C, accompanied by high capacity retention of 76%. Moreover, Chen et al. fabricated a “tube on cube” nanohybrid as a compact sulfur host through an electrospinning method followed with pyrolysis process (Fig. 9b), which comprised a fibrous carbon skeleton, highly porous carbon cube filler, and abundant CNT tentacles [193]. Benefiting from the excellent electrical conductivity, abundant active interfaces, and strong chemical/physical confinement of polysulfides, the sulfur cathodes delivered a superior rate capability of ~623 mAh g^{-1} at 10 C and impressive cyclic stability up to 2000 cycles. Remarkably, with a high S loading and an optimized electrolyte, high energy densities of 348.8 Wh kg^{-1} and 327.6 Wh L^{-1} were achieved at the system level, demonstrating the potential for application in practical Li–S batteries. In addition, Ma et al. utilized flower-like metal hydroxides as precursors for in situ growth of a carbon matrix and N-doped CNTs on the surface of Co particles via a CVD method followed by an acidic etching process (Fig. 9c) [194]. The carbon matrix ensured outstanding structural integrity of sulfur electrode and promote the electron transfer, while the doping N atoms and Co nanoparticles promoted the fast intermediate conversions. The sulfur cathode fabricated with a high sulfur content and high areal sulfur loading of 6.5 mg cm^{-2} exhibited a high areal capacity of 4.37 mAh cm^{-2} and avoided self-discharge issues.

Metal oxides: Metal oxides with high polarities have been extensively employed as adsorbents for trapping intermediate polysulfides through chemical bonding. However, metal oxides usually exhibit poor electrical conductivity, which affects the electron transfer and ion transport during charge/discharge cycles, thereby resulting in a deterioration of electrochemical performance, especially at high rates. The combination of CNTs with metal oxides can effectively resolve the weak polysulfide adsorption of pure CNTs and the low electrical conductivity of metal oxides.

CNTs can readily form flexible interconnected networks that serve as conductive matrices to support metal oxides in the voids and spaces between CNTs. Wei et al. prepared VO_x hollow nanospheres by a hydrothermal method, and they were further mixed with SWCNTs to obtain a flexible binder-free composite [200]. It was revealed that SWCNTs intertwined around the VO_x nanospheres and generated a high-speed electron pathway, whereas VO_x nanospheres provided a strong chemical affinity for intermediate polysulfides. As a result, the sulfur composite film exhibited a high specific capacity of 1069 mAh g^{-1} at 1.0 C

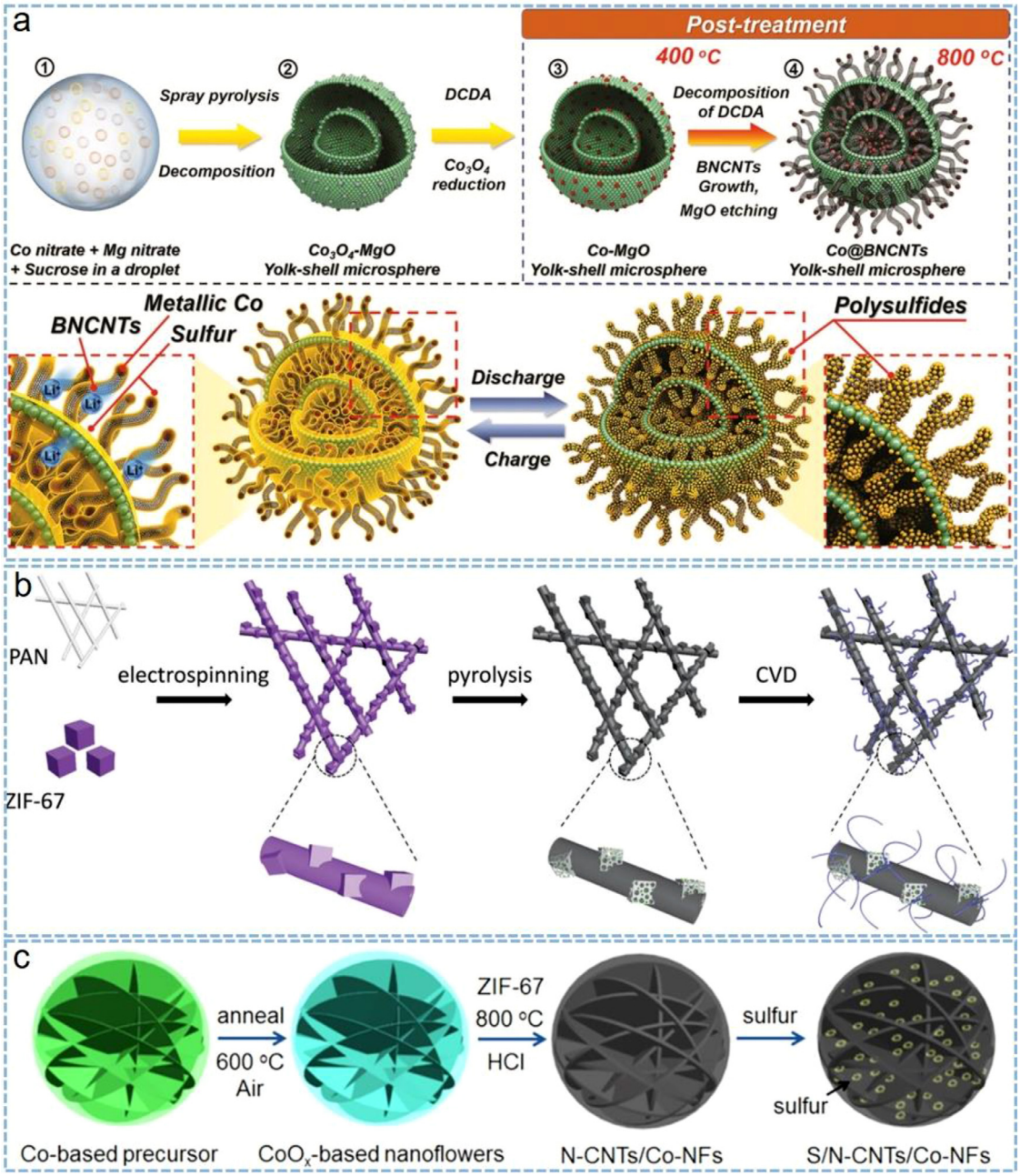

Fig. 9. (a) Schematic of the synthesis of Co/B, N-doped CNT/S composite and its working mechanism in Li–S batteries. Reproduced with permission [192]. Copyright 2018, Wiley-VCH. (b) Schematic of Co, N co-doped CNT/carbon structure. Reproduced with permission [193]. Copyright 2018, Royal Society of Chemistry. (c) Schematic of the synthesis of S/N-doped CNT/Co nanoflowers. Reproduced with permission [194]. Copyright 2018, American Chemical Society.

and excellent rate performance of 614 mAh g^{-1} at 20 C. Furthermore, other metal oxides, such as MoO_3 [201], SnO_2 [202], Co_3O_4 [203], and $NiFe_2O_4$ [204], have been combined with CNTs to serve as sulfur hosts, and the final sulfur cathodes have demonstrated enhanced electrochemical performance compared with the sulfur cathodes constructed using bare CNT hosts.

CNTs are popular as supports for loading metal oxides [205-221]. Sun et al. reported a robust sulfur host comprised of hollow mesoporous titania embedded within CNTs [205]. The titania particles are linked via CNTs (**Fig. 10a**), and this feature ensures effective electron transfer during the electrochemical cycles. After the infiltration of elemental sulfur into the pores of the hollow mesoporous titania, the resultant sulfur cathodes exhibited an exceptional electrochemical performance with excellent capacity retentions at high rates of 1.0, 2.0, and 5.0 C. Moreover, a flexible hybrid consisting of carbon foam@CNTs decorated with MgO particles was synthesized to serve as a stable sulfur host through a solution-based method followed by carbonization [206]. The dense CNTs uniformly wrapped in carbon foam skeletons built an interconnected conductive network for rapid ion/electron transport, whereas MgO particles and N-doping carbon matrix significantly restricted polysulfide dissolution and the shuttle effect. As such, the as-obtained sulfur cathodes, with an extremely high areal sulfur loading of 14.4 mg cm^{-2}, demonstrated a high initial areal capacity of 10.4 mAh cm^{-2} and retained 8.8 mAh cm^{-2} after 50 cycles. With a relatively low areal sulfur loading of 1.2 mg cm^{-2}, the sulfur cathodes maintained a high specific capacity of 390 mAh g^{-1} after 800 cycles at 2.0 C, accompanied by an extremely low capacity decay of 0.06% per cycle and an average CE of ~98%.

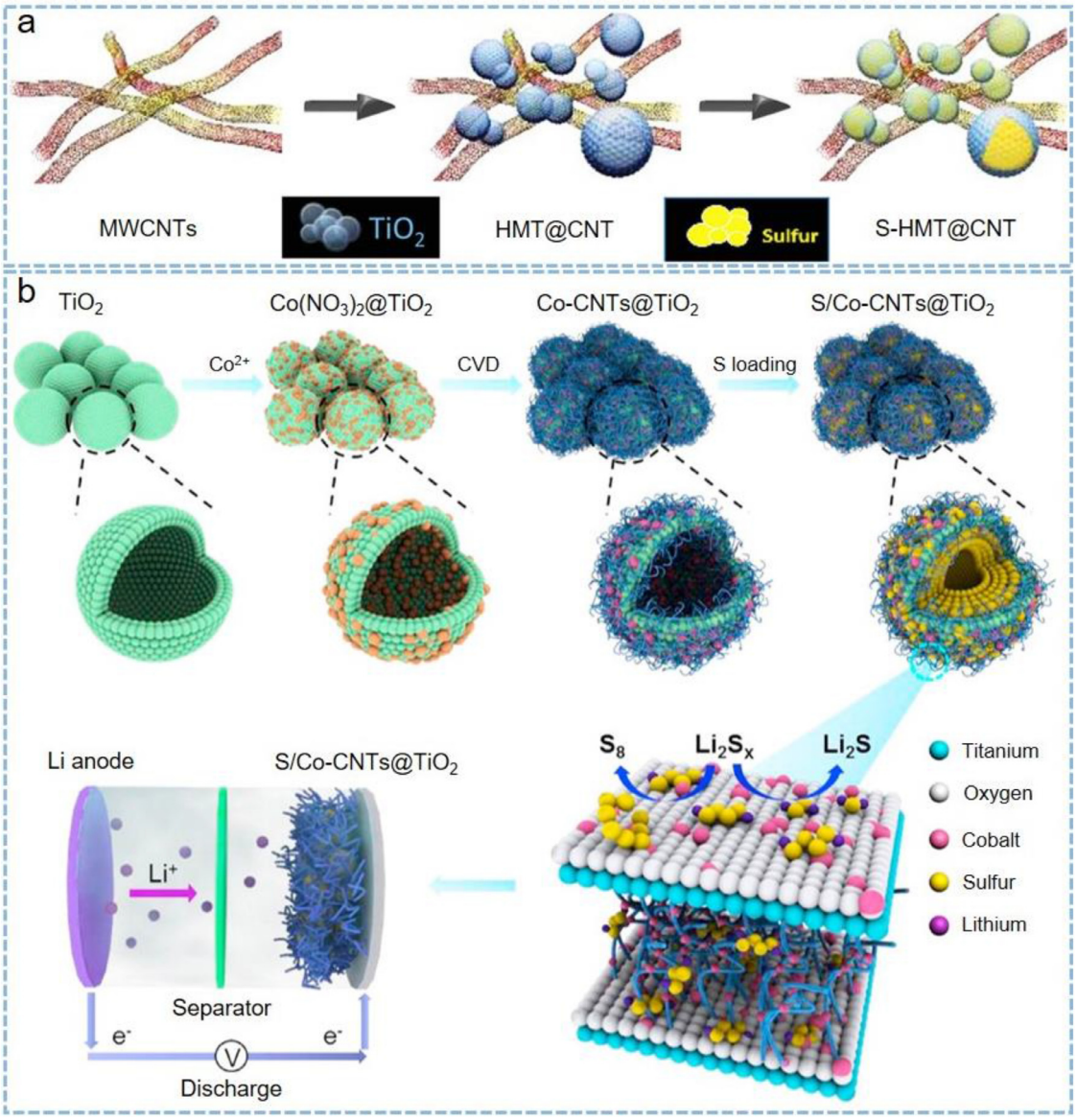

Fig. 10. (a) Schematic of the synthesis of S/hollow mesoporous TiO_2@CNT composite. Reproduced with permission [205]. Copyright 2016, Wiley-VCH. (b) Schematic of the fabrication of S/Co-doped CNT@TiO_2 microspheres and its working mechanism in Li–S batteries. Reproduced with permission [222]. Copyright 2021, Elsevier.

In addition, CNTs can be grown in situ within sulfur hosts to improve electrical conductivity and enhance the overall structural integrity. The CNTs grown in situ within the host produce intriguing micro-and nanostructures, which cannot be achieved via simple physical mixing. A novel 3D hierarchical sulfur host assembled using hollow TiO_2 spheres and a vertically rooted CNT network was fabricated by Wang and coworkers via a CVD method [222]. As shown in Fig. 10b, the 3D CNT network promotes long-range electrical conductivity, whereas the TiO_2 microspheres with hollow and porous structures buffer the volume changes and suppress polysulfide dissolution and shuttle effects. Consequently, the sulfur cathodes delivered a high specific capacity of 1135 mAh g^{-1} at 0.2 C and a remarkable long-term cyclic stability for 500 cycles with an ultralow capacity fading rate of 0.072% per cycle. Even at a high areal sulfur loading of 5.9 mg cm^{-2}, the sulfur cathode exhibited a remarkable electrochemical performance (4.33 mAh cm^{-2} at 0.2 C). A similar improvement was observed in the unique TiO_2/Co_3O_4-CNT host [223].

Metal sulfides: Metal sulfides have high electrical conductivity and high polarity, which make them good sulfur hosts for Li–S batteries. The combination of CNTs with metal sulfides can form an interconnected conductive network that enables fast electron transfer [224-236]. For instance, Chen et al. reported a microstructure comprising CNTs inserted in hollow Co_3S_4 nanoboxes through a self-templated method, serving as an efficient sulfur host for Li–S batteries (**Fig. 11a**) [224]. The CNT framework in the composite rendered ultrafast charge transfer and the hollow Co_3S_4 nanoboxes contributed to efficient polysulfide retention via both physical confinement and chemical bonding. Furthermore, the sulfur cathodes delivered a high specific capacity of 1535 mAh g^{-1} at 0.2 C and demonstrated cyclic stability across 500 cycles. Increasing the testing temperature to 50°C resulted in high capacity retention (718 mAh g^{-1} after 300 cycles at 0.2 C) and a good rate capability (446 mAh g^{-1} at 0.5 C). Moreover, Manthiram et al. decorated the CNT surface with 1T-ReS_2 nanosheets through a self-assembly method, which served as polysulfide conversion electrocatalysts for Li–S batteries [225]. Thanks to the high electrical conductivity and rich nano-porosity in the composite, the architecture facilitates fast electron transfer and ion diffusion and provides abundant active sites for catalyzing polysulfide conversion. After sulfur infiltration, the as-fabricated sulfur cathodes demonstrated a high specific capacity with excellent long-term

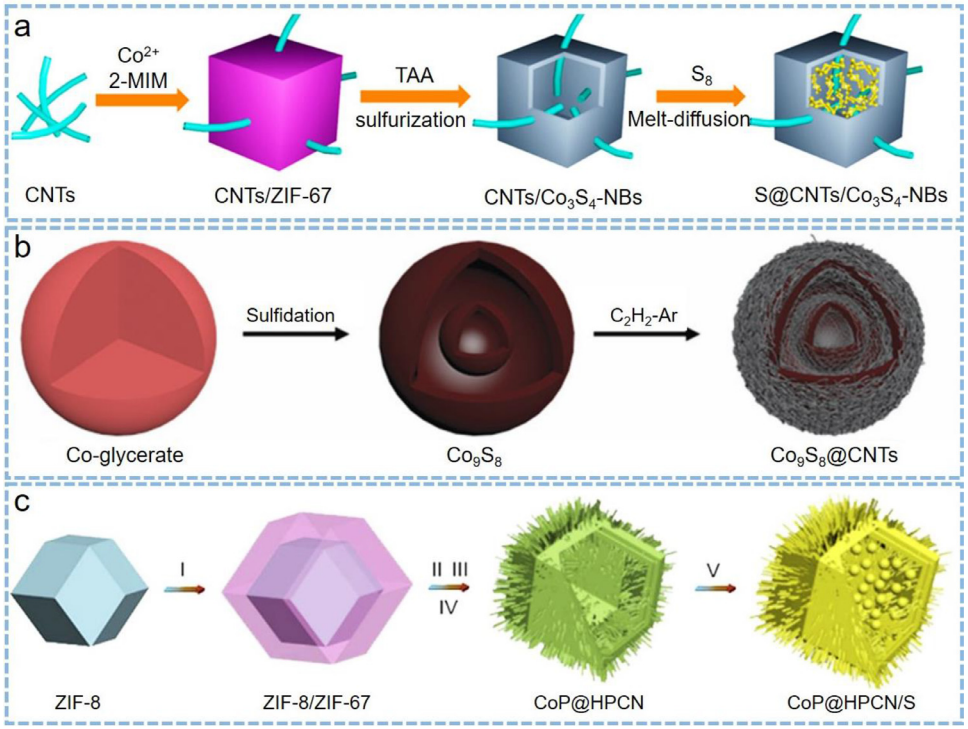

Fig. 11. (a) Schematic of the synthesis of S@CNT/Co_3S_4 nanoboxes. Reproduced with permission [224]. Copyright 2017, American Chemical Society. (b) Schematic of the fabrication of Co_9S_8@CNTs. Reproduced with permission [226]. Copyright 2019, Royal Society of Chemistry. (c) Schematic of the synthesis of hollow polyhedron/CNT confined CoP/S. Reproduced with permission [36]. Copyright 2019, Elsevier.

cyclic stability (capacity retention of 71.7% over 1000 cycles at 1.0 C). The in situ growth of CNTs ensures a strong combination between the CNTs and metal sulfides, which is conducive to the transfer of electrons and ions. Qian et al. prepared an integrated hierarchical double-shelled Co_9S_8@CNT nanostructure for Li–S batteries via a solvothermal method followed by a CVD process using C_2H_2 as the carbon source (Fig. 11b) [226]. In such a structure, the CNT components offered well-maintained structural integrity and high electron pathway throughout the cathode, while the Co_9S_8 species entrapped polysulfides and further boosted the polysulfide redox kinetics. As a result, the sulfur cathode demonstrated a high specific capacity of 1415 mAh g^{-1} at 0.2 C, a high rate capability of 677 mAh g^{-1} at 10 C, and an unprecedented long-term cyclic stability over 1000 cycles with an extremely low capacity decay of 0.0448% per cycle. Upon further increasing the areal sulfur loading to 5.5 mg cm^{-2}, a remarkable areal capacity of 4.3 mAh cm^{-2} was retained.

Metal phosphides: Emerging metal phosphides including CoP [36], MoP [237], NiP [238], and Co_2P [239], have been hybridized with CNTs to make sulfur hosts, owing to their high chemical affinity for polysulfides and high catalytic activity in promoting polysulfide conversion. Chen et al. fabricated a hollow polyhedral/CNT-confined CoP nanoparticle superstructure via a phosphatization of Co_3O_4 embedded hollow polyhedron/CNTs (Fig. 11c) [36]. The high porosity, cavities, and multidirectional channels of the sulfur host accommodate the volume expansion and entrap sulfur species, whereas the inserted CoP nanoparticles act as the adsorbent and electrocatalyst to bind the polysulfides and catalyze their conversion to Li_2S. Owing to these advantages, the final sulfur cathodes exhibited an excellent rate performance (~528 mAh g^{-1} at 3.0 C) and cyclic stability (capacity retention of 84.9% after 200 cycles) with an areal sulfur loading of 2.3 mg cm^{-2}. Furthermore, Lu et al. investigated the influence of highly polar NiP/CNTs on Li–S battery performance [238], whereas Wang et al. demonstrated the effects of MoP/CNTs on polysulfide conversions [237]. Both studies proved that excellent electrochemical performance can be achieved using metal phosphides/CNT hosts for Li–S batteries.

MXene: Recently, MXene nanosheets have become a promising sulfur stockpile because of their high electrical conductivity, strong chemical affinity, and good mechanical strength [240, 241]. Unfortunately, the significant stacking and aggregation of MXene nanosheets inhibit ionic transfer, thus limiting the efficient utilization of active sulfur species and polysulfide conversion kinetics. The insertion of CNTs into the interlayers of MXene nanosheets can prevent the re-stacking of MXene nanosheets and enhance the electrical conductivity of sulfur composites to improve sulfur utilization [242]. For instance, Nazar et al. fabricated interwoven MXene nanosheet/CNT composites through a filtrated method, which was then used as the sulfur host [243]. The CNTs were well interconnected on MXene sheets, thereby an enhanced electrochemical performance was achieved using these composites, as compared with Li–S batteries using MXene nanosheets as the sulfur host. Moreover, Chen et al. prepared MXene/CNT hierarchical porous hollow microsphere host via a spray-dry method [244]. CNTs ensure the structural stability of sulfur cathodes, whereas MXene nanosheets adsorb intermediate polysulfides and promote the conversion kinetics of polysulfides, and the microspherical structure ensures high stability during cycles. As a result, the sulfur cathodes exhibited a high specific capacity of 1451 mAh g^{-1} at 0.2 C, a remarkable rate capability of 686 mAh g^{-1} even at 8.0 C, and stable cyclic performance over 500 cycles. A similar improvement was observed upon using porous MXene/CNT microspheres, as reported by Han and coworkers [245].

Others: In addition to the abovementioned metal-based composites, other polar materials, including graphene/Al_3Ni_2 [246], boron nitride (BN) [247, 248], 3D Al foam [249], carbon/$Al_2(OH)_{2.76}F_{3.24}$ [250], Fe/Fe_3C nanoparticles [251], and Co-MoC [47], have been combined with CNTs to serve as S hosts for Li–S batteries. Huang et al. prepared a 3D network comprising CNT/graphene/S-Al_3Ni_2 for Li–S batteries via the physical mixing method [246]. The 3D network and Al species provide channels for fast electron transfer and ion transport, the Ni species accelerate the polysulfide conversion kinetics, whereas the CNTs serve as the conductive channels for electron transfer. In this manner, the sulfur cathodes exhibited a high specific capacity of 2.05 mAh cm^{-2} over 200 cycles at 2.76 mA cm^{-2}, accompanied by a capacity retention of 85.9%. To improve the adsorption of polysulfides, CNT/BN fibers were fabricated through a physical mixing method and used as an effective sulfur host for Li–S batteries [247]. The CNTs act as the additive for separating BN, and further serve as the high-speed pathways to promote

electron transfer. This structure enables the loading and entrapment of active sulfur species and localizes soluble long-chain polysulfides within sulfur cathodes. When used as the sulfur host in Li–S batteries, the as-fabricated sulfur cathodes demonstrated a high initial specific capacity of 1222 mAh g^{-1} at 0.1 C and outstanding cyclic stability with a capacity of 482 mAh g^{-1} after 500 cycles at 4.0 C.

4.1.5. CNTs hybridized with MOFs

MOFs with a high specific surface area and abundant pores are considered to be good hosts for Li–S batteries. However, MOFs usually exhibit extremely low electronic conductivity, which restricts electron transfer during electrochemical reactions. Incorporating CNTs in MOFs alleviates these issues and enhances the structural stability of sulfur hosts. Cao et al. prepared a sulfur host comprising a 3D porous MOF@CNT framework with CNTs uniformly distributed in MOFs through the solution-based method [252]. The long CNTs intercalated the MOFs together and ensured the high electrical conductivity of the entire electrode. After sulfur infiltration, the as-fabricated sulfur cathode demonstrated a high specific capacity of 1380 mAh g^{-1} at 0.1 C and remarkable cyclic stability with negligible capacity decay (over 500 cycles). Even with a high areal sulfur loading of 8.0 mg cm^{-2}, an impressive areal capacity of ~11 mAh cm^{-2} was obtained at 0.1 C. Furthermore, a few other MOF/CNT hosts have been designed to improve the electrochemical performance of Li–S batteries [253, 254]. These studies demonstrated that the utilization of MOFs can resolve the issues faced by Li–S batteries, indicating their potential for practical applications.

4.2. CNT-based Se hosts

Carbonaceous materials are typically employed hosts to accommodate the volume changes of Se and entrap the polyselenides [255-259]. Zhang et al. developed a low-cost and highly efficient solution-based technique to fabricate Se/MWCNT composites using ethylenediamine as the solvent (1.0 M LiTFSI in DOL/DME, 1:1 in v/v) [255]. Besides the accommodation of volume expansion, the existence of CNTs served as the support and conductive network. Compared to the melt infiltration method, the solution-based approach enables the homogenous distribution of small Se particles on the CNT skeleton, thus leading to enhanced battery performance. The Se content is another crucial parameter that determines the specific capacity of CNT/Se composites. To elevate the Se content in the component, Mukkabla et al. loaded the Se nanoparticles on the cetyltrimethylammonium bromide-functionalized MWCNTs with a high Se content of ~72 wt% using a facile hydrothermal method [256]. The surface-functionalized MWCNTs with high electrical conductivity enhanced the adsorption capability of intermediates, thereby improving the utilization ratio of Se. The as-prepared Li–Se batteries (1.0 M LiTFSI in DOL/DME, 1:1 in v/v) showed a substantially prolonged lifespan. Moreover, to further enhance capability for suppressing the shuttle effects of polyselenides, Dutta et al. infused the Se into the cavity of CNTs [257]. As the polyselenides are completely confined within the precincts of the CNT cavity, the as-prepared Se-CNT composite delivered exceptionally stable battery performance at widely varying current densities in 1.0 M $LiPF_6$/EC-DMC (1:1 in v/v). Various micro-and nanostructures based on the CNT matrix were designed to facilitate Se loading and better accommodate the volume expansion of Se. For example, Feng et al. fabricated CNT microspheres using an ultrasonic spray method and subsequently loaded Se via a molten-diffusion strategy (1.0 M $LiPF_6$ in EC/DMC, 1:1 in v/v) [258]. As shown in **Fig. 12a**, the CNT microspheres possessed abundant pores and voids for loading Se and mitigating volume changes, and the spherical morphology ensured the high structural integrity. When Se/CNT microspheres were used as the cathode, the Li–Se batteries exhibited an initial specific capacity of 626 mAh g^{-1} at 0.2 C, a high rate capability with a specific capacity of 390 mAh g^{-1} at 5.0 C, and remarkable cyclic performance with a capacity retention of 80% after 500 cycles at 1.0 C.

Although the construction of CNTs with various micro-and nanostructures enhanced the polyselenide retention during cycles, the Se loading mass and electrochemical performance are still not satisfactory for practical applications. CNTs combined with various carbon matrices produce intriguing architectures and are capable of restricting polyselenides. Moreover, the coupling with CNTs improved the structural integrity of the entire Se host, thereby improving the electrochemical performance, especially the long-term cyclic stability. To date, graphene [260-264], CNFs [264], and porous carbon matrices [265, 266], have been integrated with CNTs. For instance, He et al. fabricated a 3D free-standing graphene-CNT@Se aerogel, with CNT/Se sandwiched between graphene nanosheets, via a simple solvothermal method (Fig. 12b) [260]. The unique 3D mesoporous and conductive network offers highly efficient channels for electron transfer and ion diffusion, and the hierarchical features, originating from the interconnections between graphene and CNT, restrict polyselenide dissolution and prevent Se volume expansion during electrochemical cycles. Therefore, the Li–Se batteries (1.0 M LiTFSI in DOL/DME, 1:1 in v/v) exhibited a high reversible capacity of 632.7 mAh g^{-1} at 0.2 C and a high rate capability of 192.9 mAh g^{-1} at 10 C. Moreover, Han et al. prepared a flexible, self-standing graphene-Se@CNT composite film via vacuum filtration method, which has been utilized as a cathode in Li–Se batteries (1.2 M $LiPF_6$ in EC/EMC, 3:7 in v/v) without binders and additives [261]. The graphene-CNT matrix with tight interactions releases the strain/stress arising due to volume expansion, provides a conductive framework with open channels for electron transfer and ion diffusion, and restricts polyselenide dissolution. The graphene-Se@CNT composite demonstrated a high specific capacity of 400 mAh g^{-1} at 0.1 C and stable cyclic performance (315 mAh g^{-1} after 100 cycles at 0.1 C). Remarkably, an MWCNT/CNF free-standing substrate has also been used to prevent the dissolution of polyselenide intermediates, which is promising in making flexible Li–Se batteries (1.0 M $LiPF_6$ in EC/DMC, 1:1 in W/W) [264]. In addition, a tube-in-tube structure comprising MWCNTs encapsulated by highly porous carbon was synthesized via a hard template-assisted method [265]. Such a design facilitated the encapsulation and further confinements of Se species and enhanced the electrical conductivity of the entire electrode. The Se host had a high pore volume of 2.167 cm^3 g^{-1} and a remarkable surface area of 1131 m^2 g^{-1}, enabling a high Se loading content of 70 wt%. After Se infiltration, the cathodes (1.0 M $LiPF_6$ in EC/DEC, 1:1 in v/v) exhibited a specific capacity of 625 mAh g^{-1} at 0.2 C, an outstanding rate performance (190 mAh g^{-1} at 10 C), and impressive cyclic stability with a negligible capacity decay of 0.01% per cycle for 4000 cycles at 1.0 C. Inspired by the confinement of small sulfur molecules in micropores, Xin et al. further extend this strategy to study the electrochemistry of small Se molecules confined in slit micropores versus Li (electrolyte: 1.0 M $LiPF_6$ in EC/DMC, 1:1 in W/W) [266]. A pyrolytic microporous carbon sheath was coated on an MWCNT core via an ultrasonic spraying method, and Se was further penetrated into the micropores of the outer shell to form the Se–C composite (Se/CNT@MPC). Benefiting from the CNT-formed spherical morphology and intrinsic high electrical conductivity, the Se/CNT@MPC composites have been characterized by high specific capacities and good cyclic stability, which promise Li–Se batteries with a high volumetric energy density of 2308 Wh L^{-1}.

4.3. CNT-based Te hosts

In light of the less shuttle effect, Yin et al. adopted the S-doping strategy to synthesize $Te_{1-x}S_x$ nanorod cathodes via a melting-diffusion-vaporization method for Li-Te batteries. They concluded that the transport kinetics of Li^+ and electrons can be accelerated by S-doping thanks to the redistribution of electrons between low electronegative Te and high electronegative S. As a result, the optimal $Te_{0.92}S_{0.08}$ cathode without any carbonous matrix exhibits a high volumetric capacity of 1615 mAh cm^{-3} over 100 cycles at 0.1 C [267]. Making Te/carbon composites appears to be another viable approach to surmount these issues, which attracts enormous interest [22, 268]. For example, He et al. em-

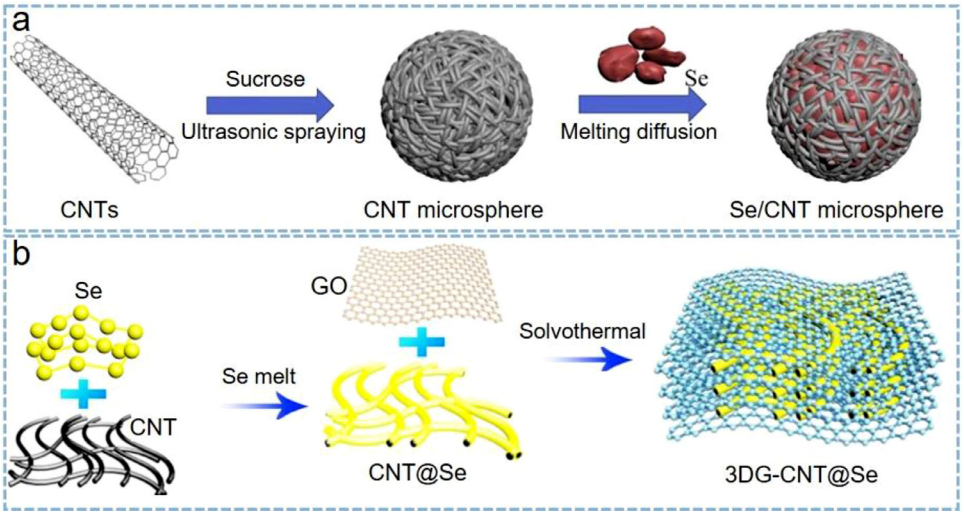

Fig. 12. (a) Schematic of the synthesis of Se/CNT microsphere. Reproduced with permission [258]. Copyright 2019, Elsevier. (b) Schematic of the synthesis of 3D graphene/CNT/Se composite. Reproduced with permission [260]. Copyright 2016, American Chemical Society.

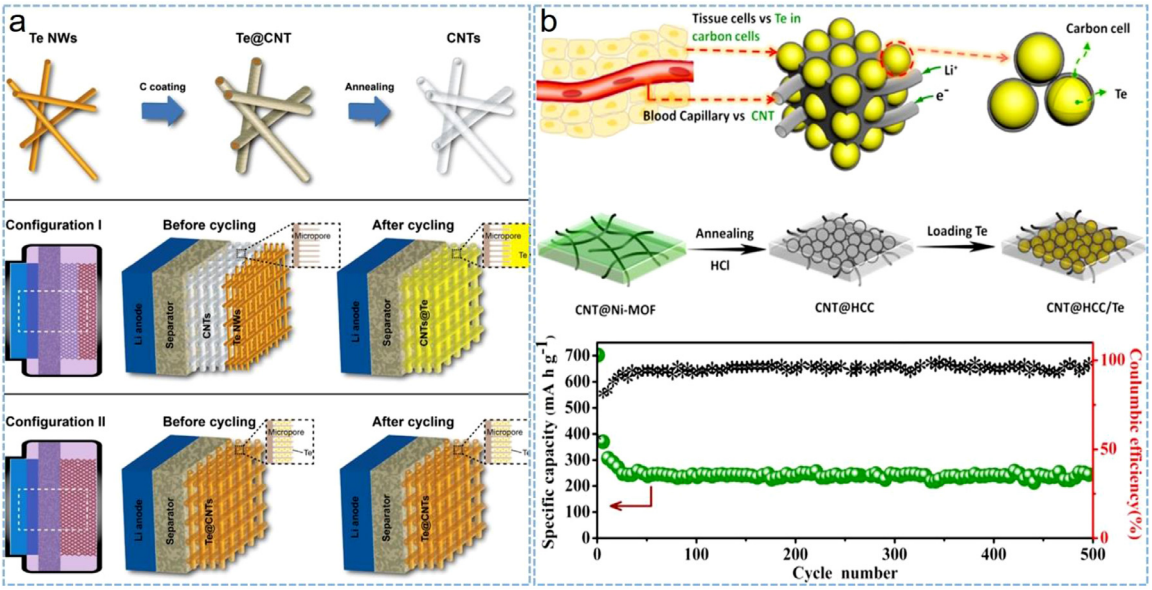

Fig. 13. (a) Schematic of the synthesis of Se/CNT composite and the proposed two types of working mechanisms proposed. Reproduced with permission [269]. Copyright 2016, Wiley-VCH. (b) Schematic of the synthesis of CNT@hollow carbon cell/Te cathode and the cyclic performance (0.5 C) of Li–Te batteries. Reproduced with permission [270]. Copyright 2018, Elsevier.

ployed MOF-derived carbon polyhedra to serve as the host with a high Te loading of 77 wt%. An ultrahigh initial capacity of 2615.2 mAh cm^{-3} was delivered [268]. Considering the excellent characteristics of CNTs, Yu et al. incorporated CNTs with Te nanowires to fabricate composite electrodes through the solution-based method combined with the carbonization process (**Fig. 13a**) [269]. A CNT aerogel with high electrical conductivity and porous structure was used, which enables fast electron/ionic transport and the efficient trapping of active species. In addition, CNTs enhance the integrity of the Te cathodes, thereby facilitating a stable cyclic performance. As a result, the fabricated Li–Te batteries exhibited remarkable electrochemical performance, in terms of a high specific capacity of 548 mAh g^{-1} at 0.1 C, excellent rate capability of 215 mAh g^{-1} at 5.0 C, and good cyclic stability with almost no capacity decay for 200 cycles. Moreover, Xu et al. reported a muscle-like electrode via the carbonization of CNTs/MOFs precursor for high-performance Li–Te batteries (Fig. 13b) [270]. Hollow carbon cells were utilized to confine Te, accommodating the volume change and restricting the loss of active species, whereas the CNTs provide abundant channels for both electron and ion transfer during electrochemical cycles. Owing to such an intriguing design, Li–Te batteries showed good rate performance (124 mAh g^{-1} at 5.0 C) and high cyclic stability with a specific capacity of ~240 mAh g^{-1} after 500 cycles at 0.5 C. These studies demonstrated that CNT networks play a significant role in resolving/alleviating the issues of Te cathodes in Li–Te batteries. Overall, the application of CNTs in Li–Te batteries is still in its infancy stage with very few works have been reported. This may be attributed to the high cost and low abundance of Te elements. In addition, the conversion mechanisms of Li–Te batteries in different electrolyte systems have not been well studied, which can be accomplished with the assist of start-of-the-art techniques and computational approaches with different scales. Further works should focus on the construction of high volumetric-energy-density CNT-based Te cathodes to realize task-specific applications such as aerospace engineering, safety and rescue, and medical devices which required limited space.

5. CNT-based interlayers/separators

Functionalized interlayers and/or separators are widely used to intercept the shuttling of polychalcogenides for improving the utilization

of active species (Table 4). Before moving to in-depth discussions of CNT-based interlayers and separators, the differences between these two terms are revisited to avoid any misunderstandings. In general, the interlayer is a freestanding film inserted in-between the existing separator and electrode, whereas the functional separator is a physicochemical modification on the routine separators by hybridizing with materials (*e.g.*, nanocarbon and inorganic nanomaterials). The CNT-based interlayer and CNT-modified separators indeed have almost the same functions in cutting off the polychalcogenide shuttling, but differences remain. First, an interlayer should be free-standing, while a CNT-modified separator normally requires a binder to form a dense coating film on the pristine separator. In this regard, different fabrication methods should be used to prepare CNT-based interlayer and CNT-modified separators. Second, the relatively dense structure of CNT-modified separators inevitably introduces high resistance to the transfer of Li-ions. For comparison, CNT interlayers require a porous structure and high surface area to reduce the weight and offer more sites for intermediate adsorption, respectively. Third, an interlayer has other functions, such as upper current collectors and structure stabilizer of the chalcogen cathode, whereas CNT-modified separators mainly focus on the block of intermediate shuttling.

5.1. CNT-based interlayers for Li-S batteries

The rational construction of sulfur hosts has effectively resolved the issues associated with Li–S batteries. As an alternative strategy, the introduction of interlayers to prevent polysulfide shuttling is simple and effective (**Table 4**). Ideally, interlayers should meet the following requirements: (1) high electrical conductivity for fast electron transfer, (2) high chemical affinity for adsorbing intermediate polysulfides, (3) ability to catalyze the conversion of long-chain polysulfides, (4) large surface area to ensure adequate contact with polysulfides, and (5) sufficient electrolyte penetration and compatibility. Although pure CNTs have been used as interlayers in Li–S batteries to enhance electrochemical performance [271-274], the weak interactions between CNTs and polysulfides can not effectively prevent polysulfide shuttling. Thus, CNTs combined with other materials including carbon matrices, polar metal compounds, polymers, and MOFs, have emerged as interlayers for Li–S batteries.

5.1.1. Carbon-based interlayers

Constructing pure carbon-based architectures can prevent the dissolution and shuttle effect of intermediate polysulfides by physical restriction. To inhibit the dissolution of polysulfides, GO, $C_{60,}$ and g-C_3N_4 have been coupled with CNTs [275-278]. These carbon-based architectures usually have hierarchical and porous structures, thus facilitating the contact and penetration of electrolytes. As a typical study, Lee et al. prepared a flexible carbon-based membrane comprising graphene oxide (GO) and CNTs (**Fig. 14a**), via a simple vacuum filtration approach [275]. Owing to the oxygen-containing functional groups on GO and the high electrical conductivity of CNTs, polysulfides were strongly adsorbed in the interlayer with a high specific capacity of 1591.56 mAh g^{-1} at 0.2 C. Moreover, Ma et al. employed an N-deficient g-C_3N_4/CNT composite as the polysulfide barrier for Li–S batteries [277]. The defect chemistry of g-C_3N_4 enhanced its chemical affinity to polysulfides and promoted fast polysulfide conversion during cycles. Hence, the Li–S batteries displayed a high reversible capacity of 1128 mAh g^{-1} at 0.2 C and 567 mAh g^{-1} after 500 cycles at 1.0 C.

5.1.2. CNT/metal oxide-based interlayers

Similar to their utilization in the fabrication of sulfur hosts, metal oxides with high polarity can be hybridized with CNTs to fabricate interlayers. Metal oxides used in the fabrication of interlayers include MnO [279], TiO_2 [280, 281], ZnO [282], MoO_3 [283], and $CoNiFeO_x$ [284], and the prepared interlayers have significantly enhanced the electrochemical performance of Li–S batteries by confining polysulfides in the cathodic region. Wang et al. developed an ultrathin MnO_2/GO/CNT interlayer as an efficient polysulfide trapping shield for Li–S batteries through a simple layer-by-layer procedure (Fig. 14b) [279]. Owing to their physical confinement in the hierarchical nanostructures and chemical confinement by the oxygen-containing groups of GO and MnO_2, the intermediate polysulfides are well preserved and stored in the cathodic region, thus preventing their further diffusion toward the Li anode. Moreover, the long-range CNTs enhance the structural integrity and electrical conductivity of the entire electrode during cycles. Consequently, Li–S batteries with high sulfur loading contents of 60–80 wt% demonstrated a high rate capability of 747 mAh g^{-1} at 10 C along with an extremely low capacity fading rate of 0.029% per cycle. Notably, a low self-discharge rate was achieved with a capacity retention of 93.0% after 20 days of rest. In addition, Sun et al. fabricated an interlayer consisting of mesoporous TiO_2 threaded by CNTs via a vacuum-filtrated method [280]. Because of the good polysulfide suppression by both physical and chemical adsorption, the Li–S batteries displayed a low capacity decay of 0.07% per cycle for 500 cycles at 0.5 C.

5.1.3. Others

Other materials, such as metal sulfides [41], phosphides [285], polymers [286, 287], fluorides [288], and COFs [289], have also been used to construct functional interlayers by their rational combination with CNTs. The as-fabricated interlayers exhibited merits similar to that of interlayers comprising CNTs and metal oxides, thus effectively restricting polysulfide shuttling. Wang et al. verified that the Li–S battery performance was enhanced significantly when an ultrathin and lightweight MoS_2/CNT interlayer was used [41]. Notably, the CNTs served as a conductive network and supporting skeleton, whereas MoS_2 nanosheets adsorbed the polysulfides well through strong chemical affinity. A high specific capacity of 1237 mAh g^{-1} at 0.2 C and a remarkable capacity of 784 mAh g^{-1} at 10 C were obtained. Moreover, they developed a multifunctional interlayer consisting of MoP_2 and CNTs by a typical flux method to prevent polysulfide dissolution [285]. The CNTs not only act as the support for MoP_2 but offer fast electron transfer and good structural stability for the whole electrode. Consequently, the Li–S batteries equipped with the MoP_2/CNTs interlayer exhibited a reversible capacity of 905 mAh g^{-1} for 100 cycles at 0.2 C, accompanied by a capacity fading rate of 0.152% per cycle. These studies demonstrated that the introduction of interlayers is an effective solution for producing high-performance Li–S batteries.

5.2. CNT-modified separators for Li-S batteries

The modification of the separator is another feasible approach to intercept the polysulfide shuttling in Li–S batteries (**Table 4**) that is compatible with the current production line [290-292]. Carbonaceous materials and polar ingredients have been introduced into CNT matrices to improve their capability in preventing polysulfide shuttling [293]. Wu et al. used a CVD method to synthesize a 3D graphene@CNT composite, which is then coated on a separator to restrict polysulfide dissolution [294]. With S/carbon black as cathode, the Li–S batteries exhibited a high reversible capacity of 935.1 mAh g^{-1} at 0.2 C, and good cyclic stability with a specific capacity of 755.6 mAh g^{-1} after 200 cycles at 1.0 C. Moreover, Xia et al. fabricated an ultralight coating layer comprising MWCNTs and carbon quantum dots for Li–S batteries by a hydrothermal method [295]. The MWCNTs with excellent electrical conductivity and the carbon quantum dots capable of chemically adsorbing polysulfides built a physical shield against polysulfides. Benefiting from the synergistic effects of MWCNTs and carbon quantum dots, Li–S batteries displayed a high specific capacity of 1330.8 mAh g^{-1} and outstanding cyclic performance with a low capacity fading rate of 0.05% per cycle over 1000 cycles at 0.5 C. In addition, a porous carbon matrix [42], and g-C_3N_4 [296] have been integrated with CNTs to functionalize the separators for Li–S batteries, resulting in improved electrochemical performance.

Table 4
Electrochemical performance comparison of Li–S batteries with CNT-based interlayers and coating layers.

CNT-based layers	Morphology	Methods	Areal sulfur loading (mg cm^{-2})/electrode area	Sulfur content (wt.%)	Electrolyte/S ratio	Rate capability	Cyclic performance	Ref.
CNT interlayer	Porous structure	Filtration	3.0/1.54	80	–	1112 mAh g^{-1} at 0.1 C	Capacity retention of 95.8% after 100 cycles at 0.5 C	[272]
GO/CNT interlayer	Porous structure	Vacuum filtration	~1.0	27.8	20	469 mAh g^{-1} at 2.0 C	671 mAh g^{-1} after 300 cycles at 0.2 C	[276]
MnO_2/GO/CNT interlayer	Hierarchical porous structure	Layer-by-layer method	1.11~2.37	60~80	–	747 mAh g^{-1} at 10 C	Capacity fading rate of 0.029% after 2500 cycles at 1.0 C	[279]
MoP_2/CNT interlayer	Porous structure	Flux method	1.2	70	–	360 mAh g^{-1} at 5.0 C	905 mAh g^{-1} after 100 cycles at 0.2 C	[285]
CNT coating layer	Porous structure	Vacuum filtration	3.0	–	10	~1000 mAh g^{-1} at 2.0 C	1056 mAh g^{-1} after 400 cycles at 0.5 C	[290]
MWCNT/carbon quantum coating layer	Porous structure	Vacuum filtration	1.3~1.5	60	–	666.7 mAh g^{-1} at 3.0 C	1330.8 mAh g^{-1} after 1000 cycles at 0.5 C	[295]
Nb_2O_5/CNT coating layer	Tubular structure	Solvothermal method	1.3~1.5/1.13	80	14.6~15.4	507 mAh g^{-1} at 5.0 C	992 mAh g^{-1} after 100 cycles at 0.2 C	[297]
Sb_2S_3/CNT coating layer	Layered structure	Exfoliation method	~1.0	65	50	530 mAh g^{-1} at 2.0 C	Capacity fading rate of 0.05% after 200 cycles at 2.0 C	[307]
Ni@N-doped graphene/CNT coating layer	Porous structure	In situ growth method	1.0~1.2	70	~30	710.9 mAh g^{-1} at 5.0 C	265 mAh g^{-1} after 500 cycles at 10 C	[313]
Co_2B/CNT coating layer	Particle interconnected structure	Self-templated method	3.6	72.45	–	1172.8 mAh g^{-1} at 5.0 C	Capacity fading rate of 0.0072% after 3000 cycles at 5.0 C	[309]

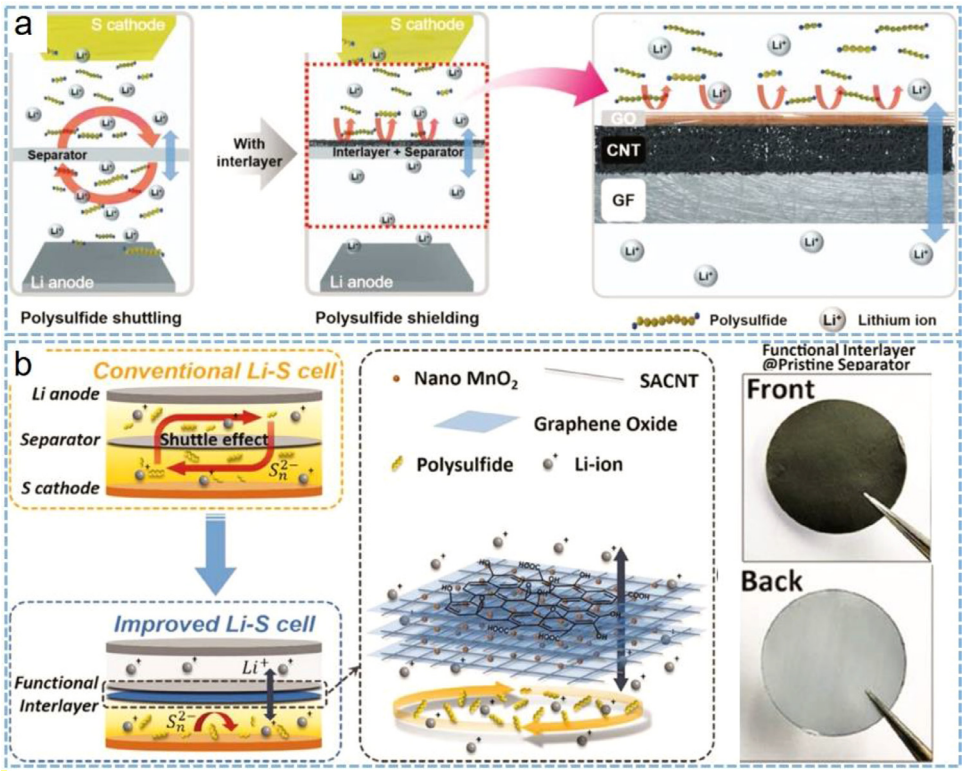

Fig. 14. (a) Schematic of the Li–S cell configuration with CNT/graphene interlayer. Reproduced with permission [275]. Copyright 2019, Wiley-VCH. (b) Schematic of the Li–S cell configuration with MnO_2/CNT/graphene interlayer. Reproduced with permission [279]. Copyright 2017, Wiley-VCH.

Although the coating layers comprising CNTs and other carbon matrices enhanced polysulfide utilization, the restriction was physical, and the electrochemical performance deteriorated, especially the long cyclic stability. Metal oxides with a strong chemical affinity to intermediate polysulfides have recently been combined with CNTs to modify the separator [297-304]. In addition, metal oxides can catalyze fast polysulfide conversion reactions during cycles. For example, Liu et al. employed a solvothermal method to make Nb_2O_5/CNT composite [297]. The construction of a conductive and catalytic Nb_2O_5/CNT layer provides a long-distance electron transfer network, strong chemisorption properties, and abundant catalytic sites for polysulfide conversion. As a result, a high specific capacity of 1286 mAh g^{-1} at 0.2 C, accompanied by a capacity decay rate of 0.23% per cycle, was achieved. Similarly, a lightweight multifunctional Sc_2O_3@CNT capping layer prepared by a solvothermal method was developed for loading onto the separator of Li–S batteries [298]. Benefiting from the synergistic effects of both physical and chemical confinement due to Sc_2O_3 and CNTs, the Li–S batteries demonstrated significantly enhanced electrochemical performance, in terms of specific capacity, rate capability, and long-term cyclic stability.

Additionally, other fillers, including polymers [305, 306], metal sulfides [307, 308], Co_2B [309], MOFs [310, 311], and metals [312, 313], have been integrated with CNTs to modify Li–S battery separators. Considering metal sulfides as a typical example, Kim et al. reported the use of a novel Sb_2S_3 nanosheet/CNT coupling layer on the separator surface via vacuum filtration for Li–S batteries [307]. The employment of 2D Sb_2S_3 nanosheets enables the exposure of a large surface area and therefore the abundant active sites, which are conducive to the chemical confinement of intermediate polysulfides, while the CNTs guarantee the high stability of Sb_2S_3 nanosheets and improve the reaction kinetics. The Li–S batteries with this modified separator demonstrated a high specific capacity and a remarkable capacity fading rate of 0.05% over 200 cycles at 2.0 C. Furthermore, theoretical simulations verified the important role of Sb_2S_3 nanosheets in trapping polysulfides and creating a low energy barrier for Li-ion diffusion. Wang et al. reported an efficient polysulfide barrier of Ni@N-doped graphene nanosheets/CNT hybrids via a CVD method [313]. The Ni@N-doped graphene nanosheets/CNT hybrids are capable of providing a large surface area for polysulfide adsorption, accelerating the electron transfer, and boosting polysulfide conversion kinetics. Consequently, the Li–S batteries exhibited a high specific capacity of 265 mAh g^{-1} after 500 cycles at 10 C. All these studies provide new insights into the utilization of CNTs to modify separators for enhancing the performance of Li–S batteries.

5.3. CNT-modified separators for Li-Se batteries

Similar to Li–S batteries, CNTs have been used to modify the separator for Li–Se batteries. As a representative example, Wang et al. prepared a mixture comprising an ultrathin cetrimonium bromide (CTAB)/CNTs/MXene hybrid by filtration to modify the separators in Li–Se batteries (1.0 M LiTFSI in DOL/DME, 1:1 in v/v) [314]. Owing to the existence of Lewis acid-base interactions between CTAB/MXene and polyselenides, polyselenide dissolution was well suppressed. Moreover, CNTs can be inserted into the MXene layers to facilitate electrolyte infiltration and ionic transport. As such, the Li–Se batteries demonstrated extremely high cyclic performance with a low capacity fading rate of 0.05% per cycle at 1.0 C. All these excellent results imply that the utilization of CNT-based composites is a promising approach for promoting commercial applications of Li–Se batteries.

To sum up, unremitting efforts have been paid to the construction of CNT-based interlayers/separators for LCBs and impressive electrochemical results were achieved. Notably, the combination of cathode design and functionalized interlayers/separators is capable to further improve the electrochemical performance. However, it is worth noting that most of the current results are based on the coin cells, and the overuse of Li supply and electrolyte amount artificially exaggerates the realistic performance. In addition, the addition of non-active components inevitably negates the energy density of the whole system. In this regard, much attention should be paid to the practical parameters used in industry, thus creating safe, low-cost, and high-performance LCBs.

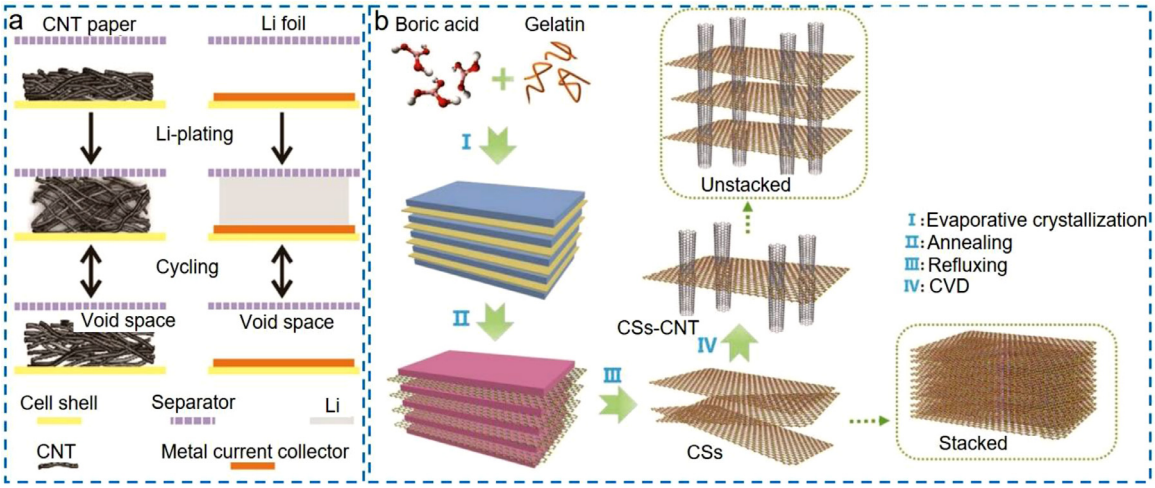

Fig. 15. (a) Schematic of volume expansion Li/CNT and Li-metal anodes during Li- plating/stripping. Reproduced with permission [324]. Copyright 2018, Wiley-VCH. (b) Schematic illustration of the synthesis of CSs-CNT and its behavior as the host material for Li metal anode. Reproduced with permission [327]. Copyright 2019, Wiley-VCH.

As discussed in the above sections, the utilization of CNTs in Li–S batteries have been extensively studied as compared to that in Li–Se and Li–Te batteries. This can be partially attributed to the higher specific energy of Li–S batteries. As shown in the above discussions, the volumetric energy densities of Li–Se and Li–Te batteries are comparable to Li–S batteries, indicating their great potential for applications in devices that require limited packing space. It is worth noting that a large proportion of carbon-based host materials are needed in Li–S batteries, which will inevitably further reduce their gravimetric and volumetric energy densities. Regarding the short history of Li–Se and Li–Te batteries begun in the past several years, the published papers in these two battery systems are still much fewer than those in Li–S counterparts. Meanwhile, the substantial achievement in Li–S batteries has triggered a surge of interest in Li–Se and Li–Te batteries, thus accelerating the development of Li–Se and Li–Te batteries. Currently, most of the studies focus on the construction of host materials for Li–Se and Li–Te batteries. Other strategies including the fabrication of interlayers and modification of separators need more exploration and optimization regarding the similar shuttling effects. With the continuous efforts on the exploration of CNTs for LCBs, their commercialization will be witnessed soon.

6. CNT-based composites for Li metal anodes

Besides the issues associated with chalcogen cathodes, the practical applications of LCBs are also hindered by the uneven Li deposition/dissolution, severe volume change of Li anode, and unstable SEI films, thus resulting in uncontrollable Li dendrite growth and low Coulombic efficiency [315]. Various strategies have been proposed to resolve these issues, including new electrolyte formulation, artificial SEI design, novel Li hosts [316-318]. CNTs with high electrical conductivity and tunable surface characteristics are well suited for Li metal hosts. various CNT architectures, including 3D CNT network/skeleton/framework [319-321], CNT sphere [322], CNT sponge [49, 323], and CNT paper [324] have been reported to improve the stability of Li metal anode. Yu et al. prepared a Li metal host consisting of CNTs with trenches in a free-standing porous CNT sponge using a novel mechanochemical method [49]. The created trenches provided lithiophilic surface for Li metal anodes, and the large specific surface area significantly reduced the local current density for uniform Li deposition. As a result, when coupled with sulfur cathodes, the as-achieved batteries exhibited a remarkable specific areal capacity of 13.3 mAh cm^{-2}, attributing to the improved reaction kinetics and decreased overpotentials. Moreover, Ji et al. synthesized a lightweight mechanically robust CNT paper as the freestanding framework to resolve the issues faced by Li metal anode (Fig. 15a) [324]. Benefiting from the intrinsic physicochemical properties (large surface area, high electrical conductivity, and elastic properties) of CNTs, the Li metal dendrites were greatly suppressed. Consequently, a high areal capacity of 10 mAh cm^{-2} with 90.9% of Li metal utilization for 1000 cycles at 10 mA cm^{-2} was finally achieved.

Surface functionalization has also been developed to enhance the interaction between Li and CNTs for governing the growth of Li [325, 326]. Xiong et al. fabricated a lithiophilic amide-functionalized CNT skeleton for Li metal anodes [325]. The functionalized CNT skeletons with a large surface area not only reduced the local current density but also promoted the uniform growth of Li metal thanks to the strong interactions between Li^+ and lithiophilic functional groups. Consequently, the as-obtained electrodes showed a low overpotential of 14 mV, accompanied by high Coulombic efficiency of ~97.8% for 300 cycles. More impressively, the amide-functionalized CNT skeleton displayed dendrite-free morphology for 1800 h, which is remarkable compared to the untreated counterpart. The weak interactions and poor contact among individual CNT have led to large contact resistance and weak structural integrity, which may degrade during repeated volume expansion and shrinkage. To resolve the above issues, Sun et al. prepared a new structure comprising of an N-doped CNT forest planted on the surface of N-doped carbon sheets (CSs-CNT) (Fig. 15b) [327]. The N atoms provided abundant Li nucleation sites, the voids accommodated the volume expansion of Li, resulting in smooth and uniform Li deposition. More importantly, the adoption of CSs-CNT enhanced the total structural stability and the capacity for encapsulating Li metal. Eventually, the electrode exhibited a high Coulombic efficiency of 98.8% for 2000 h with a low overpotential. In addition, Wang et al. confirmed that a self-standing CNT aerogel integrated with amorphous carbon coating can serve as a stable host for encapsulating Li metal [328].

Metal oxides with a high affinity to Li have been incorporated into CNT frameworks to act as nucleation sites during the Li plating process [50, 329, 330]. Li et al. fabricated stretchable fiber-shaped Li metal anodes by using the CNT fibers modified with lithiophilic ZnO nanowire arrays to infiltrate molten Li [50]. The CNT fiber provides a well-defined conductive network for electron transfer and served as a support for ZnO nanowires, while the ZnO nanowire arrays increase the lithiophilicity of CNT fiber (Fig. 16a). As a result, the composite Li anode showed excellent cyclic stability under a strain of 100%, accompanying a dendrite-free morphology during long-term cycles. Moreover, Hu et al. synthesized a 3D CNT sponge modified with an Al_2O_3 coating layer for serving as a metallic Li host [329]. The Al_2O_3 decorated CNT sponge with

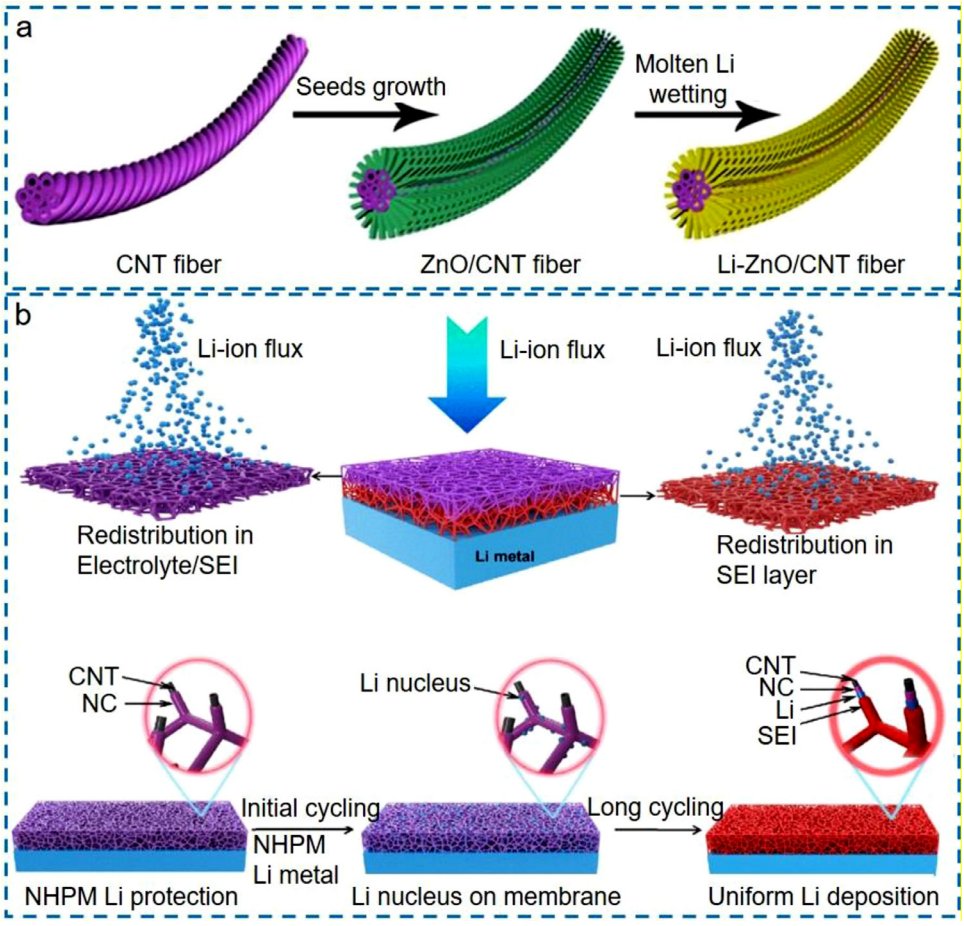

Fig. 16. (a) Schematical illustration of the fabrication process of the fiber-shaped Li metal anode. Reproduced with permission [50]. Copyright 2019, Elsevier. (b) Schematical illustration of the redistributed Li^+ flux in the presence of NHPM as well as the nucleation and uniform deposition of Li^+ on NHPM. Reproduced with permission [334]. Copyright 2021, Elsevier.

a large surface area lowers the local current density for Li deposition and offers abundant nucleation sites to induce homogeneous Li growth. The as-prepared electrode displayed a stable voltage with an extremely low overpotential of 16–30 mV for 100 h at 1.0 mA cm^{-2}. Impressively, the electrode showed a dendrite-free morphology, with a Coulombic efficiency of 92.4% for 80 cycles at 1.0 mA cm^{-2}. Other metal oxides, such as Sb_2MoO_6 [331] and SiO_2 [332], were also hybridized with CNT architectures to realize stable and reversible Li plating/stripping.

Besides the design and construction of Li metal hosts, the introduction of modification layers on Li metal anodes is another easy and effective way to suppress Li dendrite growth [333-335]. Lu and co-workers developed an MWCNT interlayer to alleviate the problematic Li dendrite growth [333]. The structure can efficiently relieve the volume expansion of Li metal during deposition, thus leading to smooth Li morphology and stable cyclic stabilities under various current rates. Moreover, He et al. prepared a hierarchical porous layer comprising CNT core and N-doped hierarchically porous membranes (NHPM) to homogenize Li^+ ions at electrolyte/SEI interface (Fig. 16b) [334]. The doped N atoms are capable to adsorb Li^+ and reduce the energy barrier for Li^+ diffusion on the carbon surface, while the high specific surface area provides more nucleation sites and lowers the local current density on Li anode. The modified Li anodes exhibited a remarkable Coulombic efficiency of ~99% and a dendrite-free morphology for 500 h even under 8 mA cm^{-2}.

Owing to their ultrahigh electrical conductivity, large specific surface areas, and excellent mechanical properties, CNTs are widely deemed to be a promising material to construct Li hosts and protective layers. Through surface modification and hybridization, CNT-based assemblies have shown exciting performance in guiding uniform Li deposition and maintaining electrode integrity. However, the construction of CNT architectures requires multi-steps and high costs. In addition, the performance of CNT assemblies is usually worse than the building units because of the weak interactions and large contact resistance. In this regard, crosslinked CNT frameworks are desired and deserve more attention. Since Li tends to nucleate on the top region of conductive skeletons, proper modification of CNTs at different locations, such as designing conductivity and lithiophilicity gradients, is the key to achieving better Li deposition and utilization in 3D conductive hosts.

7. Conclusions and perspectives

LCBs with high theoretical capacities and energy densities have been recognized as promising alternatives to LIBs. However, the practical application of LCBs is hindered by the severe volume expansion of chalcogen cathodes, dissolution and diffusion of intermediates in ether-based electrolytes, sluggish redox reaction kinetics, and problematic Li dendrite growth. CNTs with diverse micro-and nanostructures have been adopted to resolve these issues with much improved electrochemical performance. This review discusses the recent advances in CNTs for LCBs with respect to their diversified roles in the cathode, anode, and interlayer/separator. Although significant progress has been achieved, issues and challenges remain to be resolved. The following are some of the main challenges in the development of CNT-based LCBs.

(1) Scalable manufacturing of CNTs remains a hurdle for practical applications in LCBs. The CNT synthesis with controllable chirality, super-alignment, and predetermined size and length is still challenging. Although the fabrication cost of CNTs has been reduced significantly, the available products are still expensive than other carbonaceous materials (*e.g.*, carbon black), especially for SWCNTs and super-aligned CNTs. In addition, the processing of CNT assemblies is

still difficult because of the strong coupling among CNT structures and the inert surface properties, and post-treatments.

(2) High-performance CNT assemblies should be constructed for both the cathode, interlayer, separator, and anode. Up to date, various CNT assemblies, including 0D microspheres, 1D fibers, 2D films, and 3D aerogels/foams, have been developed to load a high mass of chalcogens and Li metal. Although CNT itself has shown excellent mechanical strength and electrical conductivity, the assemblies exhibit relatively poor properties caused by the weak interactions and poor contact among individual CNTs. In this regard, interconnected structures should be constructed to establish fast electron/ion transportation and good structural stability. Since CNT assemblies normally have a large surface area, low packing density, and high porosity, the volumetric energy densities of LCBs are debated. On the other hand, large surface area and high porosity are required to allow high active material loading [336], provide abundant active sites to promote chalcogen redox reactions and guide Li deposition and accommodate the volume variation during electrochemical processes. In this regard, the balance among different critical parameters is necessary to improve the overall performance.

(3) The precise control in the functionalization of CNTs is crucial to LCBs and needs systematic study. The inert surface of pure CNTs brings about good chemical stability but leads to poor interaction with soluble intermediates, causing serious shuttling effects. Surface modification by heteroatoms, functional groups, and polar inorganic species can offer strong interactions with soluble polychalcogenides and Li metal, thus ensuring high chalcogen utilization and homogeneous Li growth. However, these treatments inevitably induce defects, thus giving rise to lower electrical conductivity, degraded mechanical stability, and inferior chemical stability. More importantly, the surface modification should be tailored to meet the requirements for each component in LCBs. For example, when serving as the chalcogen hosts and intermediate blocking layers, components that can chemically anchor soluble intermediates and catalyze the conversion are of great interest and should be implanted into the CNT skeletons to achieve high chalcogen utilization. To promote dendrite-free Li growth, the lithiophilicity of CNT substrates should be modulated by heteroatom doping and by introducing nucleation seeds [337,338]. In addition, modifying CNTs with different properties at different locations precisely (*i.e.*, graded structure) is another intriguing direction that deserves more attention for the applications in LCBs.

(4) Apart from the rational design of CNT skeletons, other components that significantly affect the performance of LCBs should also be explored to push their commercialization. Currently, ether-based electrolytes are widely used in research; however, the notorious shuttle effects in such electrolytes trigger continuous intermediate dissolution and significant side reactions that corrode the Li anode, which results in inferior cyclic stability. In addition, ether electrolytes are extremely volatile and highly flammable, thus causing serious safety concerns. Therefore, safer electrolytes that are compatible with both Li anodes and chalcogen cathodes are required. Very recently, the development of all-solid-state inorganic electrolytes is flourishing, which is expected to resolve the shuttling of soluble intermediates and prevent Li dendrite growth [56]. In addition, practical cell parameters should be used to evaluate the realistic performance of LCBs.

(5) The working mechanisms of different LCBs should be determined and clarified. Owing to the different physicochemical properties of chalcogens, the working mechanisms of LCBs may differ slightly. It has been reported that the working principles of Li–S and Li–Se batteries in ether and carbonate electrolytes show huge differences and are still controversial. For the Li–Te system, the mechanistic studies are far behind those in Li–S counterpart, offering a great opportunity in this field. More importantly, understanding the reaction mechanisms of LCBs, especially those of Li–Se and Li–Te batteries, is of great importance to select suitable strategies for improving their performance. In this regard, there is an urgent need to employ advanced characterization techniques, such as in situ Raman spectroscopy, in situ ultraviolet spectroscopy, and in situ transmission electron microscopy, as well as high-throughput calculations to understand the fundamental mechanisms in detail.

In summary, CNTs with unique physical and chemical properties have gained tremendous interest for use in LCBs. Although great progress has been achieved, research in this regard is still in its infancy. Thus, numerous efforts are urgently needed to devote to further experimental research and theoretical simulations. Given the rapid development and thorough understanding of the multiple functions and working mechanisms of CNTs in LCBs, the commercialization of LCBs is expected to be realized soon.

Declaration of competing interest

The authors declare that they have no known competing financial interests or personal relationships that could have appeared to influence the work reported in this paper.

Acknowledgments

This project was financially supported by the National Key Research and Development Program of China (2017YFA0208200), the Natural Science Foundation of China (22005003, 22022505, 21872069), the Fundamental Research Funds for the Central Universities of China (0205-14380266), the Scientific Research Foundation of Anhui University of Technology for Talent Introduction (DT19100069), the Yong Scientific Research Foundation of Anhui University of Technology (QZ202003), the Natural Science Foundation of Jiangsu Province (BK20180008) and the Shenzhen Fundamental Research Program of Science, Technology and Innovation Commission of Shenzhen Municipality (JCYJ20180307155007589).

References

[1] B. Dunn, H. Kamath, J.-M. Tarascon, Electrical energy storage for the grid: a battery of choices, Science 334 (2011) 928–935.
[2] J. Jiang, Y. Li, J. Liu, X. Huang, C. Yuan, X.W. Lou, Recent advances in metal oxide-based electrode architecture design for electrochemical energy storage, Adv. Mater. 24 (2012) 5166–5180.
[3] J.B. Goodenough, Y. Kim, Challenges for rechargeable Li batteries, Chem. Mater. 22 (2010) 587–603.
[4] P.G. Bruce, B. Scrosati, J.-M. Tarascon, Nanomaterials for rechargeable lithium batteries, Angew. Chem. Int. Ed. 47 (2008) 2930–2946.
[5] V. Etacheri, R. Marom, R. Elazari, G. Salitra, D. Aurbach, Challenges in the development of advanced Li-ion batteries: a review, Energy Environ. Sci. 4 (2011) 3243–3262.
[6] E. Yoo, J. Kim, E. Hosono, H.-S. Zhou, T. Kudo, I. Honma, Large reversible Li storage of graphene nanosheet families for use in rechargeable lithium ion batteries, Nano Lett 8 (2008) 2277–2282.
[7] N. Yabuuchi, K. Kubota, M. Dahbi, S. Komaba, Research development on sodium-ion batteries, Chem. Rev. 114 (2014) 11636–11682.
[8] Z. Jian, W. Luo, X. Ji, Carbon Electrodes for K-ion batteries, J. Am. Chem. Soc. 137 (2015) 11566–11569.
[9] G. Wang, L. Zhang, J. Zhang, A review of electrode materials for electrochemical supercapacitors, Chem. Soc. Rev. 41 (2012) 797–828.
[10] J. Wu, M. Ihsan-Ul-Haq, F. Ciucci, B. Huang, J.-K. Kim, Rationally designed nanostructured metal chalcogenides for advanced sodium-ion batteries, Energy Storage Mater. 34 (2021) 582–628.
[11] L. Ma, Y. Lv, J. Wu, C. Xia, Q. Kang, Y. Zhang, H. Liang, Z. Jin, Recent advances in anode materials for potassium-ion batteries: a review, Nano Res (2021) doi.org/10.1007/s12274-021-3439-3.
[12] A. Manthiram, Y. Fu, S.-H. Chung, C. Zu, Y.-S. Su, Rechargeable lithium–sulfur batteries, Chem. Rev. 114 (2014) 11751–11787.
[13] C.-P. Yang, S. Xin, Y.-X. Yin, H. Ye, J. Zhang, Y.-G. Guo, An advanced selenium—carbon cathode for rechargeable lithium–selenium batteries, Angew. Chem. Int. Ed. 52 (2013) 8363–8367.
[14] J. He, Y. Chen, W. Lv, K. Wen, Z. Wang, W. Zhang, Y. Li, W. Qin, W. He, Three-dimensional hierarchical reduced graphene oxide/tellurium nanowires: a high-performance freestanding cathode for Li–Te batteries, ACS Nano 10 (2016) 8837–8842.

[15] T. Zhou, W. Lv, J. Li, G. Zhou, Y. Zhao, S. Fan, B. Liu, B. Li, F. Kang, Q.-H. Yang, Twinborn TiO2–TiN heterostructures enabling smooth trapping–diffusion–conversion of polysulfides towards ultralong life lithium–sulfur batteries, Energy Environ. Sci. 10 (2017) 1694–1703.
[16] M. Liu, X. Qin, Y.-B. He, B. Li, F. Kang, Recent innovative configurations in high--energy lithium–sulfur batteries, J. Mater. Chem. A 5 (2017) 5222–5234.
[17] X. Xu, D. Zhou, X. Qin, K. Lin, F. Kang, B. Li, D. Shanmukaraj, T. Rojo, M. Armand, G. Wang, A room-temperature sodium–sulfur battery with high capacity and stable cycling performance, Nat. Commun. 9 (2018) 3870.
[18] H.-J. Peng, J.-Q. Huang, Q. Zhang, A review of flexible lithium–sulfur and analogous alkali metal–chalcogen rechargeable batteries, Chem. Soc. Rev. 46 (2017) 5237–5288.
[19] S. Li, Z. Fan, Encapsulation methods of sulfur particles for lithium-sulfur batteries: a review, Energy Storage Mater. 34 (2021) 107–127.
[20] Y.-X. Yin, S. Xin, Y.-G. Guo, L.-J. Wan, Lithium–sulfur batteries: electrochemistry, materials, and prospects, Angew. Chem. Int. Ed. 52 (2013) 13186–13200.
[21] J. Xu, J. Ma, Q. Fan, S. Guo, S. Dou, Recent progress in the design of advanced cathode materials and battery models for high-performance lithium-X (X = O_2, S, Se, Te, I_2, Br_2) Batteries, Adv. Mater. 29 (2017) 1606454.
[22] Y. Liu, J. Wang, Y. Xu, Y. Zhu, D. Bigio, C. Wang, Lithium–tellurium batteries based on tellurium/porous carbon composite, J. Mater. Chem. A 2 (2014) 12201–12207.
[23] J. Wu, Q. Liang, X. Yu, Q.-F. Lü, L. Ma, X. Qin, G. Chen, B. Li, Deep eutectic solvents for boosting electrochemical energy storage and conversion: a review and perspective, Adv. Funct. Mater. 31 (2021) 2011102.
[24] P. Bonnick, J. Muldoon, The Dr Jekyll and Mr Hyde of lithium sulfur batteries, Energy Environ. Sci. 13 (2020) 4808–4833.
[25] X. Ji, K.T. Lee, L.F. Nazar, A highly ordered nanostructured carbon–sulphur cathode for lithium–sulphur batteries, Nat. Mater. 8 (2009) 500–506.
[26] A. Manthiram, Y. Fu, Y.-S. Su, Challenges and prospects of lithium–sulfur batteries, Acc. Chem. Res. 46 (2013) 1125–1134.
[27] A. Eftekhari, The rise of lithium–selenium batteries, Sustain. Energy Fuels 1 (2017) 14–29.
[28] Y. Li, Y. Zhang, Q. Xu, L. Hu, B. Shen, H. Liu, C. Dai, S. Bao, M. Xu, Nitrogen–doped carbon as a host for tellurium for high-rate Li–Te and Na–Te batteries, ChemSusChem 12 (2019) 1196–1202.
[29] H. Pan, Z. Cheng, J. Chen, R. Wang, X. Li, High sulfur content and volumetric capacity promised by a compact freestanding cathode for high-performance lithium–sulfur batteries, Energy Storage Mater. 27 (2020) 435–442.
[30] Q. Wu, L. Yang, X. Wang, Z. Hu, From carbon-based nanotubes to nanocages for advanced energy conversion and storage, Acc. Chem. Res. 50 (2017) 435–444.
[31] R. Fang, K. Chen, L. Yin, Z. Sun, F. Li, H.-M. Cheng, The regulating role of carbon nanotubes and graphene in lithium-ion and lithium–sulfur Batteries, Adv. Mater. 31 (2019) 1800863.
[32] H. Wei, Y. Liu, X. Zhai, F. Wang, X. Ren, F. Tao, T. Li, G. Wang, F. Ren, Application of carbon nanotube-based materials as interlayers in high-performance lithium-sulfur batteries: a review, Front. Energy Res. 8 (2020) 585795.
[33] T. Chen, B. Cheng, G. Zhu, R. Chen, Y. Hu, L. Ma, H. Lv, Y. Wang, J. Liang, Z. Tie, Z. Jin, J. Liu, Highly efficient retention of polysulfides in “sea urchin”-like carbon nanotube/nanopolyhedra superstructures as cathode material for ultralong-life lithium–sulfur batteries, Nano Lett 17 (2017) 437–444.
[34] X.-M. Liu, Z.d. Huang, S.w. Oh, B. Zhang, P.-C. Ma, M.M.F. Yuen, J.-K. Kim, Carbon nanotube (CNT)-based composites as electrode material for rechargeable Li-ion batteries: a review, Compos. Sci. Technol. 72 (2012) 121–144.
[35] P. Zuo, H. Zhang, M. He, Q. Li, Y. Ma, C. Du, X. Cheng, H. Huo, Y. Gao, G. Yin, Clew–like N-doped multiwalled carbon nanotube aggregates derived from metal-organic complexes for lithium-sulfur batteries, Carbon 122 (2017) 635–642.
[36] Z. Ye, Y. Jiang, J. Qian, W. Li, T. Feng, L. Li, F. Wu, R. Chen, Exceptional adsorption and catalysis effects of hollow polyhedra/carbon nanotube confined CoP nanoparticles superstructures for enhanced lithium–sulfur batteries, Nano Energy 64 (2019) 103965.
[37] J. Meng, C. Niu, L. Xu, J. Li, X. Liu, X. Wang, Y. Wu, X. Xu, W. Chen, Q. Li, Z. Zhu, D. Zhao, L. Mai, General oriented formation of carbon nanotubes from metal–organic frameworks, J. Am. Chem. Soc. 139 (2017) 8212–8221.
[38] C. Wang, J. Kim, J. Tang, M. Kim, H. Lim, V. Malgras, J. You, Q. Xu, J. Li, Y. Yamauchi, New strategies for novel MOF-derived carbon materials based on nanoarchitectures, Chem 6 (2020) 19–40.
[39] X. Wang, A. Dong, Y. Hu, J. Qian, S. Huang, A review of recent work on using metal–organic frameworks to grow carbon nanotubes, Chem. Commun. 56 (2020) 10809–10823.
[40] C. Tang, Q. Zhang, M.-Q. Zhao, J.-Q. Huang, X.-B. Cheng, G.-L. Tian, H.-J. Peng, F. Wei, Nitrogen-doped aligned carbon nanotube/graphene sandwiches: facile catalytic growth on bifunctional natural catalysts and their applications as scaffolds for high-rate lithium-sulfur batteries, Adv. Mater. 26 (2014) 6100–6105.
[41] L. Yan, N. Luo, W. Kong, S. Luo, H. Wu, K. Jiang, Q. Li, S. Fan, W. Duan, J. Wang, Enhanced performance of lithium-sulfur batteries with an ultrathin and lightweight MoS_2/carbon nanotube interlayer, J. Power Sources 389 (2018) 169–177.
[42] L. Tan, X. Li, Z. Wang, H. Guo, J. Wang, L. An, Multifunctional separator with porous carbon/multi-walled carbon nanotube coating for advanced lithium–sulfur batteries, ChemElectroChem 5 (2018) 71–77.
[43] M.-Q. Zhao, X.-F. Liu, Q. Zhang, G.-L. Tian, J.-Q. Huang, W. Zhu, F. Wei, Graphene/single-walled carbon nanotube hybrids: one-step catalytic growth and applications for high-rate Li–S batteries, ACS Nano 6 (2012) 10759–10769.
[44] C. Jin, W. Zhang, Z. Zhuang, J. Wang, H. Huang, Y. Gan, Y. Xia, C. Liang, J. Zhang, X. Tao, Enhanced sulfide chemisorption using boron and oxygen dually doped multi-walled carbon nanotubes for advanced lithium–sulfur batteries, J. Mater. Chem. A 5 (2017) 632–640.
[45] L. Ma, H.L. Zhuang, S. Wei, K.E. Hendrickson, M.S. Kim, G. Cohn, R.G. Hennig, L.A. Archer, Enhanced Li–S batteries using amine-functionalized carbon nanotubes in the cathode, ACS Nano 10 (2016) 1050–1059.
[46] D. Cheng, Y. Zhao, X. Tang, T. An, X. Wang, H. Zhou, D. Zhang, T. Fan, Densely integrated Co, N-codoped graphene@carbon nanotube porous hybrids for high-performance lithium-sulfur batteries, Carbon 149 (2019) 750–759.
[47] X. Zhou, L. Li, J. Yang, L. Xu, J. Tang, Cobalt and molybdenum carbide nanoparticles grafted on nitrogen-doped carbon nanotubes as efficient chemical anchors and polysulfide conversion catalysts for lithium-sulfur batteries, ChemElectroChem 7 (2020) 3767–3775.
[48] D. Zhu, T. Long, B. Xu, Y. Zhao, H. Hong, R. Liu, F. Meng, J. Liu, Recent advances in interlayer and separator engineering for lithium-sulfur batteries, J. Energy Chem. 57 (2021) 41–60.
[49] G. Yang, J. Tan, H. Jin, Y.H. Kim, X. Yang, D.H. Son, S. Ahn, H. Zhou, C. Yu, Creating effective nanoreactors on carbon nanotubes with mechanochemical treatments for high-areal-capacity sulfur cathodes and lithium anodes, Adv. Funct. Mater. 28 (2018) 1800595.
[50] X. Wang, Z. Pan, J. Yang, Z. Lyu, Y. Zhong, G. Zhou, Y. Qiu, Y. Zhang, J. Wang, W. Li, Stretchable fiber-shaped lithium metal anode, Energy Storage Mater 22 (2019) 179–184.
[51] X. Zhou, P. Gao, S. Sun, D. Bao, Y. Wang, X. Li, T. Wu, Y. Chen, P. Yang, Amorphous, crystalline and crystalline/amorphous selenium nanowires and their different (de)lithiation mechanisms, Chem. Mater. 27 (2015) 6730–6736.
[52] Z.W. Seh, Y. Sun, Q. Zhang, Y. Cui, Designing high-energy lithium–sulfur batteries, Chem. Soc. Rev. 45 (2016) 5605–5634.
[53] Y.-H. Wang, X.-T. Li, W.-P. Wang, H.-J. Yan, S. Xin, Y.-G. Guo, Chalcogen cathode and its conversion electrochemistry in rechargeable Li/Na batteries, Sci. China Chem. 63 (2020) 1402–1415.
[54] Z. Li, L. Yin, Nitrogen-doped MOF-derived micropores carbon as immobilizer for small sulfur molecules as a cathode for lithium sulfur batteries with excellent electrochemical performance, ACS Appl. Mater. Interfaces 7 (2015) 4029–4038.
[55] J. Wu, J. Liu, Z. Lu, K. Lin, Y.-Q. Lyu, B. Li, F. Ciucci, J.-K. Kim, Non-flammable electrolyte for dendrite-free sodium-sulfur battery, Energy Storage Mater. 23 (2019) 8–16.
[56] L.-P. Hou, H. Yuan, C.-Z. Zhao, L. Xu, G.-L. Zhu, H.-X. Nan, X.-B. Cheng, Q.-B. Liu, C.-X. He, J.-Q. Huang, Q. Zhang, Improved interfacial electronic contacts powering high sulfur utilization in all-solid-state lithium–sulfur batteries, Energy Storage Mater. 25 (2020) 436–442.
[57] Y. Liu, L. Si, X. Zhou, X. Liu, Y. Xu, J. Bao, Z. Dai, A selenium-confined microporous carbon cathode for ultrastable lithium–selenium batteries, J. Mater. Chem. A 2 (2014) 17735–17739.
[58] C. Luo, J. Wang, L. Suo, J. Mao, X. Fan, C. Wang, In situ formed carbon bonded and encapsulated selenium composites for Li–Se and Na–Se batteries, J. Mater. Chem. A 3 (2015) 555–561.
[59] J. Zhang, L. Fan, Y. Zhu, Y. Xu, J. Liang, D. Wei, Y. Qian, Selenium/interconnected porous hollow carbon bubbles composites as the cathodes of Li–Se batteries with high performance, Nanoscale 6 (2014) 12952–12957.
[60] J. Zhang, Y. Xu, L. Fan, Y. Zhu, J. Liang, Y. Qian, Graphene–encapsulated selenium/polyaniline core–shell nanowires with enhanced electrochemical performance for Li–Se batteries, Nano Energy 13 (2015) 592–600.
[61] C. Luo, Y. Xu, Y. Zhu, Y. Liu, S. Zheng, Y. Liu, A. Langrock, C. Wang, Selenium@mesoporous carbon composite with superior lithium and sodium storage capacity, ACS Nano 7 (2013) 8003–8010.
[62] J. Sun, Z. Du, Y. Liu, W. Ai, K. Wang, T. Wang, H. Du, L. Liu, W. Huang, State-of-the-art and future challenges in high energy lithium–selenium batteries, Adv. Mater. 33 (2021) 2003845.
[63] Y. Cui, A. Abouimrane, C.-J. Sun, Y. Ren, K. Amine, Li–Se battery: absence of lithium polyselenides in carbonate based electrolyte, Chem. Commun. 50 (2014) 5576–5579.
[64] Y. Zhang, W. Lu, P. Zhao, M.H. Aboonasr Shiraz, D. Manaig, D.J. Freschi, Y. Liu, J. Liu, A durable lithium–tellurium battery: effects of carbon pore structure and tellurium content, Carbon 173 (2021) 11–21.
[65] J. Zhang, Y.-X. Yin, Y. You, Y. Yan, Y.-G. Guo, A high-capacity tellurium@carbon anode material for lithium-ion batteries, Energy Technol 2 (2014) 757–762.
[66] N. Ding, S.-F. Chen, D.-S. Geng, S.-W. Chien, T. An, T.S.A. Hor, Z.-L. Liu, S.-H. Yu, Y. Zong, Tellurium@ordered macroporous carbon composite and free-standing tellurium nanowire mat as cathode materials for rechargeable lithium–tellurium batteries, Adv. Energy Mater. 5 (2015) 1401999.
[67] Y. Li, L. Hu, B. Shen, C. Dai, Q. Xu, D. Liu, J. Jiang, Y. Li, M. Xu, Rib-like hierarchical porous carbon as reservoir for long-life and high-rate Li-Te batteries, Electrochim. Acta 250 (2017) 10–15.
[68] G. Liang, J. Wu, X. Qin, M. Liu, Q. Li, Y.-B. He, J.-K. Kim, B. Li, F. Kang, Ultrafine TiO_2 decorated carbon nanofibers as multifunctional interlayer for high-performance lithium–sulfur battery, ACS Appl. Mater. Interfaces 8 (2016) 23105–23113.
[69] J. Wu, F. Ciucci, J.-K. Kim, Molybdenum disulfide based nanomaterials for rechargeable batteries, Chem. Eur. J. 26 (2020) 6296–6319.
[70] H. Tabassum, A. Mahmood, B. Zhu, Z. Liang, R. Zhong, S. Guo, R. Zou, Recent advances in confining metal-based nanoparticles into carbon nanotubes for electrochemical energy conversion and storage devices, Energy Environ. Sci. 12 (2019) 2924–2956.
[71] X.-Y. Yang, J.-J. Xu, Z.-W. Chang, D. Bao, Y.-B. Yin, T. Liu, J.-M. Yan, D.-P. Liu, Y. Zhang, X.-B. Zhang, Blood-capillary-inspired, free-standing, flexible, and low–cost super-hydrophobic N-CNTs@SS cathodes for high-capacity, high-rate, and stable Li-air batteries, Adv. Energy Mater. 8 (2018) 1702242.

[72] X. Liu, Q. Zhang, J. Huang, S. Zhang, H. Peng, F. Wei, Hierarchical nanostructured composite cathode with carbon nanotubes as conductive scaffold for lithium-sulfur batteries, J. Energy Chem. 22 (2013) 341–346.
[73] J. Yan, X. Liu, X. Wang, B. Li, Long-life, high-efficiency lithium/sulfur batteries from sulfurized carbon nanotube cathodes, J. Mater. Chem. A 3 (2015) 10127–10133.
[74] M. Hagen, S. Dörfler, H. Althues, J. Tübke, M.J. Hoffmann, S. Kaskel, K. Pinkwart, Lithium–sulphur batteries – binder free carbon nanotubes electrode examined with various electrolytes, J. Power Sources 213 (2012) 239–248.
[75] L. Zhu, W. Zhu, X.-B. Cheng, J.-Q. Huang, H.-J. Peng, S.-H. Yang, Q. Zhang, Cathode materials based on carbon nanotubes for high-energy-density lithium–sulfur batteries, Carbon 75 (2014) 161–168.
[76] Q. Zhang, N. Huang, Z. Huang, L. Cai, J. Wu, X. Yao, CNTs@S composite as cathode for all-solid-state lithium-sulfur batteries with ultralong cycle life, J. Energy Chem. 40 (2020) 151–155.
[77] J. Hu, T. Zhao, X. Ji, X. Peng, W. Jin, W. Yang, L. Zhang, J. Gao, A. Dang, H. Li, T. Li, Synthesis and electrochemical property of amorphous carbon nanotubes wrapped sulfur particles as cathode material for lithium-sulfur batteries, Chem. Phys. Lett. 688 (2017) 59–65.
[78] L. Qu, P. Liu, P. Zhang, T. Wang, Y. Yi, P. Yang, X. Tian, M. Li, B. Yang, Carbon-nanotube/sulfur cathode with in-situ assembled Si_3N_4/graphene interlayer for high-rate and long cycling-life lithium-sulfur batteries, Electrochim. Acta 296 (2019) 155–164.
[79] S.-C. Han, M.-S. Song, H. Lee, H.-S. Kim, H.-J. Ahn, J.-Y. Lee, Effect of multiwalled carbon nanotubes on electrochemical properties of lithium/sulfur rechargeable batteries, J. Electrochem. Soc. 150 (2003) A889–A893.
[80] C. Fu, M.B. Oviedo, Y. Zhu, A. von Wald Cresce, K. Xu, G. Li, M.E. Itkis, R.C. Haddon, M. Chi, Y. Han, B.M. Wong, J. Guo, Confined lithium–sulfur reactions in narrow-diameter carbon nanotubes reveal enhanced electrochemical reactivity, ACS Nano 12 (2018) 9775–9784.
[81] S. Kim, H. Song, Y. Jeong, Flexible catholyte@carbon nanotube film electrode for high-performance lithium sulfur battery, Carbon 113 (2017) 371–378.
[82] Y. Zhou, C. Zhou, Q. Li, C. Yan, B. Han, K. Xia, Q. Gao, J. Wu, Enabling prominent high-rate and cycle performances in one lithium–sulfur battery: designing permselective gateways for Li^+ transportation in holey-CNT/S cathodes, Adv. Mater. 27 (2015) 3774–3781.
[83] Z.-Z. Pan, W. Lv, Y.-B. He, Y. Zhao, G. Zhou, L. Dong, S. Niu, C. Zhang, R. Lyu, C. Wang, H. Shi, W. Zhang, F. Kang, H. Nishihara, Q.-H. Yang, A nacre-like carbon nanotube sheet for high performance Li-polysulfide batteries with high sulfur loading, Adv. Sci. 5 (2018) 1800384.
[84] J.-G. Wang, H. Liu, X. Zhang, X. Li, X. Liu, F. Kang, Green synthesis of hierarchically porous carbon nanotubes as advanced materials for high-efficient energy storage, Small 14 (2018) 1703950.
[85] Y. Feng, H. Zhang, Y. Zhang, X. Qu, C–S bonds in sulfur-embedded graphene, carbon nanotubes, and flake graphite cathodes for lithium–sulfur batteries, ACS Omega 4 (2019) 16352–16359.
[86] J. Shi, Q. Kang, Y. Mi, Q. Xiao, Nitrogen-doped hollow porous carbon nanotubes for high-sulfur loading Li–S batteries, Electrochim. Acta 324 (2019) 134849.
[87] L. Chen, C. Xu, L. Yang, M. Zhou, B. He, Z. Chen, Z. Li, M. Shi, Z. Hou, Y. Kuang, Nitrogen-doped holey carbon nanotubes: dual polysulfides trapping effect towards enhanced lithium-sulfur battery performance, Appl. Surf. Sci. 454 (2018) 284–292.
[88] X.L. Wang, J. Chen, B. Jin, Q. Jiang, E.M. Jin, S.M. Jeong, Electrochemical performance of electrospun lotus–root–structure porous multichannel carbon nanotubes for lithium–sulfur battery applications, J. Electroanal. Chem. 878 (2020) 114564.
[89] J.S. Lee, J. Jun, J. Jang, A. Manthiram, Sulfur-immobilized, activated porous carbon nanotube composite based cathodes for lithium–sulfur batteries, Small 13 (2017) 1602984.
[90] W. Wei, P. Liu, Rational porous design for carbon nanotubes derived from tubular polypyrrole as sulfur host for lithium-sulfur batteries, Microporous Mesoporous Mater. 311 (2021) 110705.
[91] Z. Xiao, Z. Yang, H. Nie, Y. Lu, K. Yang, S. Huang, Porous carbon nanotubes etched by water steam for high-rate large-capacity lithium–sulfur batteries, J. Mater. Chem. A 2 (2014) 8683–8689.
[92] L. Sun, D. Wang, Y. Luo, K. Wang, W. Kong, Y. Wu, L. Zhang, K. Jiang, Q. Li, Y. Zhang, J. Wang, S. Fan, Sulfur embedded in a mesoporous carbon nanotube network as a binder-free electrode for high-performance lithium–sulfur batteries, ACS Nano 10 (2016) 1300–1308.
[93] K. Mi, Y. Jiang, J. Feng, Y. Qian, S. Xiong, Hierarchical carbon nanotubes with a thick microporous wall and inner channel as efficient scaffolds for lithium–sulfur batteries, Adv. Funct. Mater. 26 (2016) 1571–1579.
[94] J.H. Kim, K. Fu, J. Choi, S. Sun, J. Kim, L. Hu, U. Paik, Hydroxylated carbon nanotube enhanced sulfur cathodes for improved electrochemical performance of lithium–sulfur batteries, Chem. Commun. 51 (2015) 13682–13685.
[95] J. Wu, S. Ding, S. Ye, C. Lai, Grafting polymeric sulfur onto carbon nanotubes as highly-active cathode for lithium–sulfur batteries, J. Energy Chem. 42 (2020) 27–33.
[96] Y.C. Jeong, K. Lee, T. Kim, J.H. Kim, J. Park, Y.S. Cho, S.J. Yang, C.R. Park, Partially unzipped carbon nanotubes for high-rate and stable lithium–sulfur batteries, J. Mater. Chem. A 4 (2016) 819–826.
[97] J.S. Lee, A. Manthiram, Hydroxylated N-doped carbon nanotube-sulfur composites as cathodes for high-performance lithium-sulfur batteries, J. Power Sources 343 (2017) 54–59.
[98] Y.-W. Xu, B.-H. Zhang, G.-R. Li, S. Liu, X.-P. Gao, Covalently bonded sulfur anchored with thiol-modified carbon nanotube as a cathode material for lithium–sulfur batteries, ACS Appl. Energy Mater. 3 (2020) 487–494.
[99] X.Z. Ma, B. Jin, P.M. Xin, H.H. Wang, Multiwalled carbon nanotubes-sulfur composites with enhanced electrochemical performance for lithium/sulfur batteries, Appl. Surf. Sci. 307 (2014) 346–350.
[100] W. Liang, Y. Tang, L. Liu, C. Zhu, R. Sheng, Effective trapping of polysulfides using functionalized thin-walled porous carbon nanotubes as sulfur hosts for lithium—sulfur batteries, Inorg. Chem. 59 (2020) 8481–8486.
[101] C. Xu, H. Zhou, C. Fu, Y. Huang, L. Chen, L. Yang, Y. Kuang, Hydrothermal synthesis of boron-doped unzipped carbon nanotubes/sulfur composite for high-performance lithium-sulfur batteries, Electrochim. Acta 232 (2017) 156–163.
[102] F. Li, J. Tao, Z. Zou, C. Li, Z. Hou, J. Zhao, Aminomethyl-functionalized carbon nanotubes as a host of small sulfur clusters for high-performance lithium–sulfur batteries, ChemSusChem 13 (2020) 2761–2768.
[103] R. Ummethala, M. Fritzsche, T. Jaumann, J. Balach, S. Oswald, R. Nowak, N. Sobczak, I. Kaban, M.H. Rümmeli, L. Giebeler, Lightweight, free-standing 3D interconnected carbon nanotube foam as a flexible sulfur host for high performance lithium-sulfur battery cathodes, Energy Storage Mater 10 (2018) 206–215.
[104] Z. Fang, Y. Luo, H. Wu, L. Yan, F. Zhao, Q. Li, S. Fan, J. Wang, Mesoporous carbon nanotube aerogel-sulfur cathodes: a strategy to achieve ultrahigh areal capacity for lithium-sulfur batteries via capillary action, Carbon 166 (2020) 183–192.
[105] K. Hori, Y. Yamada, T. Momma, S. Noda, High-energy density Li_xSi-S full cell based on 3D current collector of few-wall carbon nanotube sponge, Carbon 161 (2020) 612–621.
[106] W. Wang, Y. Li, Y. Feng, J. Han, F. Zhang, P. Long, C. Peng, C. Cao, Y. Cao, H. Yang, W. Feng, Asymmetric self-supporting hybrid fluorinated carbon nanotubes/carbon nanotubes sponge electrode for high-performance lithium-polysulfide battery, Chem. Eng. J. 349 (2018) 756–765.
[107] L. Guo, X. Li, Z. Xu, S. Zhou, X. Zhang, J. Ni, Y. Cheng, Z. Yang, Spatial effects between two 3D self-supported carbon-nanotube-based skeleton as binder-free cathodes for lithium-sulfur batteries, ChemistrySelect 5 (2020) 11383–11390.
[108] M. Li, R. Carter, A. Douglas, L. Oakes, C.L. Pint, Sulfur vapor-infiltrated 3D carbon nanotube foam for binder-free high areal capacity lithium–sulfur battery composite cathodes, ACS Nano 11 (2017) 4877–4884.
[109] L. Wang, Y. Zhao, M.L. Thomas, H.R. Byon, In situ synthesis of bipyramidal sulfur with 3D carbon nanotube framework for lithium–sulfur batteries, Adv. Funct. Mater. 24 (2014) 2248–2252.
[110] X. Pu, G. Yang, C. Yu, Liquid-type cathode enabled by 3D sponge-like carbon nanotubes for high energy density and long cycling life of Li-S batteries, Adv. Mater. 26 (2014) 7456–7461.
[111] M.D. Patel, E. Cha, C. Kang, B. Gwalani, W. Choi, High performance rechargeable Li-S batteries using binder-free large sulfur-loaded three-dimensional carbon nanotubes, Carbon 118 (2017) 120–126.
[112] J. Wang, X. Yan, Z. Zhang, H. Ying, R. Guo, W. Yang, W.-Q. Han, Facile preparation of high-content N-doped CNT microspheres for high-performance lithium storage, Adv. Funct. Mater. 29 (2019) 1904819.
[113] D. Gueon, J.T. Hwang, S.B. Yang, E. Cho, K. Sohn, D.-K. Yang, J.H. Moon, Spherical macroporous carbon nanotube particles with ultrahigh sulfur loading for lithium—sulfur battery cathodes, ACS Nano 12 (2018) 226–233.
[114] K. Xiang, M. Chen, J. Hu, S. Wang, X. Wen, Y. Zhu, H. Chen, H. Shu, Intertwined nitrogen-doped carbon nanotube microsphere as polysulfide grappler for high-performance lithium-sulfur batteries, ChemElectroChem 6 (2019) 1466–1474.
[115] Y. Qiu, X. Wu, M. Wang, L. Fan, D. Tian, B. Guan, D. Tang, N. Zhang, 3D hierarchical CNT-based host with high sulfur loading for lithium-sulfur batteries, ChemElectroChem 6 (2019) 5698–5704.
[116] T. Wang, G. Cui, Y. Zhao, A. Nurpeissova, Z. Bakenov, Porous carbon nanotubes microspheres decorated with strong catalyst cobalt nanoparticles as an effective sulfur host for lithium-sulfur battery, J. Alloys Compd. 853 (2021) 157268.
[117] X. Ye, J. Ma, Y.-S. Hu, H. Wei, F. Ye, MWCNT porous microspheres with an efficient 3D conductive network for high performance lithium–sulfur batteries, J. Mater. Chem. A 4 (2016) 775–780.
[118] J. Guo, Y. Xu, C. Wang, Sulfur-impregnated disordered carbon nanotubes cathode for lithium–sulfur batteries, Nano Lett. 11 (2011) 4288–4294.
[119] M.-Q. Zhao, H.-J. Peng, G.-L. Tian, Q. Zhang, J.-Q. Huang, X.-B. Cheng, C. Tang, F. Wei, Hierarchical vine-tree-like carbon nanotube architectures: in-situ CVD self-assembly and their use as robust scaffolds for lithium-sulfur batteries, Adv. Mater. 26 (2014) 7051–7058.
[120] J.-Q. Huang, Q. Zhang, S.-M. Zhang, X.-F. Liu, W. Zhu, W.-Z. Qian, F. Wei, Aligned sulfur-coated carbon nanotubes with a polyethylene glycol barrier at one end for use as a high efficiency sulfur cathode, Carbon 58 (2013) 99–106.
[121] G. Zhou, D.-W. Wang, F. Li, P.-X. Hou, L. Yin, C. Liu, G.Q. Lu, I.R. Gentle, H.-M. Cheng, A flexible nanostructured sulphur–carbon nanotube cathode with high rate performance for Li-S batteries, Energy Environ. Sci. 5 (2012) 8901–8906.
[122] W. Deng, A. Hu, X. Chen, S. Zhang, Q. Tang, Z. Liu, B. Fan, K. Xiao, Sulfur-impregnated 3D hierarchical porous nitrogen-doped aligned carbon nanotubes as high-performance cathode for lithium-sulfur batteries, J. Power Sources 322 (2016) 138–146.
[123] R. Carter, B. Davis, L. Oakes, M.R. Maschmann, C.L. Pint, A high areal capacity lithium–sulfur battery cathode prepared by site-selective vapor infiltration of hierarchical carbon nanotube arrays, Nanoscale 9 (2017) 15018–15026.
[124] X.-B. Cheng, J.-Q. Huang, Q. Zhang, H.-J. Peng, M.-Q. Zhao, F. Wei, Aligned carbon nanotube/sulfur composite cathodes with high sulfur content for lithium–sulfur batteries, Nano Energy 4 (2014) 65–72.
[125] H.-N. Fan, S.-L. Chen, X.-H. Chen, Q.-L. Tang, A.-P. Hu, W.-B. Luo, H.-K. Liu, S.-X. Dou, 3D selenium sulfide@carbon nanotube array as long-life and high-rate cathode material for lithium storage, Adv. Funct. Mater. 28 (2018) 1805018.
[126] K. Xi, B. Chen, H. Li, R. Xie, C. Gao, C. Zhang, R.V. Kumar, J. Robertson, Soluble polysulphide sorption using carbon nanotube forest for enhancing cycle performance in a lithium–sulphur battery, Nano Energy 12 (2015) 538–546.

[127] Z. Yuan, H.-J. Peng, J.-Q. Huang, X.-Y. Liu, D.-W. Wang, X.-B. Cheng, Q. Zhang, Hierarchical free-standing carbon-nanotube paper electrodes with ultrahigh sulfur-loading for lithium–sulfur batteries, Adv. Funct. Mater. 24 (2014) 6105–6112.
[128] X. Ding, Z. Pan, N. Liu, L. Li, X. Wang, G. Xu, J. Yang, J. Yang, N. Yu, M. Liu, W. Li, Y. Zhang, Freestanding carbon nanotube film for flexible straplike lithium/sulfur batteries, Chem. Eur. J. 25 (2019) 3775–3780.
[129] K. Jin, X. Zhou, L. Zhang, X. Xin, G. Wang, Z. Liu, Sulfur/carbon nanotube composite film as a flexible cathode for lithium–sulfur batteries, J. Phys. Chem. C 117 (2013) 21112–21119.
[130] L. Sun, M. Li, Y. Jiang, W. Kong, K. Jiang, J. Wang, S. Fan, Sulfur nanocrystals confined in carbon nanotube network as a binder-free electrode for high-performance lithium sulfur batteries, Nano Lett 14 (2014) 4044–4049.
[131] R. Fang, G. Li, S. Zhao, L. Yin, K. Du, P. Hou, S. Wang, H.-M. Cheng, C. Liu, F. Li, Single-wall carbon nanotube network enabled ultrahigh sulfur-content electrodes for high-performance lithium-sulfur batteries, Nano Energy 42 (2017) 205–214.
[132] F. Jin, S. Xiao, L. Lu, Y. Wang, Efficient activation of high-loading sulfur by small CNTs confined inside a large CNT for high-capacity and high-rate lithium–sulfur batteries, Nano Lett 16 (2016) 440–447.
[133] Y. Zhao, W. Wu, J. Li, Z. Xu, L. Guan, Encapsulating MWNTs into hollow porous carbon nanotubes: a tube-in-tube carbon nanostructure for high-performance lithium-sulfur batteries, Adv. Mater. 26 (2014) 5113–5118.
[134] T. Liu, S. Sun, W. Song, X. Sun, Q. Niu, H. Liu, T. Ohsaka, J. Wu, A lightweight and binder-free electrode enabled by lignin fibers@carbon-nanotubes and graphene for ultrastable lithium–sulfur batteries, J. Mater. Chem. A 6 (2018) 23486–23494.
[135] L. Sun, W. Kong, Y. Jiang, H. Wu, K. Jiang, J. Wang, S. Fan, Super-aligned carbon nanotube/graphene hybrid materials as a framework for sulfur cathodes in high performance lithium sulfur batteries, J. Mater. Chem. A 3 (2015) 5305–5312.
[136] Y.-L. Ding, P. Kopold, K. Hahn, P.A. van Aken, J. Maier, Y. Yu, Facile solid-state growth of 3D well-interconnected nitrogen-rich carbon nanotube–graphene hybrid architectures for lithium–sulfur batteries, Adv. Funct. Mater. 26 (2016) 1112–1119.
[137] L. Sun, H. Li, M. Zhao, G. Wang, High-performance lithium-sulfur batteries based on self-supporting graphene/carbon nanotube foam@sulfur composite cathode and quasi-solid-state polymer electrolyte, Chem. Eng. J. 332 (2018) 8–15.
[138] S. Huang, L. Zhang, J. Wang, J. Zhu, P.K. Shen, In situ carbon nanotube clusters grown from three-dimensional porous graphene networks as efficient sulfur hosts for high-rate ultra-stable Li–S batteries, Nano Res 11 (2018) 1731–1743.
[139] D. Su, M. Cortie, G. Wang, Fabrication of N-doped graphene–carbon nanotube hybrids from prussian blue for lithium–sulfur batteries, Adv. Energy Mater. 7 (2017) 1602014.
[140] Q.Q. Wang, J.B. Huang, G.R. Li, Z. Lin, B.H. Liu, Z.P. Li, A facile and scalable method to prepare carbon nanotube-grafted-graphene for high performance Li-S battery, J. Power Sources 339 (2017) 20–26.
[141] L. Zhu, H.-J. Peng, J. Liang, J.-Q. Huang, C.-M. Chen, X. Guo, W. Zhu, P. Li, Q. Zhang, Interconnected carbon nanotube/graphene nanosphere scaffolds as free–standing paper electrode for high-rate and ultra-stable lithium–sulfur batteries, Nano Energy 11 (2015) 746–755.
[142] S. Baik, J.H. Park, J.W. Lee, One-pot conversion of carbon dioxide to CNT-grafted graphene bifunctional for sulfur cathode and thin interlayer of Li–S battery, Electrochim. Acta 330 (2020) 135264.
[143] H. Shi, X. Zhao, Z.-S. Wu, Y. Dong, P. Lu, J. Chen, W. Ren, H.-M. Cheng, X. Bao, Free-standing integrated cathode derived from 3D graphene/carbon nanotube aerogels serving as binder-free sulfur host and interlayer for ultrahigh volumetric-energy-density lithium sulfur batteries, Nano Energy 60 (2019) 743–751.
[144] W.G. Chong, J.-Q. Huang, Z.-L. Xu, X. Qin, X. Wang, J.-K. Kim, Lithium–sulfur battery cable made from ultralight, flexible graphene/carbon nanotube/sulfur composite fibers, Adv. Funct. Mater. 27 (2017) 1604815.
[145] Y. Chen, S. Lu, J. Zhou, W. Qin, X. Wu, Synergistically assembled Li_2S/FWNTs@reduced graphene oxide nanobundle forest for free-standing high-performance Li_2S cathodes, Adv. Funct. Mater. 27 (2017) 1700987.
[146] J. Wang, Z. Meng, W. Yang, X. Yan, R. Guo, W.-Q. Han, Facile synthesis of rGO/g-C_3N_4/CNT microspheres via an ethanol-assisted spray-drying method for high-performance lithium–sulfur batteries, ACS Appl. Mater. Interfaces 11 (2019) 819–827.
[147] Y. Chen, S. Lu, X. Wu, J. Liu, Flexible carbon nanotube–graphene/sulfur composite film: free-standing cathode for high-performance lithium/sulfur batteries, J. Phys. Chem. C 119 (2015) 10288–10294.
[148] X. Li, X. Pu, S. Han, M. Liu, C. Du, C. Jiang, X. Huang, T. Liu, W. Hu, Enhanced performances of Li/polysulfide batteries with 3D reduced graphene oxide/carbon nanotube hybrid aerogel as the polysulfide host, Nano Energy 30 (2016) 193–199.
[149] J.L. Gómez-Urbano, J.L. Gómez-Cámer, C. Botas, T. Rojo, D. Carriazo, Graphene oxide-carbon nanotubes aerogels with high sulfur loadings suitable as binder-free cathodes for high performance lithium sulfur batteries, J. Power Sources 412 (2019) 408–415.
[150] J. He, Y. Chen, P. Li, F. Fu, Z. Wang, W. Zhang, Three-dimensional CNT/graphene–sulfur hybrid sponges with high sulfur loading as superior-capacity cathodes for lithium–sulfur batteries, J. Mater. Chem. A 3 (2015) 18605–18610.
[151] H. Wu, L. Xia, J. Ren, Q. Zheng, C. Xu, D. Lin, A high-efficiency N/P co-doped graphene/CNT@porous carbon hybrid matrix as a cathode host for high performance lithium–sulfur batteries, J. Mater. Chem. A 5 (2017) 20458–20472.
[152] S. Niu, W. Lv, C. Zhang, Y. Shi, J. Zhao, B. Li, Q.-H. Yang, F. Kang, One-pot self--assembly of graphene/carbon nanotube/sulfur hybrid with three dimensionally interconnected structure for lithium–sulfur batteries, J. Power Sources 295 (2015) 182–189.
[153] Z. Luo, Z. Tao, X. Li, D. Xu, C. Xuan, Z. Wang, T. Tang, J. Wen, M. Li, J. Xiao, Ferroconcrete-like helical carbon nanotube/reduced graphene oxide heterostructure 3D networks as sulfur hosts for high-performance Li-S batteries, Front. Energy Res. 7 (2020) 157.
[154] Y. Hwa, H.K. Seo, J.-m. Yuk, E.J. Cairns, Freeze-dried sulfur–graphene oxide–carbon nanotube nanocomposite for high sulfur-loading lithium/sulfur cells, Nano Lett 17 (2017) 7086–7094.
[155] H. Köse, B.Ş. Kurt, Ş. Dombaycıoğlu, A.O. Aydın, Rational design of cathode structure based on free-standing S/rGO/CNT nanocomposite for Li-S batteries, Synth. Met. 267 (2020) 116471.
[156] L. Ji, M. Rao, S. Aloni, L. Wang, E.J. Cairns, Y. Zhang, Porous carbon nanofiber—sulfur composite electrodes for lithium/sulfur cells, Energy Environ. Sci. 4 (2011) 5053–5059.
[157] S. Wang, L. Xia, L. Yu, L. Zhang, H. Wang, X.W. Lou, Free-standing nitrogen-doped carbon nanofiber films: integrated electrodes for sodium-ion batteries with ultralong cycle life and superior rate capability, Adv. Energy Mater. 6 (2016) 1502217.
[158] Y.-Z. Zhang, Z. Zhang, S. Liu, G.-R. Li, X.-P. Gao, Free-standing porous carbon nanofiber/carbon nanotube film as sulfur immobilizer with high areal capacity for lithium–sulfur battery, ACS Appl. Mater. Interfaces 10 (2018) 8749–8757.
[159] Y. Chen, X. Li, K.-S. Park, J. Hong, J. Song, L. Zhou, Y.-W. Mai, H. Huang, J.B. Goodenough, Sulfur encapsulated in porous hollow CNTs@CNFs for high-performance lithium–sulfur batteries, J. Mater. Chem. A 2 (2014) 10126–10130.
[160] N. Deng, W. Kang, J. Ju, L. Fan, X. Zhuang, X. Ma, H. He, Y. Zhao, B. Cheng, Polyvinyl alcohol-derived carbon nanofibers/carbon nanotubes/sulfur electrode with honeycomb-like hierarchical porous structure for the stable-capacity lithium/sulfur batteries, J. Power Sources 346 (2017) 1–12.
[161] Z. Shan, Y. He, N. Liu, J. Li, M. Li, Y. Zhang, Spontaneously rooting carbon nanotube incorporated N-doped carbon nanofibers as efficient sulfur host toward high performance lithium-sulfur batteries, Appl. Surf. Sci. 539 (2021) 148209.
[162] J. Song, T. Xu, M.L. Gordin, P. Zhu, D. Lv, Y.-B. Jiang, Y. Chen, Y. Duan, D. Wang, Nitrogen-doped mesoporous carbon promoted chemical adsorption of sulfur and fabrication of high-areal-capacity sulfur cathode with exceptional cycling stability for lithium-sulfur batteries, Adv. Funct. Mater. 24 (2014) 1243–1250.
[163] J. Schuster, G. He, B. Mandlmeier, T. Yim, K.T. Lee, T. Bein, L.F. Nazar, Spherical ordered mesoporous carbon nanoparticles with high porosity for lithium–sulfur batteries, Angew. Chem. Int. Ed. 51 (2012) 3591–3595.
[164] H. Pan, Z. Cheng, Z. Xiao, X. Li, R. Wang, The fusion of imidazolium-based ionic polymer and carbon nanotubes: one type of new heteroatom-doped carbon precursors for high-performance lithium–sulfur batteries, Adv. Funct. Mater. 27 (2017) 1703936.
[165] X. Chen, Y. Xu, F.-H. Du, Y. Wang, Covalent organic framework derived boron/oxygen codoped porous carbon on CNTs as an efficient sulfur host for lithium–sulfur batteries, Small Methods 3 (2019) 1900338.
[166] S. Liang, Y. Xia, C. Liang, Y. Gan, H. Huang, J. Zhang, X. Tao, W. Sun, W. Han, W. Zhang, A green and facile strategy for the low-temperature and rapid synthesis of Li_2S@PC–CNT cathodes with high Li_2S content for advanced Li–S batteries, J. Mater. Chem. A 6 (2018) 9906–9914.
[167] T. Xu, J. Song, M.L. Gordin, H. Sohn, Z. Yu, S. Chen, D. Wang, Mesoporous Carbon—Carbon Nanotube–Sulfur Composite Microspheres for High-Areal-Capacity Lithium–Sulfur Battery Cathodes, ACS Appl. Mater. Interfaces 5 (2013) 11355–11362.
[168] J. Cai, C. Wu, S. Yang, Y. Zhu, P.K. Shen, K. Zhang, Templated and Catalytic Fabrication of N-Doped Hierarchical Porous Carbon–Carbon Nanotube Hybrids as Host for Lithium–Sulfur Batteries, ACS Appl. Mater. Interfaces 9 (2017) 33876–33886.
[169] H.-J. Peng, J.-Q. Huang, M.-Q. Zhao, Q. Zhang, X.-B. Cheng, X.-Y. Liu, W.-Z. Qian, F. Wei, Nanoarchitectured Graphene/CNT@Porous Carbon with Extraordinary Electrical Conductivity and Interconnected Micro/Mesopores for Lithium-Sulfur Batteries, Adv. Funct. Mater. 24 (2014) 2772–2781.
[170] G.D. Park, Y.C. Kang, Aerosol-assisted synthesis of porous and hollow carbon–carbon nanotube composite microspheres as sulfur host materials for high-performance Li-S batteries, Appl. Surf. Sci. 495 (2019) 143637.
[171] H. Yu, B. Zhang, F. Sun, G. Jiang, N. Zheng, C. Xu, Y. Li, Core-shell polyhedrons of carbon nanotubes-grafted graphitic carbon@nitrogen doped carbon as efficient sulfur immobilizers for lithium-sulfur batteries, Appl. Surf. Sci. 450 (2018) 364–371.
[172] M.D. Walle, M. Zhang, K. Zeng, Y. Li, Y.-N. Liu, MOFs-derived nitrogen-doped carbon interwoven with carbon nanotubes for high sulfur content lithium–sulfur batteries, Appl. Surf. Sci. 497 (2019) 143773.
[173] C. Luo, S. Niu, G. Zhou, W. Lv, B. Li, F. Kang, Q.-H. Yang, Dual-functional hard template directed one-step formation of a hierarchical porous carbon–carbon nanotube hybrid for lithium–sulfur batteries, Chem. Commun. 52 (2016) 12143–12146.
[174] B. Fan, D. Zhao, W. Zhou, W. Xu, X. Liang, G. He, Z. Wu, L. Li, Nitrogen-Doped Hollow Carbon Polyhedrons with Carbon Nanotubes Surface Layers as Effective Sulfur Hosts for High-Rate, Long-Lifespan Lithium–Sulfur Batteries, ChemElectroChem 7 (2020) 4990–4998.
[175] J. Ren, Z. Song, X. Zhou, Y. Chai, X. Lu, Q. Zheng, C. Xu, D. Lin, A Porous Carbon Polyhedron/Carbon Nanotube Based Hybrid Material as Multifunctional Sulfur Host for High-Performance Lithium-Sulfur Batteries, ChemElectroChem 6 (2019) 3410–3419.
[176] Z. Tao, J. Xiao, H. Wang, F. Zhang, Novel cathode structure based on spiral carbon nanotubes for lithium–sulfur batteries, J. Electroanal. Chem. 851 (2019) 113477.
[177] W. Bao, Z. Zhang, C. Zhou, Y. Lai, J. Li, Multi-walled carbon nanotubes @ mesoporous carbon hybrid nanocomposites from carbonized multi-walled carbon nanotubes @ metal–organic framework for lithium sulfur battery, J. Power Sources 248 (2014) 570–576.
[178] S. Luo, W. Sun, J. Ke, Y. Wang, S. Liu, X. Hong, Y. Li, Y. Chen, W. Xie, C. Zheng, A 3D conductive network of porous carbon nanoparticles interconnected with carbon nanotubes as the sulfur host for long cycle life lithium–sulfur batteries, Nanoscale 10 (2018) 22601–22611.

[179] W. Yang, W. Yang, A. Song, G. Sun, G. Shao, 3D interconnected porous carbon nanosheets/carbon nanotubes as a polysulfide reservoir for high performance lithium–sulfur batteries, Nanoscale 10 (2018) 816–824.
[180] H. Lu, C. Zhang, Y. Zhang, Y. Huang, M. Liu, T. Liu, Simultaneous growth of carbon nanotubes on inner/outer surfaces of porous polyhedra: advanced sulfur hosts for lithium-sulfur batteries, Nano Res 11 (2018) 6155–6166.
[181] X.-W. Wu, H. Xie, Q. Deng, H.-X. Wang, H. Sheng, Y.-X. Yin, W.-X. Zhou, R.-L. Li, Y.-G. Guo, Three-dimensional carbon nanotubes forest/carbon cloth as an efficient electrode for lithium–polysulfide batteries, ACS Appl. Mater. Interfaces 9 (2017) 1553–1561.
[182] Z. Gao, N. Song, Y. Zhang, Y. Schwab, J. He, X. Li, Carbon nanotubes derived from yeast-fermented wheat flour and their energy storage application, ACS Sustain. Chem. Eng. 6 (2018) 11386–11396.
[183] W. He, X. He, M. Du, S. Bie, J. Liu, Y. Wang, M. Liu, Z. Zou, W. Yan, H. Zhao, Three-dimensional functionalized carbon nanotubes/graphitic carbon nitride hybrid composite as the sulfur host for high-performance lithium–sulfur batteries, J. Phys. Chem. C 123 (2019) 15924–15934.
[184] S. Huang, X. Wang, R. Hu, X. Wang, X. Yang, N. Zhao, W. Lei, L. Zhu, J. Peng, Polypyrrole-S-coated MWCNT composites as cathode materials for lithium-sulfur batteries, Ionics 26 (2020) 5455–5462.
[185] H. Li, L. Sun, G. Wang, Self-assembly of polyethylene glycol-grafted carbon nanotube/sulfur composite with nest-like structure for high-performance lithium–sulfur batteries, ACS Appl. Mater. Interfaces 8 (2016) 6061–6071.
[186] X. Hong, J. Jin, T. Wu, Y. Lu, S. Zhang, C. Chen, Z. Wen, A rGO–CNT aerogel covalently bonded with a nitrogen-rich polymer as a polysulfide adsorptive cathode for high sulfur loading lithium sulfur batteries, J. Mater. Chem. A 5 (2017) 14775–14782.
[187] J. Wang, C. Lv, Y. Zhang, L. Deng, Z. Peng, Polyphenylene wrapped sulfur/multi-walled carbon nano-tubes via spontaneous grafting of diazonium salt for improved electrochemical performance of lithium-sulfur battery, Electrochim. Acta 165 (2015) 136–141.
[188] G. Hu, Z. Sun, C. Shi, R. Fang, J. Chen, P. Hou, C. Liu, H.-M. Cheng, F. Li, A sulfur-rich copolymer@CNT hybrid cathode with dual-confinement of polysulfides for high-performance lithium–sulfur batteries, Adv. Mater. 29 (2017) 1603835.
[189] A. Abdul Razzaq, Y. Yao, R. Shah, P. Qi, L. Miao, M. Chen, X. Zhao, Y. Peng, Z. Deng, High-performance lithium sulfur batteries enabled by a synergy between sulfur and carbon nanotubes, Energy Storage Mater 16 (2019) 194–202.
[190] L. Yin, J. Wang, J. Yang, Y. Nuli, A novel pyrolyzed polyacrylonitrile-sulfur@MWCNT composite cathode material for high-rate rechargeable lithium/sulfur batteries, J. Mater. Chem. 21 (2011) 6807–6810.
[191] T.S. Sahu, S. Choi, P. Jaumaux, J. Zhang, C. Wang, D. Zhou, G. Wang, Squalene-derived sulfur-rich copolymer@3D graphene-carbon nanotube network cathode for high-performance lithium-sulfur batteries, Polyhedron 162 (2019) 147–154.
[192] S.-K. Park, J.-K. Lee, Y.C. Kang, Yolk–shell structured assembly of bamboo-like nitrogen-doped carbon nanotubes embedded with Co nanocrystals and their application as cathode material for Li–S batteries, Adv. Funct. Mater. 28 (2018) 1705264.
[193] G. Li, W. Lei, D. Luo, Y. Deng, Z. Deng, D. Wang, A. Yu, Z. Chen, Stringed "tube on cube" nanohybrids as compact cathode matrix for high-loading and lean-electrolyte lithium–sulfur batteries, Energy Environ. Sci. 11 (2018) 2372–2381.
[194] L. Ma, H. Lin, W. Zhang, P. Zhao, G. Zhu, Y. Hu, R. Chen, Z. Tie, J. Liu, Z. Jin, Nitrogen-doped carbon nanotube forests planted on cobalt nanoflowers as polysulfide mediator for ultralow self-discharge and high areal-capacity lithium–sulfur batteries, Nano Lett 18 (2018) 7949–7954.
[195] Z. Wang, J. Shen, S. Ji, X. Xu, S. Zuo, Z. Liu, D. Zhang, R. Hu, L. Ouyang, J. Liu, M. Zhu, B,N codoped graphitic nanotubes loaded with Co nanoparticles as superior sulfur host for advanced Li–S batteries, Small 16 (2020) 1906634.
[196] C. Hu, C. Yang, J. Yang, N. Han, R. Yuan, Y. Chen, H. Liu, T. Xie, R. Chen, H. Zhou, W. Liu, X. Sun, An entangled cobalt–nitrogen–carbon nanotube array electrode with synergetic confinement and electrocatalysis of polysulfides for stable Li–S batteries, ACS Appl. Energy Mater. 2 (2019) 2904–2912.
[197] R. Liu, Q. Kang, W. Liu, Z. Liu, Y. Liu, Y. Wang, J. Chen, B. Hultman, X. Lin, Y. Li, P. Li, Z. Huang, X. Feng, G. Wu, L. Yu, Y. Ma, Carbon nanotube-connected yolk–shell carbon nanopolyhedras with cobalt and nitrogen doping as sulfur immobilizers for high-performance lithium–sulfur batteries, ACS Appl. Energy Mater. 1 (2018) 6487–6496.
[198] A.H. Shao, Z. Zhang, D.-G. Xiong, J. Yu, J.-X. Cai, Z.-Y. Yang, Facile synthesis of a "two-in-one" sulfur host featuring metallic-cobalt-embedded N-doped carbon nanotubes for efficient lithium-sulfur batteries, ACS Appl. Mater. Interfaces 12 (2020) 5968–5978.
[199] J. Zhao, C. Liu, H. Deng, S. Tang, C. Liu, S. Chen, J. Guo, Q. Lan, Y. Li, Y. Liu, M. Ye, H. Liu, J. Liang, Y.-C. Cao, In-situ catalytic growth carbon nanotubes from metal organic frameworks for high performance lithium-sulfur batteries, Mater. Today Energy 8 (2018) 134–142.
[200] M. Zhang, Y. Yang, X. Zhang, M. Cheng, H. Yuan, K. Amin, A. Ahmad, L. Mao, W. Yan, Z. Wei, Flexible VO_x nanosphere@SWCNT hybrid films with dual-confinement function of polysulfides for high-performance lithium–sulfur batteries, Adv. Mater. Interfaces 5 (2018) 1800766.
[201] D. Chen, X.-Y. Yue, X.-L. Li, J. Bao, Q.-Q. Qiu, X.-J. Wu, X. Zhang, Y.-N. Zhou, Freestanding double-layer MoO_3/CNT@S membrane: a promising flexible cathode for lithium–sulfur batteries, ACS Appl. Mater. Interfaces 12 (2020) 2354–2361.
[202] Q. Liu, Q. Jiang, L. Jiang, J. Peng, Y. Gao, Z. Duan, X. Lu, Preparation of SnO_2@rGO/CNTs/S composite and application for lithium-sulfur battery cathode material, Appl. Surf. Sci. 462 (2018) 393–398.
[203] D. Bosubabu, J. Sivaraj, P. Gurunathan, K. Ramesha, Hollow Co_3O_4 microspheres grafted with nitrogen-doped carbon nanotubes as efficient sulfur host for high performing lithium–sulfur batteries, Energy Fuels 34 (2020) 16810–16818.
[204] H. Wang, N. Zhang, Y. Li, P. Zhang, Z. Chen, C. Zhang, X. Qiao, Y. Dai, Q. Wang, S. Liu, Unique flexible $NiFe_2O_4$@S/rGO–CNT electrode via the synergistic adsorption/electrocatalysis effect toward high-performance lithium–sulfur batteries, J. Phys. Chem. Lett. 10 (2019) 6518–6524.
[205] J.-Y. Hwang, H.M. Kim, S.-K. Lee, J.-H. Lee, A. Abouimrane, M.A. Khaleel, I. Belharouak, A. Manthiram, Y.-K. Sun, High-energy, high-rate, lithium–sulfur batteries: synergetic effect of hollow TiO_2-webbed carbon nanotubes and a dual functional carbon-paper interlayer, Adv. Energy Mater. 6 (2016) 1501480.
[206] M. Xiang, H. Wu, H. Liu, J. Huang, Y. Zheng, L. Yang, P. Jing, Y. Zhang, S. Dou, H. Liu, A flexible 3D multifunctional MgO-decorated carbon foam@CNTs hybrid as self-supported cathode for high-performance lithium-sulfur batteries, Adv. Funct. Mater. 27 (2017) 1702573.
[207] R. Liu, F. Guo, X. Zhang, J. Yang, M. Li, W. Miaomiao, H. Liu, M. Feng, L. Zhang, Novel "bird-nest" structured Co_3O_4/acidified multiwall carbon nanotube (ACNT) hosting materials for lithium–sulfur batteries, ACS Appl. Energy Mater. 2 (2019) 1348–1356.
[208] Y. Li, D. Ye, W. Liu, B. Shi, R. Guo, H. Zhao, H. Pei, J. Xu, J. Xie, A MnO_2/graphene oxide/multi-walled carbon nanotubes-sulfur composite with dual-efficient polysulfide adsorption for improving lithium-sulfur batteries, ACS Appl. Mater. Interfaces 8 (2016) 28566–28573.
[209] R. Carter, L. Oakes, N. Muralidharan, A.P. Cohn, A. Douglas, C.L. Pint, Polysulfide anchoring mechanism revealed by atomic layer deposition of V_2O_5 and sulfur-filled carbon nanotubes for lithium–sulfur batteries, ACS Appl. Mater. Interfaces 9 (2017) 7185–7192.
[210] Z. Zhang, S. Basu, P. Zhu, H. Zhang, A. Shao, N. Koratkar, Z. Yang, Highly sulfiphilic Ni-Fe bimetallic oxide nanoparticles anchored on carbon nanotubes enable effective immobilization and conversion of polysulfides for stable lithium-sulfur batteries, Carbon 142 (2019) 32–39.
[211] H. Li, J. Wang, Y. Zhao, S. Yang, Y. Tian, Y. Wang, S–ZnO/CNTs microspheres prepared by spray drying for improved cathodes in lithium-sulfur batteries, ChemElectroChem 6 (2019) 3454–3459.
[212] G. Gao, P. Zhai, Q. Zhang, C.J. Shearer, J. Zhao, J.G. Shapter, Fe_3O_4@S nanoparticles embedded/coated on the multi-wall carbon nanotubes for rechargeable lithium batteries, Chem. Eng. J. 333 (2018) 268–275.
[213] D. Xiao, C. Lu, C. Chen, S. Yuan, CeO_2-webbed carbon nanotubes as a highly efficient sulfur host for lithium-sulfur batteries, Energy Storage Mater 10 (2018) 216–222.
[214] X. Wen, K. Xiang, Y. Zhu, L. Xiao, H. Liao, X. Chen, H. Chen, Nb_2O_5-decorated nitrogen-doped carbon nanotube microspheres for highly efficient sulfur confinement in lithium–sulfur batteries, Ind. Eng. Chem. Res. 58 (2019) 8724–8733.
[215] M. Yuan, Y. Zhao, Z. Sun, Z. Bakenov, Rational design of MOFs-derived Fe_3O_4@C interwoven with carbon nanotubes as sulfur host for advanced lithium-sulfur batteries, J. Electroanal. Chem. 877 (2020) 114608.
[216] J. Lee, Y. Jeon, J. Oh, M. Kim, L.Y.S. Lee, Y. Piao, γ-Fe_2O_3 nanoparticles anchored in MWCNT hybrids as efficient sulfur hosts for high-performance lithium-sulfur battery cathode, J. Electroanal. Chem. 858 (2020) 113806.
[217] T. An, D. Deng, M. Lei, Q.-H. Wu, Z. Tian, M. Zheng, Q. Dong, MnO modified carbon nanotubes as a sulfur host with enhanced performance in Li/S batteries, J. Mater. Chem. A 4 (2016) 12858–12864.
[218] T. Ma, M. Liu, T. Huang, A. Yu, Al_2O_3-doped ZnO coating of carbon nanotubes as cathode material for lithium-sulfur batteries, J. Power Sources 398 (2018) 75–82.
[219] Y. Zhou, H. Shu, Y. Zhou, T. Sun, M. Han, Y. Chen, M. Chen, Z. Chen, X. Yang, X. Wang, Flower-like $Bi_4Ti_3O_{12}$/carbon nanotubes as reservoir and promoter of polysulfide for lithium sulfur battery, J. Power Sources 453 (2020) 227896.
[220] A. Chen, W. Liu, H. Hu, T. Chen, B. Ling, K. Liu, Three-dimensional TiO_2-B nanotubes/carbon nanotubes intertwined network as sulfur hosts for high performance lithium−sulfur batteries, J. Power Sources 400 (2018) 23–30.
[221] W. Dong, L. Meng, X. Hong, S. Liu, D. Shen, Y. Xia, S. Yang, MnO_2/rGO/CNTs framework as a sulfur host for high-performance Li-S batteries, Molecules 25 (2020) 1989.
[222] X. Zhang, Y. Li, J. Li, A. Jia, D. Sun, Y. Wang, Vertically rooting carbon nanotubes on cobalt-loaded hollow Titanium Dioxide spheres as conductive multifunctional sulfur hosts for superior lithium-sulfur performance, J. Alloys Compd. 854 (2021) 157267.
[223] W. Qiu, J. Li, Y. Zhang, G. Kalimuldina, Z. Bakenov, Carbon nanotubes assembled on porous TiO_2 matrix doped with Co_3O_4 as sulfur host for lithium–sulfur batteries, Nanotechnology 32 (2020) 075403.
[224] T. Chen, Z. Zhang, B. Cheng, R. Chen, Y. Hu, L. Ma, G. Zhu, J. Liu, Z. Jin, Self-templated formation of interlaced carbon nanotubes threaded hollow Co_3S_4 nanoboxes for high-rate and heat-resistant lithium–sulfur batteries, J. Am. Chem. Soc. 139 (2017) 12710–12715.
[225] J. He, A. Bhargav, H. Yaghoobnejad Asl, Y. Chen, A. Manthiram, 1T′-ReS_2 nanosheets in situ grown on carbon nanotubes as a highly efficient polysulfide electrocatalyst for stable Li–S batteries, Adv. Energy Mater. 10 (2020) 2001017.
[226] J. Zhou, X. Liu, J. Zhou, H. Zhao, N. Lin, L. Zhu, Y. Zhu, G. Wang, Y. Qian, Fully integrated hierarchical double-shelled Co_9S_8@CNT nanostructures with unprecedented performance for Li–S batteries, Nanoscale Horiz 4 (2019) 182–189.
[227] H. Wu, L. Wang, J. Bi, Y. Li, X. Pang, Z. Li, Q. Meng, H. Liu, L. Wang, Local concentration effect-derived heterogeneous Li_2S_2/Li_2S deposition on dual-phase MWCNT/cellulose nanofiber/$NiCo_2S_4$ self-standing paper for high performance of lithium polysulfide batteries, ACS Appl. Mater. Interfaces 12 (2020) 15228–15238.
[228] L. Ma, W. Zhang, L. Wang, Y. Hu, G. Zhu, Y. Wang, R. Chen, T. Chen, Z. Tie, J. Liu, Z. Jin, Strong capillarity, chemisorption, and electrocatalytic capability of

crisscrossed nanostraws enabled flexible, high-rate, and long-cycling lithium–sulfur batteries, ACS Nano 12 (2018) 4868–4876.
[229] M. Xu, P. Dong, T. Li, H. Hua, Y. Li, X. Li, Y. Zhang, Y. Zhang, J. Zhao, Promoting kinetics of polysulfides redox reactions by the multifunctional CoS/C/CNT microspheres for high-performance lithium-sulfur batteries, Appl. Surf. Sci. 504 (2020) 144463.
[230] M.D. Walle, K. Zeng, M. Zhang, Y. Li, Y.-N. Liu, Flower-like molybdenum disulfide/carbon nanotubes composites for high sulfur utilization and high-performance lithium–sulfur battery cathodes, Appl. Surf. Sci. 473 (2019) 540–547.
[231] K. Xiang, X. Wen, J. Hu, S. Wang, H. Chen, Rational fabrication of nitrogen and sulfur codoped carbon nanotubes/MoS_2 for high-performance lithium–sulfur batteries, ChemSusChem 12 (2019) 3602–3614.
[232] S. Zhao, X. Tian, Y. Zhou, B. Ma, A. Natarajan, Three-dimensionally interconnected Co_9S_8/MWCNTs composite cathode host for lithium–sulfur batteries, J. Energy Chem. 46 (2020) 22–29.
[233] D. Cai, L. Wang, L. Li, Y. Zhang, J. Li, D. Chen, H. Tu, W. Han, Self-assembled CdS quantum dots in carbon nanotubes: induced polysulfide trapping and redox kinetics enhancement for improved lithium–sulfur battery performance, J. Mater. Chem. A 7 (2019) 806–815.
[234] W. Yang, W. Yang, L. Dong, X. Gao, G. Wang, G. Shao, Enabling immobilization and conversion of polysulfides through a nitrogen-doped carbon nanotubes/ultrathin MoS_2 nanosheet core–shell architecture for lithium–sulfur batteries, J. Mater. Chem. A 7 (2019) 13103–13112.
[235] W. Guo, Q. Zhu, Q. Lu, MCNT/MoS_2 promoting the electrochemical performance of lithium-sulfur batteries by adsorption polysulfide, Mater. Res. Express 7 (2020) 035507.
[236] J. Wu, B. Chen, Q. Liu, A. Hu, X. Lu, Q. Jiang, Preparing a composite including SnS_2, carbon nanotubes and S and using as cathode material of lithium-sulfur battery, Scripta Materialia 177 (2020) 208–213.
[237] Y. Mi, W. Liu, X. Li, J. Zhuang, H. Zhou, H. Wang, High-performance Li–S battery cathode with catalyst-like carbon nanotube-MoP promoting polysulfide redox, Nano Res 10 (2017) 3698–3705.
[238] X.-F. Yu, D.-X. Tian, W.-C. Li, B. He, Y. Zhang, Z.-Y. Chen, A.-H. Lu, One-pot synthesis of highly conductive nickel-rich phosphide/CNTs hybrid as a polar sulfur host for high-rate and long-cycle Li-S battery, Nano Res 12 (2019) 1193–1197.
[239] Z. Shi, W. Feng, X. Wang, M. Li, C. Song, L. Chen, Catalytic cobalt phosphide Co_2P/carbon nanotube nanocomposite as host material for high performance lithium-sulfur battery cathode, J. Alloys Compd. 851 (2021) 156289.
[240] X. Liang, A. Garsuch, L.F. Nazar, Sulfur cathodes based on conductive MXene nanosheets for high-performance lithium–sulfur batteries, Angew. Chem. Int. Ed. 54 (2015) 3907–3911.
[241] J. Pang, R.G. Mendes, A. Bachmatiuk, L. Zhao, H.Q. Ta, T. Gemming, H. Liu, Z. Liu, M.H. Rummeli, Applications of 2D MXenes in energy conversion and storage systems, Chem. Soc. Rev. 48 (2019) 72–133.
[242] L.-P. Lv, C.-F. Guo, W. Sun, Y. Wang, Strong surface-bound sulfur in carbon nanotube bridged hierarchical Mo_2C-based MXene nanosheets for lithium–sulfur batteries, Small 15 (2019) 1804338.
[243] X. Liang, Y. Rangom, C.Y. Kwok, Q. Pang, L.F. Nazar, Interwoven MXene nanosheet/carbon-nanotube composites as Li–S cathode hosts, Adv. Mater. 29 (2017) 1603040.
[244] X. Wang, D. Luo, J. Wang, Z. Sun, G. Cui, Y. Chen, T. Wang, L. Zheng, Y. Zhao, L. Shui, G. Zhou, K. Kempa, Y. Zhang, Z. Chen, Strain engineering of a MXene/CNT hierarchical porous hollow microsphere electrocatalyst for a high-efficiency lithium polysulfide conversion process, Angew. Chem. Int. Ed. 60 (2021) 2371–2378.
[245] J. Wang, Z. Zhang, X. Yan, S. Zhang, Z. Wu, Z. Zhuang, W.-Q. Han, Rational design of porous N-Ti_3C_2 MXene@CNT microspheres for high cycling stability in Li–S battery, Nano-Micro Lett 12 (2019) 4.
[246] Z. Guo, H. Nie, Z. Yang, W. Hua, C. Ruan, D. Chan, M. Ge, X.a. Chen, S. Huang, 3D CNTs/graphene-S-Al_3Ni_2 cathodes for high-sulfur-loading and long-life lithium—sulfur batteries, Adv. Sci. 5 (2018) 1800026.
[247] M. Li, K. Fu, Z. Wang, C. Cao, J. Yang, Q. Zhai, Z. Zhou, J. Ji, Y. Xue, C. Tang, enhanced adsorption of polysulfides on carbon nanotubes/boron nitride fibers for high-performance lithium-sulfur batteries, Chem. Eur. J. 26 (2020) 17567–17573.
[248] B. He, W.-C. Li, Y. Zhang, X.-F. Yu, B. Zhang, F. Li, A.-H. Lu, Paragenesis BN/CNTs hybrid as a monoclinic sulfur host for high rate and ultra-long life lithium–sulfur battery, J. Mater. Chem. A 6 (2018) 24194–24200.
[249] X.-B. Cheng, H.-J. Peng, J.-Q. Huang, L. Zhu, S.-H. Yang, Y. Liu, H.-W. Zhang, W. Zhu, F. Wei, Q. Zhang, Three-dimensional aluminum foam/carbon nanotube scaffolds as long- and short-range electron pathways with improved sulfur loading for high energy density lithium–sulfur batteries, J. Power Sources 261 (2014) 264–270.
[250] C. Li, Z. Xi, S. Dong, X. Ge, Z. Li, C. Wang, L. Yin, CNTs/MOFs-derived carbon/$Al_2(OH)_{2.76}F_{3.24}$/S cathodes for high-performance lithium-sulfur batteries, Energy Storage Mater 12 (2018) 341–351.
[251] Y.-S. Liu, C. Ma, Y.-L. Bai, X.-Y. Wu, Q.-C. Zhu, X. Liu, X.-H. Liang, X. Wei, K.-X. Wang, J.-S. Chen, Nitrogen-doped carbon nanotube sponge with embedded Fe/Fe_3C nanoparticles as binder-free cathodes for high capacity lithium–sulfur batteries, J. Mater. Chem. A 6 (2018) 17473–17480.
[252] H. Zhang, W. Zhao, M. Zou, Y. Wang, Y. Chen, L. Xu, H. Wu, A. Cao, 3D, mutually embedded MOF@carbon nanotube hybrid networks for high-performance lithium–sulfur batteries, Adv. Energy Mater. 8 (2018) 1800013.
[253] H. Zhang, W. Zhao, Y. Wu, Y. Wang, M. Zou, A. Cao, Dense monolithic MOF and carbon nanotube hybrid with enhanced volumetric and areal capacities for lithium–sulfur battery, J. Mater. Chem. A 7 (2019) 9195–9201.
[254] G. Xu, Y. Zuo, B. Huang, Metal-organic framework-74-Ni/carbon nanotube composite as sulfur host for high performance lithium-sulfur batteries, J. Electroanal. Chem. 830-831 (2018) 43–49.
[255] X. Wang, Z. Zhang, Y. Qu, G. Wang, Y. Lai, J. Li, Solution-based synthesis of multi-walled carbon nanotube/selenium composites for high performance lithium–selenium battery, J. Power Sources 287 (2015) 247–252.
[256] R. Mukkabla, S. Deshagani, M. Deepa, S.M. Shivaprasad, P. Ghosal, Carbon black free Selenium/CTAB decorated carbon nanotubes composite with high selenium content for Li-Se batteries, Electrochim. Acta 283 (2018) 63–74.
[257] D. Dutta, S. Gope, D.S. Negi, R. Datta, A.K. Sood, A.J. Bhattacharyya, Pressure-induced capillary encapsulation protocol for ultrahigh loading of sulfur and selenium inside carbon nanotubes: application as high performance cathode in Li–S/Se rechargeable batteries, J. Phys. Chem. C 120 (2016) 29011–29022.
[258] N. Feng, K. Xiang, L. Xiao, W. Chen, Y. Zhu, H. Liao, H. Chen, Se/CNTs microspheres as improved performance for cathodes in Li-Se batteries, J. Alloys Compd. 786 (2019) 537–543.
[259] Y. Cui, X. Zhou, W. Guo, Y. Liu, T. Li, Y. Fu, L. Zhu, Selenium nanocomposite cathode with long cycle life for rechargeable lithium-selenium batteries, Batter. Supercaps 2 (2019) 784–791.
[260] J. He, Y. Chen, W. Lv, K. Wen, P. Li, Z. Wang, W. Zhang, W. Qin, W. He, Three-dimensional hierarchical graphene-CNT@Se: a highly efficient freestanding cathode for Li–Se batteries, ACS Energy Lett 1 (2016) 16–20.
[261] K. Han, Z. Liu, H. Ye, F. Dai, Flexible self-standing graphene–Se@CNT composite film as a binder-free cathode for rechargeable Li–Se batteries, J. Power Sources 263 (2014) 85–89.
[262] J. Ge, Q. Zhang, Z. Liu, H. Yang, B. Lu, Solvothermal synthesis of graphene encapsulated selenium/carboxylated carbon nanotubes electrode for lithium–selenium battery, J. Alloys Compd. 810 (2019) 151894.
[263] J. Li, C. Zhang, C.-J. Wu, Y. Tao, L. Zhang, Q.-H. Yang, Improved performance of Li–Se battery based on a novel dual functional CNTs@graphene/CNTs cathode construction, Rare Metals 36 (2017) 425–433.
[264] L. Zeng, X. Wei, J. Wang, Y. Jiang, W. Li, Y. Yu, Flexible one-dimensional carbon–selenium composite nanofibers with superior electrochemical performance for Li–Se/Na–Se batteries, J. Power Sources 281 (2015) 461–469.
[265] K. Balakumar, N. Kalaiselvi, Selenium containing tube-in-tube carbon: a one dimensional carbon frame work for selenium cathode in Li-Se battery, Carbon 112 (2017) 79–90.
[266] S. Xin, L. Yu, Y. You, H.-P. Cong, Y.-X. Yin, X.-L. Du, Y.-G. Guo, S.-H. Yu, Y. Cui, J.B. Goodenough, The electrochemistry with lithium versus sodium of selenium confined to slit micropores in carbon, Nano Lett 16 (2016) 4560–4568.
[267] X. Ge, L. Yin, S-doping induced boosted electrochemical redox kinetics in $Te_{1-x}S_x$ nanorod cathodes for high volumetric capacity Li-Te batteries, Energy Storage Mater 20 (2019) 89–97.
[268] J. He, W. Lv, Y. Chen, K. Wen, C. Xu, W. Zhang, Y. Li, W. Qin, W. He, Tellurium-impregnated porous cobalt-doped carbon polyhedra as superior cathodes for lithium–tellurium batteries, ACS Nano 11 (2017) 8144–8152.
[269] J. Xu, S. Xin, J.-W. Liu, J.-L. Wang, Y. Lei, S.-H. Yu, Elastic carbon nanotube aerogel meets tellurium nanowires: a binder- and collector-free electrode for Li-Te batteries, Adv. Funct. Mater. 26 (2016) 3580–3588.
[270] Y. Li, M.-Q. Wang, Y. Chen, L. Hu, T. Liu, S. Bao, M. Xu, Muscle-like electrode design for Li-Te batteries, Energy Storage Mater 10 (2018) 10–15.
[271] K. Xie, K. Yuan, K. Zhang, C. Shen, W. Lv, X. Liu, J.-G. Wang, B. Wei, Dual functionalities of carbon nanotube films for dendrite-free and high energy–high power lithium–sulfur batteries, ACS Appl. Mater. Interfaces 9 (2017) 4605–4613.
[272] H.M. Kim, J.-Y. Hwang, A. Manthiram, Y.-K. Sun, High-performance lithium–sulfur batteries with a self-assembled multiwall carbon nanotube interlayer and a robust electrode–electrolyte interface, ACS Appl. Mater. Interfaces 8 (2016) 983–987.
[273] Y. Peng, Z. Wen, C. Liu, J. Zeng, Y. Wang, J. Zhao, Refining interfaces between electrolyte and both electrodes with carbon nanotube paper for high-loading lithium–sulfur batteries, ACS Appl. Mater. Interfaces 11 (2019) 6986–6994.
[274] C.-L. Lee, I.-D. Kim, A hierarchical carbon nanotube-loaded glass-filter composite paper interlayer with outstanding electrolyte uptake properties for high-performance lithium–sulphur batteries, Nanoscale 7 (2015) 10362–10367.
[275] D.K. Lee, S.J. Kim, Y.-J. Kim, H. Choi, D.W. Kim, H.-J. Jeon, C.W. Ahn, J.W. Lee, H.-T. Jung, Graphene oxide/carbon nanotube bilayer flexible membrane for high--performance Li–S batteries with superior physical and electrochemical properties, Adv. Mater. Interfaces 6 (2019) 1801992.
[276] J.-Q. Huang, Z.-L. Xu, S. Abouali, M. Akbari Garakani, J.-K. Kim, Porous graphene oxide/carbon nanotube hybrid films as interlayer for lithium-sulfur batteries, Carbon 99 (2016) 624–632.
[277] H. Ma, C. Song, N. Liu, Y. Zhao, Z. Bakenov, Nitrogen-deficient graphitic carbon nitride/carbon nanotube as polysulfide barrier of high-performance lithium-sulfur batteries, ChemElectroChem 7 (2020) 4906–4912.
[278] M.X. Tran, R. Enggar Anugrah Ardhi, G. Liu, J.Y. Kim, J.K. Lee, Plasma-polymerized C_{60}-coated CNT interlayer with physical and chemical functions for lithium–sulfur batteries, Chem. Eng. J. 401 (2020) 126075.
[279] W. Kong, L. Yan, Y. Luo, D. Wang, K. Jiang, Q. Li, S. Fan, J. Wang, Ultrathin MnO_2/graphene oxide/carbon nanotube interlayer as efficient polysulfide-trapping shield for high-performance Li–S batteries, Adv. Funct. Mater. 27 (2017) 1606663.
[280] N. Li, Z. Chen, F. Chen, G. Hu, S. Wang, Z. Sun, X. Sun, F. Li, From interlayer to lightweight capping layer: rational design of mesoporous TiO_2 threaded with CNTs for advanced Li–S batteries, Carbon 143 (2019) 523–530.
[281] C. Yan, X. Zhou, Y. Wei, S. He, A waste newspaper/multi-walled carbon nanotube/TiO_2 interlayer for improving the cycling stability of lithium–sulfur batteries by anchoring polysulfides, Dalton Trans 49 (2020) 11675–11681.

[282] Z. Sun, Y. Guo, B. Li, T. Tan, Y. Zhao, ZnO/carbon nanotube/reduced graphene oxide composite film as an effective interlayer for lithium/sulfur batteries, Solid State Sci 95 (2019) 105924.
[283] L. Luo, X. Qin, J. Wu, G. Liang, Q. Li, M. Liu, F. Kang, G. Chen, B. Li, An interwoven MoO_3@CNT scaffold interlayer for high-performance lithium–sulfur batteries, J. Mater. Chem. A 6 (2018) 8612–8619.
[284] T. Liu, S. Sun, J. Hao, W. Song, Q. Niu, X. Sun, Y. Wu, D. Song, J. Wu, Reliable interlayer based on hybrid nanocomposites and carbon nanotubes for lithium–sulfur batteries, ACS Appl. Mater. Interfaces 11 (2019) 15607–15615.
[285] Y. Luo, N. Luo, W. Kong, H. Wu, K. Wang, S. Fan, W. Duan, J. Wang, Multifunctional interlayer based on molybdenum diphosphide catalyst and carbon nanotube film for lithium–sulfur batteries, Small 14 (2018) 1702853.
[286] S. Li, H. Zhang, W. Chen, Y. Zou, H. Yang, J. Yang, C. Peng, Toward commercially viable Li-S batteries: overall performance improvements enabled by a multipurpose interlayer of hyperbranched polymer-grafted carbon nanotubes, ACS Appl. Mater. Interfaces 12 (2020) 25767–25774.
[287] J.H. Kim, J. Seo, J. Choi, D. Shin, M. Carter, Y. Jeon, C. Wang, L. Hu, U. Paik, Synergistic ultrathin functional polymer-coated carbon nanotube interlayer for high performance lithium–sulfur batteries, ACS Appl. Mater. Interfaces 8 (2016) 20092–20099.
[288] K. Zou, N. Li, X. Dai, W. Jing, M. Shi, C. Lu, Q. Tan, Y. Xin, J. Sun, Y. Chen, Y. Liu, Lightweight freestanding CeF_3 nanorod/carbon nanotube composite interlayer for lithium–sulfur batteries, ACS Appl. Nano. Mater. 3 (2020) 5732–5742.
[289] J. Yoo, S.-J. Cho, G.Y. Jung, S.H. Kim, K.-H. Choi, J.-H. Kim, C.K. Lee, S.K. Kwak, S.-Y. Lee, COF-net on CNT-net as a molecularly designed, hierarchical porous chemical trap for polysulfides in lithium–sulfur batteries, Nano Lett 16 (2016) 3292–3300.
[290] R. Ponraj, A.G. Kannan, J.H. Ahn, J.H. Lee, J. Kang, B. Han, D.-W. Kim, Effective trapping of lithium polysulfides using a functionalized carbon nanotube-coated separator for lithium–sulfur cells with enhanced cycling stability, ACS Appl. Mater. Interfaces 9 (2017) 38445–38454.
[291] J.-Q. Huang, W.G. Chong, Q. Zheng, Z.-L. Xu, J. Cui, S. Yao, C. Wang, J.-K. Kim, Understanding the roles of activated porous carbon nanotubes as sulfur support and separator coating for lithium-sulfur batteries, Electrochim. Acta 268 (2018) 1–9.
[292] S.-H. Chung, A. Manthiram, High-performance Li–S batteries with an ultra–lightweight MWCNT-coated separator, J. Phys. Chem. Lett. 5 (2014) 1978–1983.
[293] F. Gao, X. Yan, Z. Wei, M. Qu, W. Fan, Graphene/carbon nanotubes composite as a polysulfide trap for lithium-sulfur batteries, Int. J. Electrochem. Sci 14 (2019) 3301–3314.
[294] H. Wu, Y. Huang, W. Zhang, X. Sun, Y. Yang, L. Wang, M. Zong, Lock of sulfur with carbon black and a three-dimensional graphene@carbon nanotubes coated separator for lithium-sulfur batteries, J. Alloys Compd. 708 (2017) 743–750.
[295] Y. Pang, J. Wei, Y. Wang, Y. Xia, Synergetic protective effect of the ultralight MWCNTs/NCQDs modified separator for highly stable lithium–sulfur batteries, Adv. Energy Mater. 8 (2018) 1702288.
[296] X. Wang, G. Li, M. Li, R. Liu, H. Li, T. Li, M. Sun, Y. Deng, M. Feng, Z. Chen, Reinforced polysulfide barrier by g-C_3N_4/CNT composite towards superior lithium-sulfur batteries, J. Energy Chem. 53 (2021) 234–240.
[297] Y. Liu, M. Chen, Z. Su, Y. Gao, Y. Zhang, D. Long, Direct trapping and rapid conversing of polysulfides via a multifunctional Nb_2O_5-CNT catalytic layer for high performance lithium-sulfur batteries, Carbon 172 (2021) 260–271.
[298] J. Xu, Q. Zhang, X. Liang, J. Yan, J. Liu, Y. Wu, A multifunctional separator based on scandium oxide nanocrystal decorated carbon nanotubes for high performance lithium–sulfur batteries, Nanoscale 12 (2020) 6832–6843.
[299] J. Du, W. Ahmed, J. Xu, M. Zhang, Z. Zhang, X. Zhang, D. Niu, Chainmail catalyst of Fe_3O_4@C/CNTO-modified celgard separator with low metal loading for high-performance lithium–sulfur batteries, ChemistrySelect 5 (2020) 3757–3762.
[300] Z. Sun, T. Wang, Y. Zhang, K. Kempa, X. Wang, Boosting the electrochemical performance of lithium/sulfur batteries with the carbon nanotube/Fe_3O_4 coated by carbon modified separator, Electrochim. Acta 327 (2019) 134843.
[301] H. Ding, Q. Zhang, Z. Liu, J. Wang, R. Ma, L. Fan, T. Wang, J. Zhao, J. Ge, X. Lu, X. Yu, B. Lu, TiO_2 quantum dots decorated multi-walled carbon nanotubes as the multifunctional separator for highly stable lithium sulfur batteries, Electrochim. Acta 284 (2018) 314–320.
[302] P. Chen, Z. Wang, B. Zhang, J. Zhao, H. Liu, X. Guo, W. Liu, Z. Su, Multi-functional TiO_2 nanosheets/carbon nanotubes modified separator enhanced cycling performance for lithium-sulfur batteries, Int. J. Energy Res. 44 (2020) 3231–3240.
[303] X. Wu, S. Li, S. Yao, M. Liu, S. Pang, X. Shen, T. Li, S. Qin, Nanosized Ti_4O_7 supported on carbon nanotubes composite modified separator for enhanced electrochemical properties of lithium sulfur battery, Int. J. Energy Res. 45 (2021) 4331–4344.
[304] D. Li, J. Yang, X. Xu, X. Wang, J. Chen, J. Xu, N. Zhao, Synergistic inhibitory effect of ultralight CNTs-COOH@Fe_3O_4 modified separator on polysulfides shuttling for high-performance lithium–sulfur batteries, J. Membr. Sci. 611 (2020) 118300.
[305] L. Luo, S.-H. Chung, A. Manthiram, A trifunctional multi-walled carbon nanotubes/polyethylene glycol (MWCNT/PEG)-coated separator through a layer-by-layer coating strategy for high-energy Li–S batteries, J. Mater. Chem. A 4 (2016) 16805–16811.
[306] C.-H. Chang, S.-H. Chung, A. Manthiram, Ultra-lightweight PAN-iNF/MWCNT-functionalized separators with synergistic suppression of polysulfide migration for Li–S batteries with pure sulfur cathodes, J. Mater. Chem. A 3 (2015) 18829–18834.
[307] S. Yao, J. Cui, J.-Q. Huang, Z. Lu, Y. Deng, W.G. Chong, J. Wu, M. Ihsan Ul Haq, F. Ciucci, J.-K. Kim, Novel 2D Sb_2S_3 nanosheet/CNT coupling layer for exceptional polysulfide recycling performance, Adv. Energy Mater. 8 (2018) 1800710.
[308] Y.C. Jeong, J.H. Kim, S.H. Kwon, J.Y. Oh, J. Park, Y. Jung, S.G. Lee, S.J. Yang, C.R. Park, Rational design of exfoliated 1T MoS_2@CNT-based bifunctional separators for lithium sulfur batteries, J. Mater. Chem. A 5 (2017) 23909–23918.
[309] B. Guan, Y. Zhang, L. Fan, X. Wu, M. Wang, Y. Qiu, N. Zhang, K. Sun, Blocking polysulfide with Co_2B@CNT via "synergetic adsorptive effect" toward ultrahigh-rate capability and robust lithium–sulfur battery, ACS Nano 13 (2019) 6742–6750.
[310] D.H. Lee, J.H. Ahn, M.-S. Park, A. Eftekhari, D.-W. Kim, Metal-organic framework/carbon nanotube-coated polyethylene separator for improving the cycling performance of lithium-sulfur cells, Electrochim. Acta 283 (2018) 1291–1299.
[311] F. Wu, S. Zhao, L. Chen, Y. Lu, Y. Su, Y. Jia, L. Bao, J. Wang, S. Chen, R. Chen, Metal-organic frameworks composites threaded on the CNT knitted separator for suppressing the shuttle effect of lithium sulfur batteries, Energy Storage Mater 14 (2018) 383–391.
[312] G. Gnana kumar, S.-H. Chung, T. Raj kumar, A. Manthiram, Three-dimensional graphene–carbon nanotube–Ni hierarchical architecture as a polysulfide trap for lithium–sulfur batteries, ACS Appl. Mater. Interfaces 10 (2018) 20627–20634.
[313] X. Zuo, M. Zhen, C. Wang, Ni@N-doped graphene nanosheets and CNTs hybrids modified separator as efficient polysulfide barrier for high-performance lithium sulfur batteries, Nano Res 12 (2019) 829–836.
[314] F. Zhang, X. Guo, P. Xiong, J. Zhang, J. Song, K. Yan, X. Gao, H. Liu, G. Wang, Interface engineering of MXene composite separator for high-performance Li–Se and Na–Se batteries, Adv. Energy Mater. 10 (2020) 2000446.
[315] M.L. Meyerson, P.E. Papa, A. Heller, C.B. Mullins, Recent developments in dendrite-free lithium-metal deposition through tailoring of micro- and nanoscale artificial coatings, ACS Nano 15 (2021) 29–46.
[316] R.L. Sacci, J.M. Black, N. Balke, N.J. Dudney, K.L. More, R.R. Unocic, Nanoscale imaging of fundamental Li battery chemistry: solid-electrolyte interphase formation and preferential growth of lithium metal nanoclusters, Nano Lett. 15 (2015) 2011–2018.
[317] Y.-X. Zhan, P. Shi, X.-Q. Zhang, F. Ding, J.-Q. Huang, Z.H. Jin, R. Xiang, X.J. Liu, Q. Zhang, The insights of lithium metal plating/stripping in porous hosts: progress and perspectives, Energy Technol. 9 (2021) 2000700.
[318] Z. Zhang, J.L. Wang, X.F. Yan, S.L. Zhang, W.T. Yang, Z.H. Zhuang, W.-Q. Han, In-situ growth of hierarchical N-doped CNTs/Ni foam scaffold for dendrite-free lithium metal anode, Energy Storage Mater. 29 (2020) 332–340.
[319] Z.Y. Wang, Z.X. Lu, W. Guo, Q. Luo, Y.H. Yin, X.B. Liu, Y.S. Li, B.Y. Xia, Z.P. Wu, A dendrite-free lithium/carbon nanotube hybrid for lithium-metal batteries, Adv. Mater. 33 (2021) 2006702.
[320] L. Ye, M. Liao, H. Sun, Y. Yang, C. Tang, Y. Zhao, L. Wang, Y. Xu, L. Zhang, B. Wang, F. Xu, X. Sun, Y. Zhang, H. Dai, P.G. Bruce, H. Peng, Stabilizing lithium into cross-stacked nanotube sheets with an ultra-high specific capacity for lithium oxygen batteries, Angew. Chem. Int. Ed. 58 (2019) 2437–2442.
[321] S. Matsuda, Y. Kubo, K. Uosaki, S. Nakanishi, Lithium-metal deposition/dissolution within internal space of CNT 3D matrix results in prolonged cycle of lithium-metal negative electrode, Carbon 119 (2017) 119–123.
[322] Y. Wang, Y. Shen, Z. Du, X. Zhang, K. Wang, H. Zhang, T. Kang, F. Guo, C. Liu, X. Wu, W. Lu, L. Chen, A lithium–carbon nanotube composite for stable lithium anodes, J. Mater. Chem. A 5 (2017) 23434–23439.
[323] G. Yang, Y. Li, Y. Tong, J. Qiu, S. Liu, S. Zhang, Z. Guan, B. Xu, Z. Wang, L. Chen, Lithium plating and stripping on carbon nanotube sponge, Nano Lett. 19 (2019) 494–499.
[324] Z. Sun, S. Jin, H. Jin, Z. Du, Y. Zhu, A. Cao, H. Ji, L.-J. Wan, Robust expandable carbon nanotube scaffold for ultrahigh-capacity lithium-metal anodes, Adv. Mater. 30 (2018) 1800884.
[325] G. Wang, T. Liu, X. Fu, Z. Wu, M. Liu, X. Xiong, Lithiophilic amide-functionalized carbon nanotube skeleton for dendrite-free lithium metal anodes, Chem. Eng. J. 414 (2021) 128698.
[326] K. Liu, Z. Li, W. Xie, J. Li, D. Rao, M. Shao, B. Zhang, M. Wei, Oxygen-rich carbon nanotube networks for enhanced lithium metal anode, Energy Storage Mater. 15 (2018) 308–314.
[327] C. Zhao, Z. Wang, X. Tan, H. Huang, Z. Song, Y. Sun, S. Cui, Q. Wei, W. Guo, R. Li, C. Yu, J. Qiu, X. Sun, Implanting CNT forest onto carbon nanosheets as multifunctional hosts for high-performance lithium metal batteries, Small Methods 3 (2019) 1800546.
[328] J. Wang, H. Liu, H. Wu, Q. Li, Y. Zhang, S. Fan, J. Wang, Self-standing carbon nanotube aerogels with amorphous carbon coating as stable host for lithium anodes, Carbon 177 (2021) 181–188.
[329] Y. Zhang, B. Liu, E. Hitz, W. Luo, Y. Yao, Y. Li, J. Dai, C. Chen, Y. Wang, C. Yang, H. Li, L. Hu, A carbon-based 3D current collector with surface protection for Li metal anode, Nano Res. 10 (2017) 1356–1365.
[330] J. Zhou, F. Wu, G. Wei, Y. Hao, Y. Mei, L. Li, M. Xie, R. Chen, Lithium-metal host anodes with top-to-bottom lithiophilic gradients for prolonged cycling of rechargeable lithium batteries, J. Power Sources 495 (2021) 229773.
[331] W. Zhang, H. Jin, G. Chen, J. Zhang, Hierarchical 3D N-CNT/Sb_2MoO_6 for dendrite-free lithium metal battery, Chem. Eng. J. 420 (2021) 129614.
[332] T.-T. Zuo, Y.-X. Yin, S.-H. Wang, P.-F. Wang, X. Yang, J. Liu, C.-P. Yang, Y.-G. Guo, Trapping lithium into hollow silica microspheres with a carbon nanotube core for dendrite-free lithium metal anodes, Nano Lett 18 (2018) 297–301.
[333] Y. Deng, H. Lu, Y. Cao, B. Xu, Q. Hong, W. Cai, W. Yang, Multi-walled carbon nanotube interlayers with controllable thicknesses for high-capacity and long-life lithium metal anodes, J. Power Sources 412 (2019) 170–179.
[334] X. Li, Z. Chu, H. Jiang, Y. Dai, W. Zheng, A. Liu, X. Jiang, G. He, Redistributing Li-ion flux and homogenizing Li-metal growth by N-doped hierarchically porous membranes for dendrite-free lithium metal batteries, Energy Storage Mater. 37 (2021) 233–242.

[335] H. Zhang, X. Liao, Y. Guan, Y. Xiang, M. Li, W. Zhang, X. Zhu, H. Ming, L. Lu, J. Qiu, Y. Huang, G. Cao, Y. Yang, L. Mai, Y. Zhao, H. Zhang, Lithiophilic-lithiophobic gradient interfacial layer for a highly stable lithium metal anode, Nat. Commun. 9 (2018) 3729.
[336] M. Zhao, Y.-Q. Peng, B.-Q. Li, X.-Q. Zhang, J.-Q. Huang, Regulation of carbon distribution to construct high-sulfur-content cathode in lithium–sulfur batteries, J. Energy Chem. 56 (2021) 203–208.
[337] L. Ma, J. Cui, S. Yao, X. Liu, Y. Luo, X. Shen, J.-K. Kim, Dendrite-free lithium metal and sodium metal batteries, Energy Storage Mater. 27 (2020) 522–554.
[338] L. Ma, J. Wu, G. Zhu, Y. Lv, Y. Zhang, H. Pang, Recent advances in two-dimensional materials for alkali metal anodes, J. Mater. Chem. A 9 (2021) 5232–5257.